

**INTEGRATED ENERGY MANAGEMENT
SYSTEM FOR MICROGRIDS WITH HYBRID
RENEWABLE GENERATION, ENERGY
STORAGE AND CONTROLLABLE LOADS**

**BY
AHMED SALEH A. AL-AHMED**

**A Thesis Presented to the
DEANSHIP OF GRADUATE STUDIES
KING FAHD UNIVERSITY OF PETROLEUM & MINERALS
DHAHRAN, SAUDI ARABIA**

**In Partial Fulfillment of the
Requirements for the Degree of**

MASTER OF SCIENCE

In

ELECTRICAL ENGINEERING

MAY 2019

KING FAHD UNIVERSITY OF PETROLEUM & MINERALS
DHAHRAN 31261, SAUDI ARABIA

DEANSHIP OF GRADUATE STUDIES

This thesis, written by **AHMED SALEH AHMED AL-AHMED** under the direction of his thesis adviser and approved by his thesis committee, has been presented to and accepted by the Dean of Graduate Studies, in partial fulfillment of the requirements for the degree of **MASTER OF SCIENCE IN ELECTRICAL ENGINEERING**.

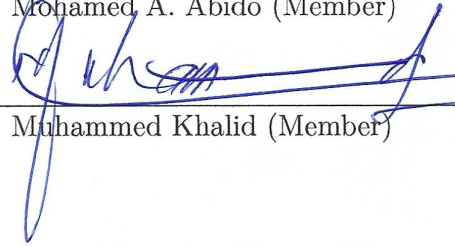
Thesis Committee



Dr. Mohammad M. Al-Muhaini (Adviser)



Dr. Mohamed A. Abido (Member)



Dr. Muhammed Khalid (Member)



Dr. Abdallah S. Al-Ahmari
Department Chairman



Dr. Salam A. Zummo
Dean of Graduate Studies

5/5/2019

Date



©Ahmed Saleh Ahmed Al-Ahmed
2019

Dedicated to my beloved mother and father.

ACKNOWLEDGMENTS

First and foremost, all praises to Allah for the strengths and his blessings and facilitation in completing this thesis.

I would like to express my sincere appreciation to my adviser, Dr. Mohammad Al-Muhaini, for his continuous support, motivation, and supervision. This thesis would never be a success without his valuable comments, and sincere advices.

I am also thankful to my fine thesis committee members whom I visited many times and was enriched by their critical remarks, resources, and point of views. My gratitude is also extended to Dr. Ibrahim Elamin and the electrical engineering department for their unlimited assistance.

Lastly, no words can describe my gratitude to my parents. Their kindness, patience, and tenderness are endless, and so are my appreciation, prayers, and love to them. I am also grateful to my brother and sisters for their unconditional support throughout my study period. Many thanks to all of my friends for being so gentle, caring and loving.

TABLE OF CONTENTS

ACKNOWLEDGMENTS	vi
LIST OF TABLES	xi
LIST OF FIGURES	xiii
NOMENCLATURE	xviii
LIST OF ABBREVIATIONS	xxii
ABSTRACT (ENGLISH)	xxiv
ABSTRACT (ARABIC)	xxvi
CHAPTER 1 INTRODUCTION	1
1.1 Introduction	1
1.2 Thesis Motivation	5
1.3 Objectives	6
1.4 Literature Review	8
1.5 Contributions	19
1.6 Thesis Structure	19
CHAPTER 2 MODELING OF MICROGRID DEMANDS AND CONTROLLABLE LOADS	22
2.1 Literature Review	25
2.2 Microgrid Demand Modeling	26

2.2.1	Residential Load Modeling	26
2.2.2	Commercial Load Modeling	31
2.2.3	Industrial Load Modeling	34
2.2.4	Hospital Load Modeling	36
2.2.5	Load Factor of All Load Types	38

CHAPTER 3 MODELING OF DISTRIBUTED ENERGY RE-SOURCES 42

3.1	Literature Review	44
3.2	PV Energy Modeling	45
3.3	Wind Energy Modeling	51
3.4	Battery Energy Storage System Modeling	55

CHAPTER 4 MICROGRID TEST SYSTEM DESIGN 60

4.1	Literature Review	62
4.2	Description of The Test System	63
4.2.1	Test-bed’s Renewable Energy Resources and Storage	63
4.2.2	Test-bed’s Demand	64
4.2.3	Configuration of The Test-bed	66
4.3	Operation of The Test System	67
4.4	Microgrid Testbed Case Studies	69
4.4.1	Case 1: Normal MG operation	71
4.4.2	Case 2: Shading Effect	72
4.4.3	Case 3: Battery Sizing change	74
4.4.4	Case 4: Fault At Industrial Bus and Shading	75
4.4.5	Case 5: Fault at Battery Bus	75
4.4.6	Case 6: MG Run for Two Simultaneous Days	76
4.4.7	Case 7: MG Run on Winter Day	77
4.4.8	Case 8: One Week Run	80

CHAPTER 5 INTELLIGENT LOAD PRIORITY LIST	82
5.1 Literature Review	83
5.2 Artificial Neural Network	86
5.3 Load Priority List Problem Formulation	88
5.4 Simulation Results and Discussion	91
CHAPTER 6 DEMAND SIDE MANAGEMENT SCHEMES	98
6.1 Fuzzy Inference Systems (FIS)	100
6.2 Implementation and Evaluation of Demand Side Management Schemes	102
6.2.1 Energy Balance Based DSM	103
6.2.2 Energy balance Based DSM Incorporated With LPL	108
6.2.3 Peak Shaving LPL based DSM on Each Load Category	112
6.2.4 Peak Shifting LPL based DSM on Each Load Category	116
6.2.5 Peak Shaving LPL based DSM of The Total Aggregated Load .	119
6.2.6 Residential Load DSM Using Load Composition	122
CHAPTER 7 INCENTIVE-BASED FEASIBILITY STUDY OF AN EFFICIENT HYBRID AC/DC MICROGRID IN SAUDI ARABIA	128
7.1 Literature Review	129
7.2 Hybrid MG Distributed Energy Resources Sizing	130
7.2.1 PV Sizing	131
7.2.2 Wind Sizing	132
7.2.3 Battery Sizing	132
7.3 Financial Costs Programs	133
7.4 Analysis and Results	139
CHAPTER 8 CONCLUSION AND FUTURE WORK	147
8.1 Conclusion	147
8.2 Future Work	149
APPENDIX A MICROGRID TEST SYSTEM	151
A.1 SIMULINK Simulation	151

A.2 Microgrid Testbed Web-page	152
APPENDIX B FUZZY RULES	157
B.1 Case 1	157
B.2 Case 2	158
B.3 Case 6	162
REFERENCES	167
VITAE	184

LIST OF TABLES

2.1	Load data specification.	24
2.2	Saudi electricity tariff [1]	24
2.3	General characteristics of the studied load types.	25
2.4	Household activities and calculation parameters	30
2.5	Summer and winter energy consumption per activity	31
3.1	Saudi Arabia daily sunshine hours.	47
3.2	Panasonic solar panel specifications.	48
3.3	Wind shear exponent based on terrain [2]	53
3.4	Wind turbine specifications	54
4.1	Classifications of the proposed microgrid test-bed	63
4.2	Maximum and average generation and load capacities of the MG test-bed	67
4.3	Microgrid test system case studies.	71
4.4	Microgrid test system case studies with different dates	71
5.1	Load categories and corresponding numerical code	90
5.2	Training input sets	91
5.3	Load criticality levels	92
6.1	DSM case studies	103
6.2	Inputs and outputs of energy balance based DSM	109
6.3	Inputs and outputs of energy balance based DSM with LPL	115
6.4	Daily load factor before and after peak clipping	115
6.5	Daily load factor before and after peak shifting	118

6.6	Daily load factor before and after peak shaving the aggregated load . .	123
6.7	Mapping of FL output and AC action	127
7.1	Consumption of the four load types	132
7.2	Wind monthly energy generation	133
7.3	Battery size calculation	134
7.4	PV technology specifications	140
7.5	High income residential customers	140
7.6	Low income residential customers	141
7.7	Commercial customers	142
7.8	Hospital load	143
7.9	Industrial customers	144
7.10	Financial parameters	144
7.11	Case study: High income residential customers	144
7.12	Case Study: Low income residential customers	145
7.13	Case study: Commercial customers	145
7.14	Case study: Hospital load	145
7.15	Case study: Industrial customers	146
B.1	Fuzzy rules of the 1 st case	158
B.2	Fuzzy rules of the 2 nd case	159
B.3	Fuzzy rules of the 6 th case	162

LIST OF FIGURES

1.1	Ever increasing world electrical energy consumption [3]	9
1.2	Demand Side Management Schemes	18
1.3	Structure and flow of the thesis	21
2.1	Microgrid configuration with the four load types in the rectangular. . .	23
2.2	The shaded region is the Eastern province in Saudi Arabia.	24
2.3	Residential annual load profile.	27
2.4	Residential hourly load profile.	28
2.5	Residential seasonal load profile.	28
2.6	Residential monthly load profile.	29
2.7	Percentage of household appliances in winter.	32
2.8	Percentage of household appliances in summer.	33
2.9	Commercial annual peak and average load profile.	33
2.10	Commercial hourly load profile.	34
2.11	Commercial seasonal load profile.	34
2.12	Commercial monthly load profile.	35
2.13	Industrial annual active power load profile.	36
2.14	Industrial daily active and reactive power load profile.	36
2.15	Industrial seasonal active power load profile.	37
2.16	Industrial monthly active and reactive consumption load profile.	37
2.17	Power factor of Industrial load.	38
2.18	Hospital annual peak and average load profile.	38
2.19	Hospital daily load profile.	39
2.20	Hospital seasonal load profile.	39

2.21	Hospital monthly load profile.	40
2.22	Monthly demand factor.	41
3.1	Microgrid configuration with Distributed Energy Resources (DERs) in the rectangular.	44
3.2	Average hourly Scaled irradiance per month.	49
3.3	Annual Temperature in Dhahran.	49
3.4	Temperature histogram of three different months.	50
3.5	Monthly PV energy output with and without the effect of temperature.	51
3.6	Wind turbine power curve [4].	52
3.7	Vestas wind turbine power curve [5].	54
3.8	Wind speed and direction at 100m altitude.	55
3.9	Wind speed and direction at 50m altitude.	55
3.10	Wind speed and direction at 5m altitude.	56
3.11	Average monthly wind speed at different altitudes.	56
3.12	Monthly wind energy output.	57
4.1	Configuration of the proposed microgrid test-bed.	62
4.2	PV hourly generation on 28 th of June.	64
4.3	Wind hourly generation on 28 th of June.	64
4.4	Hourly load profiles on 28 th of June.	65
4.5	Aggregated hourly load and generation of the MG test-bed on 28 th of June.	66
4.6	Aggregated annual day by day load and generation of the MG test-bed.	66
4.7	One line diagram of the MG test-bed.	68
4.8	Flowchart of MG test-bed operating principle.	70
4.9	Running of case 1.	72
4.10	Running of case 1, battery response.	72
4.11	Running of case 2.	73
4.12	Running of case 2, battery response.	73
4.13	Running of case 3.	74

4.14	Running of case 3, battery response.	75
4.15	Running of case 4.	76
4.16	Running of case 4, battery response.	76
4.17	Running of case 4, industrial load.	77
4.18	Running of case 5.	77
4.19	Running of case 5, battery response.	78
4.20	Running of case 6.	78
4.21	Running of case 6, battery response.	79
4.22	Running of case 7.	79
4.23	Running of case 7, battery response.	80
4.24	Running of case 8.	81
4.25	Running of case 8, battery response.	81
5.1	Multiple input, multiple output two layers feed-forward computational topology.	88
5.2	Flowchart of the proposed flexible Load Priority List (LPL).	89
5.3	Priority list when $t = 15$	94
5.4	Priority list when $t = 60$	94
5.5	Priority list when $t = 136$	94
5.6	Priority list when $t = 156$	95
5.7	Priority list when $t = 160$	95
5.8	Network Layers	96
5.9	Gradient of the neural network	96
5.10	Regression of the neural network	96
5.11	Performance of the neural network	97
6.1	Peak shaving	99
6.2	Valley filling	99
6.3	Peak shifting	99
6.4	Fuzzy Logic (FL) mapping of input and output spaces.	101
6.5	Case 1: FL input and output variables.	105

6.6 Case 1: Membership functions of the FL input. 106

6.7 Case 1: Membership function of the FL output. 106

6.8 Case 1: MG Load and generation before and after DR. 106

6.9 Case 1: MG Loads before and after DR 107

6.10 Case 1: Percentage of curtailment. 107

6.11 Case 1: Surface of the FL rules. 107

6.12 Case 1: MG test-bed response to the DSM. 108

6.13 Case 1: MG test-bed battery response to the DSM. 108

6.14 Case 2: FL input and output variables. 110

6.15 Case 2: Membership functions of the FL input. 111

6.16 Case 2: Membership functions of the FL output. 111

6.17 Case 2: MG Load and generation before and after DR. 111

6.18 Case 2: MG Loads before and after DR 112

6.19 Case 2: Priority of each load category. 112

6.20 Case 2: Percentage of curtailment of each load category. 112

6.21 Case 2: Load profile of the four load types before and after Demand
Side Management (DSM). 113

6.22 Case 2: Surface of the FL rules with time as x-axis. 113

6.23 Case 2: Surface of the FL rules with priority as x-axis. 113

6.24 Case 2: MG test-bed response to the DSM. 114

6.25 Case 2: MG test-bed battery response to the DSM. 114

6.26 MG Loads before and after peak shaving. 116

6.27 Residential load peak shaving. 116

6.28 Commercial load peak shaving. 116

6.29 Industrial load peak shaving. 117

6.30 Hospital load peak shaving. 117

6.31 Case 3: MG test-bed response to the DSM. 118

6.32 Case 3: MG test-bed battery response to the DSM. 118

6.33 MG Loads before and after peak shifting. 119

6.34 Residential load peak shifting. 119

6.35	Commercial load peak shifting.	119
6.36	Industrial load peak shifting.	120
6.37	Hospital load peak shaving.	120
6.38	Case 4: MG test-bed response to the DSM.	121
6.39	Case 4: MG test-bed battery response to the DSM.	121
6.40	MG Loads before and after peak shaving.	122
6.41	Residential load peak shaving.	122
6.42	Commercial load peak shaving.	122
6.43	Industrial load peak shaving.	123
6.44	Hospital load peak shaving.	123
6.45	Residential AC demand response FL map.	125
6.46	Inputs membership functions.	125
6.47	Outputs membership functions.	125
6.48	Profile of three houses before and after AC DSM.	126
6.49	Aggregated profile of the three houses before and after AC DSM.	126
6.50	Case 6: MG test-bed response to the DSM.	126
6.51	Case 6: MG test-bed battery response to the DSM.	127
7.1	Hybrid AC/DC microgrid configuration.	129
A.1	KFUP2MG microgrid.	153
A.2	Load and renewable generation from m.file	154
A.3	Battery controller	154
A.4	Battery ON or OFF trigger	155
A.5	Battery dynamics 1	155
A.6	Battery dynamics 2	156
A.7	Scopes to simulate the microgrid system	156

NOMENCLATURE

Indices:

b	Index of the battery
d	Index of the device used
H	Height
i	Index of type of renewable energy generation
I	Index of device idle mode
n	Total investment life
r	Rated value
R	Index of device running mode
s	Index of season of the year
STC	Standard testing condition
t	Hour
z	Index of house number

Parameters and constants:

α	Wind shear exponent
A	Area

C_P	wind maximum power coefficient
$C_{utility}$	Cost of utility power
C_1, C_2, C_3	1st, 2nd and 3rd loans, respectively
ΔT	Time spent in charging and discharging the battery
$\eta_{charge}, \eta_{discharge}$	Battery charging and discharging efficiency, respectively
η_r	Reference efficiency of PV
L_M, L_T	Derate factor of PV connections and sun-tracking, respectively
L_M, L_R	Derate factor of PV mismatch and nameplate DC rating, respectively
L_S, L_D, L_A	Derate factor of PV soiling, shading and aging, respectively
n_1, n_2, n_3	1st, 2nd and 3rd loan term
OM	Percentage of operation and maintenance cost of the capital cost
q	Number of units in a household
r_d, r_{d0}	Discount rate and equivalent discount rate, respectively
r_{inf}	Inflation rate
r_{int}, r_{int0}	Interest rate and equivalent interest rate, respectively
ρ	Air density
σ	Latitude
$T_{LOW}, T_{Medium}, T_{High}$	Low, medium and high priced tariff of utility power

Variables:

E_b	Stored energy in the battery
E^d	Average energy consumed by a device

GHI	Global horizontal irradiance
IRR	Solar radiation incident on PV
I_{sc}	Short circuit current
$P_{battery}$	Battery power
$P_b^{charge}, P_b^{discharge}$	Battery charging and discharging power, respectively
P_{Cu}	Curtailed house power
P_{DER}	Power of distributed energy resources
P_{Diff}	Power difference between microgrid supply and demand
P_H, P_S	Normal and scaled house power, respectively
P_{load}	Load power
P_{MPP}	Drop in power due to temperature effect
P_{RES}	Power of renewable energy resource
$P_{utility}$	Utility power
$P_{PV,r}, P_{PV}$	Rated and actual PV output power, respectively
$P_{PV,T}$	Actual PV output power considering temperature effect
$P_{wind,r}, P_{wind}$	Rated and actual wind output power, respectively
PWF, CRF	Present worth and capital recovery factors, respectively
S, P, Q	Apparent, active and reactive power, respectively
SoC	State of charge of the battery
S_r	Standard solar irradiance
T	Temperature

TOU^d	Time of use of a device
μ_L	Fuzzy logic membership function
ν	Wind speed
ν_c, ν_r, ν_f	Cut-in, rated and cut-off wind speed, respectively
V_{oc}	Open circuit voltage
W_I^d, W_R^d	Wattage consumption in device idle-mode and running mode, respectively
x_R^d, x_I^d	Percentage of daily run time and idle time of the device, respectively
X, Y	Priority list training input and output, respectively

Symbols:

avg	Average
$COMM$	Commercial load
$Diff$	Difference
HOS	Hospital load
IND	Industrial load
L	Fuzzy set
min	Maximum
min	Minimum
$O\&M$	Operation and maintenance cost
RES	Residential load
TAX	TAX

LIST OF ABBREVIATIONS

AC	Alternating Current
AMI	Advanced Metering Infrastructure
ANN	Artificial Neural Network
BESS	Battery Energy Storage System
DC	Direct Current
DER	Distributed Energy Resources
DG	Distributed Generation
DLC	Direct Load Control
DR	Demand Response
DSM	Demand Side Management
EA	Evolutionary Algorithms
EMS	Energy Management System
ESS	Energy Storage System
EVs	Electric Vehicles
FIL	Fuzzy Inference Logic
FL	Fuzzy Logic

IEEE	Institute of Electric and Electronics Engineers
KSA	Kingdom of Saudi Arabia
LM	Load Modeling
LPL	Load Priority List
MF	Membership Function
MG	Microgrid
MPPT	Maximum Power Point Tracking
PCC	Point of Common Coupling
PF	Power Factor
PSO	Particle Swarm Optimization
PV	Photovoltaics
RCGA	Real-Coded Genetic Algorithm
RES	Renewable Energy Sources
SAIDI	System Average Interruption Duration Index
SAIFI	System Average Interruption Frequency Index
SEC	Saudi Electricity Company
SoC	State of Charge
WT	Wind Turbine

THESIS ABSTRACT

NAME: Ahmed Saleh Ahmed Al-Ahmed

TITLE OF STUDY: Integrated Energy Management System for Microgrids with Hybrid Renewable Generation, Energy Storage and Controllable Loads

MAJOR FIELD: Electrical Engineering

DATE OF DEGREE: May 2019

The mounting number of world population and the corresponding swelling demand and reliance on electrical energy have surfaced the necessity of upgrading the current power system into a more flexible, resilient and smarter network. Microgrids avail a promising new concept that aims to encourage and facilitate the integration of renewable energy resources, energy storage systems and demand-side management. However, several hitches are objecting the way toward reposing microgrids. The lack of test system designs with real data that are capable of integrating and managing energy resources restrained researchers from appropriately bench-mark their findings. The amount of research on microgrid load side is very minimal compared to studies on control, generation or self-healing of microgrids. Furthermore, usually loads in

microgrid studies are not diverse and possess an equivalent importance level, or in the best case a predefined fixed load priority list.

In this thesis, an energy management system microgrid test-bed will be designed. Renewable Energy Resources (RES), Energy Storage System (ESS) and four load categories including residential, commercial, industrial and a hospital will be integrated into the system. Real and local data is considered for the design to enhance the practicality of the study. The energy management system utilizes intelligence control techniques mainly Artificial Neural Networks (ANN) and Fuzzy Inference System (FIS) to flexibly prioritize the demands and efficiently balance the microgrid local generation, storage, loads and transaction with the main grid. An incentive-based feasibility study of a hybrid DC/AC microgrid is evaluated and further compared with the proposed test system.

ملخص الرسالة

الاسم: أحمد بن صالح أحمد الأحمد

عنوان الدراسة: الإدارة التكاملية لطاقة الشبكات الذكية المزودة بالطاقة المتجددة وتقنيات التخزين والأحمال القابلة للتحكم

التخصص: الهندسة الكهربائية

تاريخ الدرجة العلمية: شعبان، ١٤٤٠

يشهد العالم تطوراً سريعاً في أعداد السكان وبالتالي ارتفاعاً مُتّرداً في الطلب على الطاقة الكهربائية التي أصبحت تستخدم في جميع مناح الحياة. هذا الاستعمال المفرط للطاقة الكهربائية أدى إلى زيادة الضغط على الشبكات الكهربائية الحالية مما أدى إلى تدهور موثوقيتها وارتفاع تكاليف صيانتها. تأتي الشبكات الكهربائية الذكية (Smart Microgrids) كعلاج ناجح لتخفيف الضغط على الشبكة ورفع قابليتها لتكامل مصادر الطاقة المتجددة ومصادر التخزين والأحمال غير الاعتيادية كالسيارات الكهربائية (Electric Vehicles). لذلك، وانطلاقاً من الإيمان بأهمية هذه الشبكات، نُشرت العديد من الأبحاث في هذا المجال ولكن معظمها تفتقر لوجود منصة فعالة تُطبّق الدراسات عليها وتُقارن فيها مع الدراسات الأخرى. إضافة إلى أن الإدارة المثلى لهذه الطاقة تتطلب توفر معلومات فعلية لأحمال حقيقية كي تعزز من اعتمادية الدراسة.

تعتمد هذه الدراسة على تصميم وإنشاء شبكة فاعلة ومتكاملة لإدارة الطاقة في الشبكات الذكية. هذه الشبكة تحتوي على الطاقة الكهروضوئية وطاقة الرياح وأحدث وسائل تخزين الكهرباء بالإضافة إلى قدرتها على إزاحة الأحمال لضمان استمرارية الشبكة وعدم انقطاعها وزيادة كفاءتها. كذلك الدراسة تشمل فئات مختلفة من الأحمال كالأحمال السكنية، الصناعية والتجارية والأحمال الغير قابلة للانقطاع كالمستشفيات. تستخدم هذه الدراسة أدوات التحكم الذكي كتقنية شبكة الأعصاب الصناعية (Artificial Neural Network) ونظام المنطق الضبابي (Fuzzy Inference System) هادفةً إلى تحقيق التحكم الذكي بأحمال هذه الشبكة ومولداتها وتبادل الطاقة بينها وبين الشبكة الأم. ستخدم هذه الدراسة بمناقشة نظام حوافز للتحقق من جدوى الشبكات الهجينة بدل الشبكات ذات التيار المتردد (Alternating Current).

نتائج الدراسة أثبتت كفاءة قدرة الشبكة الذكية المقترحة على الموازنة بين عرض الكهرباء وطلبه وكذلك قدرة الشبكة على تخفيض التكاليف التي يكون معظمها بسبب شراء الطاقة في أوقات الذروة من الشبكة الأساسية لعدم قدرة الشبكة الصغيرة على توفير الكهرباء الكافي لأحمالها. أثبتت النتائج كذلك قدرة تقنية التحكم بالأحمال على ترتيب أولويات إزاحة الأحمال بحيث لا تلمس الأحمال ذات الأهمية القصوى كالمستشفيات ومحطات الإطفاء ومراكز المعلومات الحيوية.

CHAPTER 1

INTRODUCTION

In this chapter, a thorough introductory material covering the thesis aspects will be presented to prepare the reader with an adequate background about the importance of the subject and the proposed contribution in the thesis. Section.1.1 gives a general introduction about the topic. Section.1.2 states the motivations behind tackling the specified problem and correspondingly section.1.3 lists the desired objectives. Lastly, Sections.1.4 and 1.6 contain the background and the suggested thesis structure, respectively.

1.1 Introduction

The rapid expansion of power systems and the diversity of power generation methods have surfaced the necessity of improving the current conventional electrical network to a smarter, more reliable and more controllable one. The typical grid has witnessed minor changes in the previous decades. However, the spiking increase and variations of generation methods and the introduction of new demand forms such as Renewable

Energy Sources (RES) and Electric Vehicles (EVs) have elevated the need of revolutionizing the existing grid into a more flexible and intelligent one; microgrids. This transition is not as easy as it sounds, since power flow schemes, reliability evaluation, and energy management systems are now much more complicated to be conducted. To build a reliable and efficient microgrid that include DER, Energy Storage System (ESS) and DSM, a precise, fast and intelligent energy management system is required.

Many Microgrids (MGs) definitions have been reciprocated in the literature [6], however a widely used one was introduced by the International Council on Large Electric Systems CIGRE C6.22 working group states that microgrids are "electricity distribution systems containing loads and distributed energy resources, (such as distributed generators, storage devices, or controllable loads) that can be operated in a controlled, coordinated way either while connected to the main power network or while islanded" [7]. The definitions of microgrids could vary between one entity to another but what still holds is that MG is a flexible, highly reliable, greener and controllable source of electricity. Many drivers motivated the adoption of the microgrid concept; these include:

1. Facilitating higher renewable energy penetration.
2. Ability of robust control of loads, generation and pricing.
3. Enhanced system reliability and power quality.
4. Reduced line losses by decentralization.

5. Ability to operate without connection to the main grid (Islanded mode).
6. Incorporation of diverse load categories.
7. Ability of outage management, fault isolation, and smart self-healing.
8. Demand side management and energy sustainability.
9. Decreased energy prices and encouragement of competitive multi-player market.
10. Reduction of pollutant deposition such as NO_2 , CO , SO_2 and CO_2 . [8].
11. Achieving utility unbundling and system restructuring.

However, several obstacles are facing the proper realization of microgrids goals. For example, the lack of microgrid test beds with real and local load and RES data, where researchers can benchmark their findings. Also, when tackled in the literature, microgrid demands are most of the time limited to one or two load categories, which in turn reduces the practicality of the findings and the eventual implementation of the conducted research to the real case situation. Furthermore, the efficient and safe operation and control of microgrids demands and DER in both on and off grid mode is an area that should be subjected to further investigation and improvement.

Microgrids are established with different capabilities and objectives; hence several MG types exist. Remote microgrids are networks that do not have a point of common coupling with the grid; thus they are continuously operated in the islanded mode. They provide higher information security since there is less or no interactions with other systems, but the reliability of the system is less than a grid-tied microgrid due to the inability of energy transaction [9],[10],[11]. Furthermore, a customer microgrid

[12] is a network that exists after a single Point of Common Coupling (PCC) with a self-controlled nature. Such types of microgrids are not highly regulated by utility standards as they have clear geographical boundaries. They are sometimes referred to as true microgrids. Utility microgrids, however, come as part of the main grid and are highly operated and governed by utility standards. These microgrids do not necessarily have a single point of common coupling with the grid, and they are usually capable of running on grid-tied and islanded operation [13],[14]. Lastly, virtual microgrids,[15], are those with DER scattered in a grid but coordinated together to supply the grid as a virtual one entity.

The research on microgrids and their feasibility need more collaborations between industry and academia to address the various issues. Among them is the lack of viable microgrid test systems that be used by researchers to benchmark their ideas. Furthermore, the microgrid concept has to be generalized to include more load categories that are Residential, commercial, governmental and industrial. Since microgrids are intelligent networks, smart Energy Management System (EMS) should be achieved to ensure a smooth operation of the MG and optimized transaction with the utility. The microgrid also has to be able to achieve a successful self-restoration by taking into account the load priorities and criticalities at different times and seasons. Lastly, more economical studies on the best MG configuration should be conducted, i.e. Direct Current (DC) MG, Alternating Current (AC) MG and hybrid AC-DC MG.

1.2 Thesis Motivation

“Microgrids are making headlines as well as headaches,” Jared Smith, a consultant at PA consulting group [16]. It is a fact that microgrids bring enormous advantages to the existing power systems and costumers as was discussed in 1.1, however, there are many hurdles that should be solved to ensure the proper deployment of MGs. The major components of MGs are distributed generation (DG), loads, storage devices, smart controllers and switches and point of common coupling (PCC). The design, control, and arrangements of these components can pose considerable challenges. How are the loads modeled and what kind of load profiles does the system have and accordingly how much renewable generation capacity has to be installed. Also, due to the intermittent behavior of renewables, a backup system is required. The back-up system may be batteries, super-capacitors, diesel generators or any other ESS. Microgrids usually have limited and intermittent energy sources; thus one of the key aspects of any microgrid is the load management and control, which enables system operators to play with the other side of the equation instead of adding costly extra generation capacity or larger cable and transformer ratings. An integrated EMS in microgrids will ensure that all local generation sources and loads are in good harmony with the main grid and that demand and supply are balanced at all times. Although MGs enhance the reliability of power systems in general, they some time contribute to deteriorating it. The huge addition of non-dispatchable energy sources such as PV and wind may introduce more frequent failures due to the unbalance between power output and loads. Moreover, the variation of the operation principle of the various energy sources can be troublesome

in case of switching or reconfiguration. All of these issues should be solved and further tested by using microgrid test beds that are capable of simulating the real situation and outputting the vital indices that guarantee the safe operation of the MG. As a result of the previous issues, the microgrid configuration should be studied, proposed and eventually implemented. With the growing number of DC-based loads such DC Air conditioners (ACs), EVs and household electronic devices as well as the existing of DC-based DERs, the DC and hybrid DC-AC microgrid connections should be studied with more depth. Feasibility studies should be done on these configurations to verify their economic benefits to the customer and the system operator.

1.3 Objectives

Driven by the gaps in the subject discussed in 1.1 and 1.2, this thesis aims to tackle and achieve the following primary objectives:

1. Provide a detailed literature survey about the discussed topics. For example, microgrids, renewable energy, energy storage systems, load models, load priority list and DSM.
2. Modeling of microgrid demands using local and real load data from Saudi Arabia. Four load types are modeled including, residential, commercial, industrial and hospital loads.
3. Modeling two microgrid renewable generation sources, which are PV and wind energy. Again, the raw data used to model generation is local and real data

from Saudi Arabia.

4. Installing a battery energy storage system to store excess energy and supply it back whenever an energy deficit in the microgrid occur.
5. Investigating the feasibility of a hybrid DC/AC microgrid configuration using the previously modeled demands, renewable generation and storage.
6. Proposing a microgrid testbed that will integrate the four load types, the hybrid renewable sources and the energy storage to achieve energy management and successful energy transaction with the main grid.
7. Test the microgrid testbed under different scenarios. Such as, battery sizing change, cloudy weather and faulty buses.
8. Proposing an intelligent flexible load priority list that ranks the microgrid loads based on the given time, available energy and reliability indices.
9. Incorporating the priority list with the microgrid testbed to achieve demand-side management that is aware of the importance of each load type.
10. Implementing and evaluating different DSM schemes on the microgrid testbed, which has the ability of load prioritization.

The structure of the thesis in solving the preceding objectives will be presented in

1.6.

1.4 Literature Review

This section will lay out a general background and literature review about the subject that will be discussed. Detailed and in-depth Literature surveys will take place locally in each section.

The rapid proliferation of population and accordingly the spiking increase of energy demand, as a result, have made the transformation to a smarter grid more important and serious than ever (Figure 1.1). Without the transformation, CO_2 emissions will continue rising to alarming levels as well the installed conventional capacity will no longer be able to meet the demand causing serious reliability issues and eventually widespread blackouts. The Kingdom of Saudi Arabia (KSA) is witnessing a swift growth in population and energy demand. The population of Saudi Arabia hit 33 million people in 2010 with a population growth of 20% between 2004 and 2010 [17]. MG technology in its large-scale version as we are proposing can be the headway to Saudi Arabian authorities to secure the system against this sudden swell. MG technology eases the incorporation of DER and DSM into the grid. In comparison to the centralized power system, the power generation in MGs is more reliable and resilient and has a higher redundancy; also the test and use of small-scale technologies in MGs are much more flexible. However, this will add up to the complexity of modeling MGs.

Generally, MGs are characterized as complex and dynamical networks that have bidirectional power flows [18]. However, these networks need more complex reliability analysis techniques and are difficult to optimize [19], [20]. The main aspects of interest

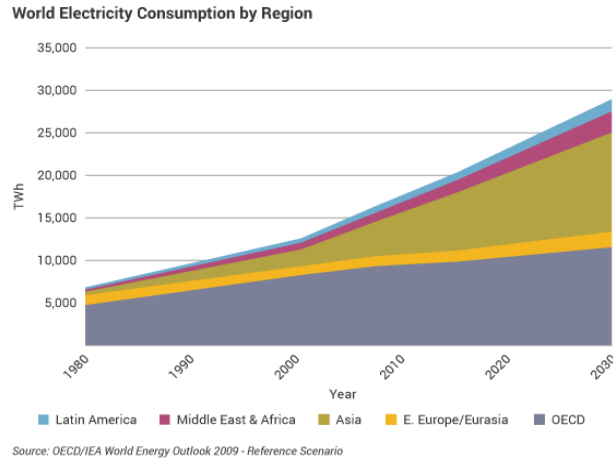


Figure 1.1: Ever increasing world electrical energy consumption [3]

in MG are integration of renewable energy resources, control of bidirectional energy flows, efficient fault restoration, and self-healing and DSM [21]. Smart restoration can be defined as bringing the power system from the faulty condition to a stable and normal one using intelligent monitoring and controlling systems, which continuously monitor, validate and test the operational mode of the grid and behave rapidly to secure the system before the loads are affected [22]. Power restoration in the MG is much more complicated than in the interconnected networks due to the existence of highly variable and uncontrollable distribution generation, distributed storage devices and variable loads [23]. While renewable generation can provide more power supply and relieve several environmental concerns, the use of conventional generation in MGs provides higher controllability, particularly in terms of maintaining the higher power quality and reliability levels. Energy storage can provide more flexibility and balance renewable generation, or provide a back-up supply, but it requires significant investments (as opposed to EV batteries, which can be used with minimal investments, only in bidirectional chargers).

DER can revolutionize the face of conventional energy generation. The Distributed Generation (DG) and energy storage devices are distributed close to the consumer premises, ensuring higher redundancy, less transmission losses, and carbon emissions. Distributed generation can take many forms. It can be renewable energy sources (RES) such as PV and wind or a conventional generation such as Diesel or coal. The generation of RES usually has very high variability. For example, the power generated from a Photovoltaics (PV) system can be very volatile, and it usually depends on the temperature, solar radiation, the efficiency of the panel and number of sun hours. Given the high input variabilities in PV over the course of the day, many papers in the literature tackled the design model of the different Maximum Power Point Tracking (MPPT) of the PV to find the optimal point to operate [24], [25], [26], [27], [28], [29], [30], [31], [32], [33], [34], [35], [36]. These PV control methods include: Incremental Conductance (IC) [26], Perturb and Observe (P&O) [33], Artificial Neural Network (ANN) [29], Genetic-based algorithm [34], sequential extremum seeking control (ESC) [35] and Fuzzy Inference Logic (FIL) [27]. The most widely used and simple methods are IC and P&O. Moreover, a MPPT that is based on intelligence control methods such as the fuzzy logic system (FLS) was offered and studied in the literature. Also, FLS and ANN can be complemented to give a versatile control method recognized as Adaptive Network-Based Fuzzy Inference System (ANFIS) [30], [31], [32]. In [36], a MPPT approach was realized using a meta-heuristic approach called Particle Swarm Optimization (PSO).

Generally, when the output of the PV system is not stable, the operation characteristics and performance of the network will be affected with further impact on

the connected local loads. Hence, to reduce the effect of the fluctuations, the excess generated power should be efficiently stored to be used in peak hours which in turn enhances the system overall performance and reliability. The ESS can prevent brown-outs and power outages, that may occur during attacks or severe climatic events [37]. In this context, several ESS can be incorporated with the PV panels. A thorough review of the energy storing in microgrids is illustrated in [38]. Systems with high power density and energy such as super-capacitors and batteries are extensively studied in the literature [38], [39], [40], [41].

Increased penetration levels of renewable-based generation resources, such as wind turbines and solar energy, pose several new challenges for network operation. While renewable resources can provide more sustainable energy supply and relieve several environmental concerns, they may also have a strong negative impact on the quality and reliability due to variations and uncertainties in their power outputs. As mentioned, energy storage can provide flexibility and balancing, as well as improved management of distribution networks, but this solution typically results in additional investment costs and reduced efficiency due to charging/discharging losses. Paper [42], attempts to reduce or ideally mitigate the effect of charging and discharging inefficiency by proposing an algorithm that ensures that the active power is balanced and hence minimizing power loss. Another primary challenge in integrating the energy storage devices is inaccurate modeling of the charging and discharging rates, based on different operational modes. In traditionally centralized grids, the actual locations of conventional energy generation, renewable generation, and energy consumption centers (e.g., big cities) are usually distant from each other. Therefore, the

need to coordinate conventional energy generation and consumption in the presence of continuous variations of renewable generation open a range of problems, ranging from optimal operation in steady state conditions, to system stability problems in case of faults and disturbances. In this context, several solutions have been introduced in the literature, including renewable energy forecasting [43], [44], [45], [46]. Given the non-dispatchable and stochastic nature of the RES, the installation of energy storage system is commonly considered, which stores the excess energy when the renewable generation is higher and then delivers energy when there is a deficit. Accordingly, it is expected that ESS would be a vital part in the promising smartgrid concept [47]. Certainly, in this case, a control strategy between the different ESS is needed to ensure smooth operation in the MG. One alternative solution is when renewable energy is generated and consumed in the local distributed network, as in the case of MGs, when the uncertainty of renewable resources is balanced locally, minimizing its negative impact on the reliability, stability, and quality of the whole transmission system . But, to achieve the best deployment of MGs, intelligent scheduling of renewable generation, storage and demand must be planned [48], [49], [50], [51]. Hence, intelligent generation-storage-load scheduling, which coordinates the microgrid and utility generation to coop with the capricious energy demand profile of MG loads is critical for the implementation of MGs. The proper scheduling of generation-side should meet two goals: 1) maintain the stability of the grid by ensuring that the combined generation from all units is equal to the aggregated electricity demand plus network losses, and 2) minimize the overall price of supplying the aggregated load, when MG control coordinates local generation and energy imported from the external grid. For achieving

these two goals, it has become imperative to develop innovative energy management and control optimization algorithms, to reduce the cost of energy when microgrids are adopted, particularly with more substantial penetration of renewable resources [52], [53]. As it is challenging to integrate variable energy resources in such problems in a uncomplicated manner, various examinations and optimization strategies are reported in, e.g., [54], [55], [56], [57], [58] and references therein.

Load Modeling (LM) is an essential step that has to be accurately designed before going to the DERs step. It is represented by a mathematical model that relates the voltage magnitude and frequency at the load bus-bar to the active and reactive power of the load or simply the current flowing into that load. The single load components at each load point are aggregated to shape the load profile. These components can range from lighting and electronic devices to motors and heaters. The load profile of a load can vary dramatically depending on chronological, environmental, religious and social factors.

To give more precise modeling, the loads are classified as static and dynamic loads. Static load models are those that relate the complex power at a bus to the voltage on that bus. From its name, the loads are represented in a time-invariant manner. A thorough look at static loads modeling and the approximation of dynamic modeling can be found in [59], [60]. Some famous models of the static representation include the ZIP model, which is a polynomial equation that relates the impedance (Z), current (I) and active power (P) in a bus. Exponential and frequency dependent models have also been investigated in the literature. Conversely, the dynamic load modeling captures the instantaneous real and reactive power as a function of real and past time instants of

the frequency and voltage at a bus [61]. The recognized dynamic load models include the induction motor (IM) model and the exponential recovery load model (ERL). A combination of a dynamic and static model is called a composite model.

Extended research in the field pointed out the importance of load modeling in a power system and its impact on the accuracy of the simulation of the dynamic performance of a system [62], [63], [64]. There are approximately three known load modeling approaches 1) component-based 2) measurement-based 3) a combination of the preceding two approaches (hybrid model). A review of load modeling is given in [65]. Component-based load modeling is a bottom-up method that aggregates the load information based on the composition of each load type and the characteristic of each load component. The component-based method was extensively studied in the literature [66], [67], [68], [69]. For example, in [66], the authors used component-based load modelling to reduce the error between reactive design and the actual real value. Their model engages quantitative analysis and test of a cluster of loads on a real configuration of a substation.

In [67], the measurement-based method is more widely used in MG given that the data can be taken from the distributed phasor measurement units (PMU). It relies on data acquisition devices that are mounted at different locations in the system. The advantage of this method is the real-time accurately acquired data that does not require any estimation or variation of variables and thus performs well in dynamic simulations. In [70], [71], [72], [73], [74], [75], measurement-based method was used at different voltage levels. In [70], the static and dynamic load model in grid-connected and islanded low-voltage (LV) microgrid was investigated. The model was developed

and then tested in a laboratory scale microgrid.

In [71], online measurement data from the Taiwan power system was gathered to derive, test and compare between different dynamic load models. The conducted numerical studies in the paper concluded that linear dynamic load models outperformed the nonlinear dynamic models when it comes to reactive power behavior modeling during disturbances. [72] utilizes the measurement-based method to build up a complete load model at the distribution level. The authors compared their model with a composite load model at transmission level and another model at the generation level. They showed that their model performs better in transient conditions. References [73] & [74], applied measurement-based dynamic load modelling using curve-fitting technique and vector-fitting technique ,respectively. [75] discusses residential microgrid scheduling by utilizing smart meters to come up with a temperature dependent thermal load model. Sensitivity analysis is implemented to reflect the impact of the uncertainties contained in the model.

A hybrid model was applied in [76], [77]. In [76], multiple data from single users is aggregated to generate the residential microgrid load profile. There are eight major electricity consumption (MEC) events, which are basically daytime, evening and long-running time events. When these events are aggregated, a residential house load profile is obtained. The model parameters for each event are acquired using Ant Colony Optimization (ACO) algorithm. The load modeling method was then validated using a real microgrid in Ohio, USA. While in [77], a dynamic equivalent active distribution network cell (ADNC) model was presented and examined. The model allows for more penetration of unconventional energy sources such as PV and wind in the distribution

network. The performance of the model was tested using the modified Institute of Electric and Electronics Engineers (IEEE) nine bus system during different levels of disturbances.

All in all, load modeling regained interests after the introduction of microgrid concepts which needs a new reformulation of previous load models in order to accommodate the different DER and the newly coming unconventional loads. Ultimately, the goal of load modeling in any system is to come up with a resilient and robust mathematical model that can ideally resemble the behavior of loads.

In accordance with the preceding literature about DER and LM, Demand Side Management (DSM) comes in between the two to match between load and generation. The article, [78], provides a very good overview about DSM and the challenges faced when incorporated with smart grids. There are different DSM schemes. Each one has certain advantages and drawbacks and mostly all of them require a well-established Advanced Metering Infrastructure (AMI). They vary in terms of reliability and the level of freedom given to the consumer. The lower the freedom is the higher the reliability. In this context, the most famous ones will be explained and further discussed (Figure 1.2).

- Direct Load Control DSM

The easiest, classic way to apply DSM is the Direct Load Control (DLC) method, in which costumers agree and enroll to be part of the demand management events. In fact, this method is the most reliable, since loads of these customers will be under the full control of the utility or the organizing entity. That is, the

utility can shed completely or curtail the load or shift it to another time depending on the situation. The enrolled costumers will be given certain incentives to encourage them to participate in such programs. In microgrid concept where higher controllability and strong information technology is achieved, demand response can be so specific. For example, sending a signal that will increase the temperature of the air conditioners in a certain area or shut down the clothes washer in a specified time period.

- Energy Efficiency DSM

This method is concerned with reducing the total system production costs and demand by increasing efficiency. Users who participate are entitled to using more efficient devices and appliances. The five-star energy efficiency model is an example of the scheme. This model has higher reliability than the coming two models, but it offers lesser freedom for the consumer.

- Price Responsive DSM

In this model, costumers can be part of the DSM program by responding to a certain signal or incentive that was sent at that particular hour. Costumers who meet the requirements and are willing to participate can benefit from the incentive given by the utility. Thus, this process is intended for short term response and it is obviously less reliable than the previous schemes since the users are not compelled to participate. Also, An example of this method is the time of use pricing and critical peak time pricing.

- Educational DSM

In contrast to DLC based DSM, the educational DSM approach is a voluntary one. It aims to raise education and awareness about the importance of energy conservation. Educational DSM is claimed to be effective for long term goals, other than rapid interventions. However, it is the least reliable one because users are not obliged to shed or curtail their loads. The users in the scheme are given full freedom on the usage of electricity.

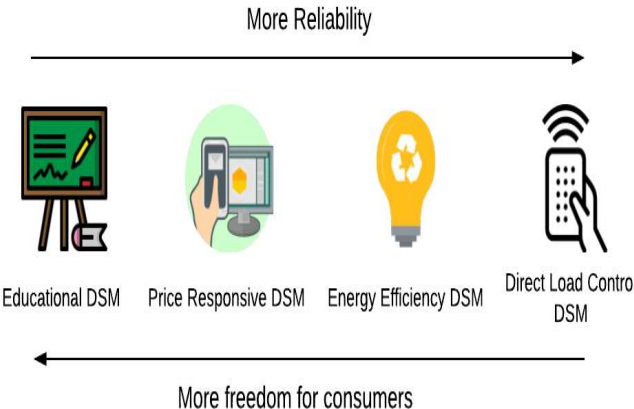


Figure 1.2: Demand Side Management Schemes

The objectives of the work in this context is to first build the test system with local and real energy sources and load data. The test system will be used to achieve and propose different DSM schemes and run the system after each scheme. An intelligent load priority list will be incorporated with the DSM. A feasibility study will be done on a hybrid DC/AC microgrid configuration to see if it can be a competitive option to the AC-based system.

1.5 Contributions

1. Model and design a microgrid test-bed with local and real loads and renewable energy sources data that will be utilized to realize the rest of the thesis goals. The test-bed and its raw data will also be available for researchers to benchmark their findings and improve the microgrid research quality in general.
2. Propose a flexible, intelligent load priority list for demand restoration, which will rank the testbed's different demand types into different priority levels based on the outage time, reliability indices and energy availability.
3. Propose different demand side management incorporated with the intelligent load priority list to optimize the microgrid transactions with the main grid increase its overall load factor.
4. Propose an incentive-based feasibility study of the microgrid test-bed when a hybrid AC/DC configuration is placed instead of the AC-based microgrid.

1.6 Thesis Structure

As stated in Section.1.5, the thesis aims to achieve four goals. A microgrid test-bed, which will be used for implementing other objectives and will be available for researchers to benchmark their ideas and findings. The second and third objectives are to propose an ANN based priority list that will be used as an input for the next step, which is proposing different DSM schemes. Furthermore, an Incentive-based economical feasibility study will be presented to compare between the AC microgrid

and the hybrid DC-AC microgrid.

Figure 1.3, shows the structure of this thesis. Firstly, the vital data required for modeling the loads and DGs is acquired from Research Institutes and Companies. The modeling of loads and the corresponding load profiles for different load categories is explained in chapter.2, while the modeling of the RES is shown in chapter.3. In section.3.4, a battery-based ESS will be sized in accordance with the available loads and generation. Chapter.4 sheds the light on the proposed AC microgrid test-bed that will be used as a study field for the remaining thesis contributions. The load priority list will be discussed in chapter.5. Based on the modeled loads, renewable energy sources, test system design and the load priority list, different load management schemes will be implemented and further evaluated. In chapter.7, the feasibility of a hybrid DC/AC microgrid will be studied. The sizing of DERs in the hybrid microgrid will differ from the sizing in the AC microgrid as our objectives are different in each of them.

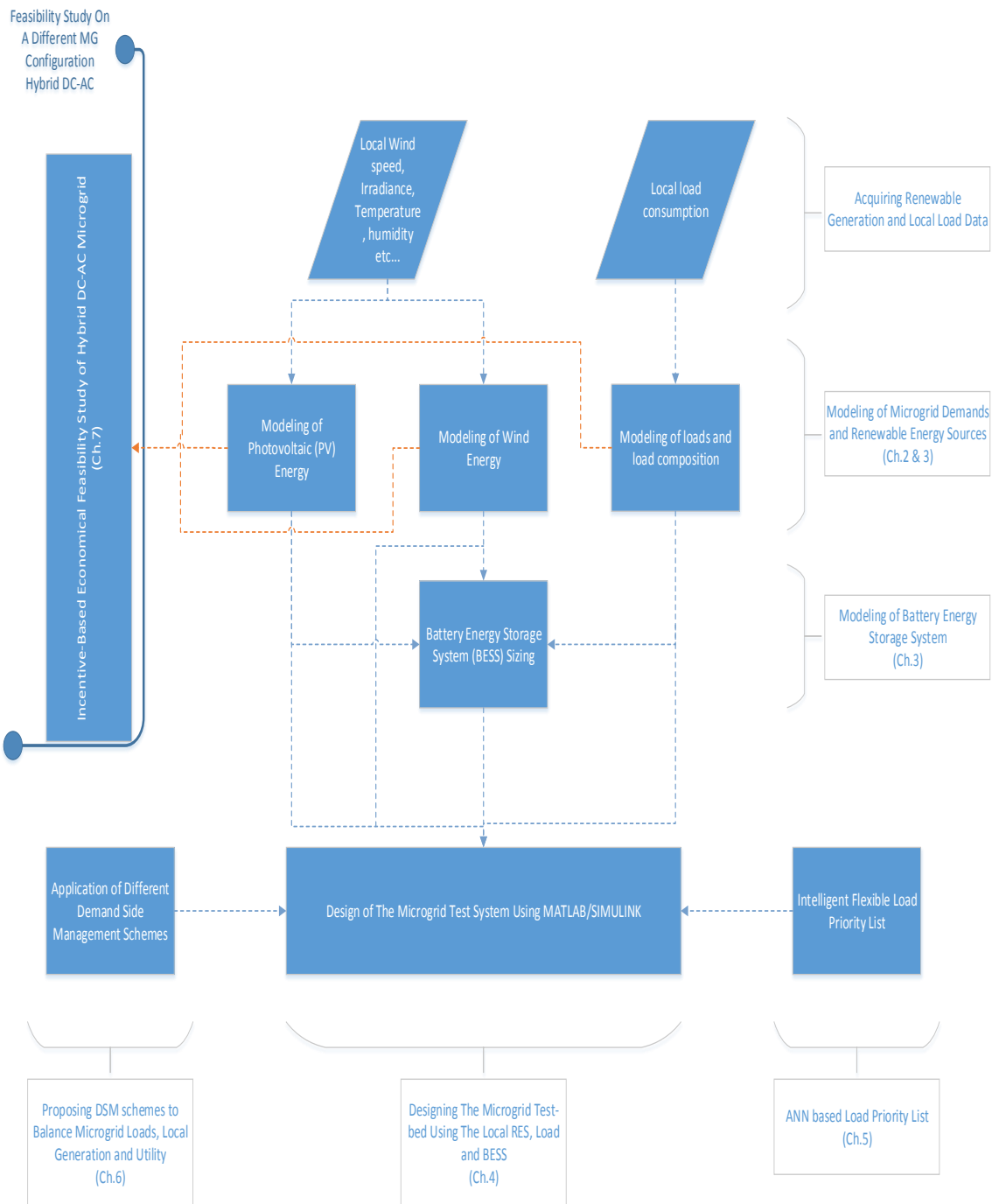


Figure 1.3: Structure and flow of the thesis

CHAPTER 2

MODELING OF MICROGRID DEMANDS AND CONTROLLABLE LOADS

In each network, there are different structure and composition of loads. Each load has to be accurately modeled by finding its monthly, daily, seasonal and annual profile. It is much more cost-effective for utilities to control the demand side rather than installing new generation units to be safe against load variations. However, the capricious variability of load profiles and the scarcity of research in the area have forced the utilities to relinquish demand-side management. In this work, we aim to generalize the microgrid concept to serve several loads at the same time. Residential, commercial, industrial and hospital load types will be modeled as shown in Figure 2.1. These load types offer a very wide range of load importance levels and different load profile characteristics as will be shown in the following sections. The modeling of the RES

and Battery Energy Storage System (BESS) will take place in the following chapter.

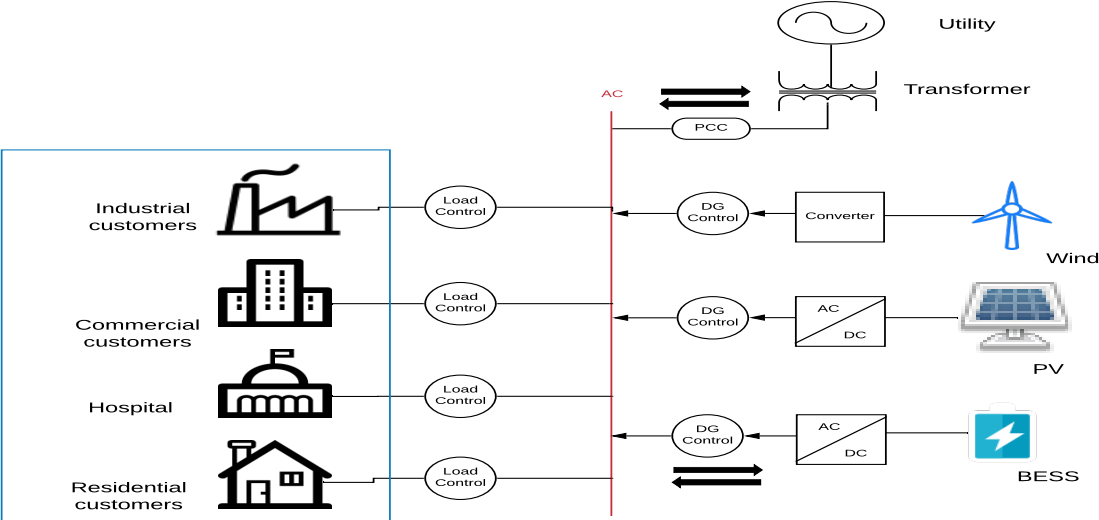


Figure 2.1: Microgrid configuration with the four load types in the rectangular.

To implement a proper sizing of Distributed Energy Resources (DERs) and calculate the efficiency of the microgrid, an accurate load modeling of the MG has to be formulated. To provide more practicality to the study, the load data was taken from the eastern region of Saudi Arabia, which is the largest area in KSA (Figure 2.2). Latitude and longitude of the location are 26.2361° N, 50.0393° E. The load data is acquired from SCADA systems for four distribution substations with four different load categories. A precise daily, weekly, seasonal and annual load profiles will be derived using MATLAB [79]. Each load profile is important to understand the load behaviour under different effects. For example, daily load profiles help us in understanding the daytime and evening variations of load consumption. Whereas, from the weekly load profile, the effect of weekdays and weekends can be observed. The monthly and annual load profiles can help us in exploring the implications of seasons

and vacations on the load profile. The load data specification is displayed in Table 2.1. It is observed that the Residential sector in KSA constitutes more than half of the total energy consumption. The Saudi electricity tariff has been just revised and the new figures are listed in Table 2.2.



Figure 2.2: The shaded region is the Eastern province in Saudi Arabia.

Table 2.1: Load data specification.

Classification	Ratings	Energy sale
Residential	69kV/13.8kV	52.3%
Commercial	69kV/13.8kV	14.5%
Industrial	69kV/13.8kV	19.3%
Governmental	69kV/13.8kV	13.9%

Table 2.2: Saudi electricity tariff [1]

Residential		Commercial		100 Halala= 1 SAR 1 SAR = 0.267\$
Tariff [Halala]	Consumption [KWh]	Tariff [Halala]	Consumption [KWh]	
18	1-6000	20	1-6000	
30	>6000	30	>6000	
Governmental		Industrial		
Tariff [Halala]	Consumption [KWh]	Tariff [Halala]	Consumption [KWh]	
32	No Limit	18	No Limit	

In this chapter, the modeling of the four load categories will be presented showing the annual, monthly, seasonal and daily load profiles. The composition of the resi-

dential load will be identified using a hybrid top-bottom and bottom-up approach. A literature review about the impact of load modeling on the system reliability and the application of DSM is placed in this chapter too. Some characteristics about the types of loads that will be studied are shown in Table 2.3.

Table 2.3: General characteristics of the studied load types.

Load Type	Controllability	Composition	Capacity	Variability
Residential	High	ACs, refrigerators, lighting, washers, etc..	Small	High
Commercial	High	ACs, lighting, elevators, coolers	Medium	High
Industrial	Low	furnaces, conveyor belts, ACs, lighting, etc..	High	Low
Hospital	Very low	ACs, medical devices and appliances, lighting	Varying	Low

2.1 Literature Review

Several papers in the literature used the load profiles to come up with efficient Demand Response (DR) programs. [80], studies the profile of three commercial users under the time of use pricing conditions and showed the profile before and after demand response. Moreover, [81] investigated the efficiency of AC and DC microgrids by using Queue theory to build up the load profile. The authors observed that load variations have a strong and direct effect on the overall microgrid efficiency. Authors in [53] derived accurate load profile for a building containing a restaurant and 12 apartments to optimize the cost of a microgrid. They found that it is better to mix residential and commercial load to increase the load factor and thus improve the price. A full literature review about load modeling can be found in section.1.4.

2.2 Microgrid Demand Modeling

2.2.1 Residential Load Modeling

The modeling of residential end users load is a very complex and time-consuming task since it is subjected to human behavior and living styles. Generally, the availability of the user and the probability of load activity exercised by the user are the two main factors that determine the shape of a residential load profile. This is called bottom-up approach load modeling which was discussed in the acquired residential data, the load profile will be built and then the power consumption of one unit will be calculated based on the average household consumption in Saudi Arabia. Then the load composition and percentage in the considered networks will be determined to achieve the objective of controllable loads.

The annual average and peak load profile are displayed in Figure 2.3. All figures were scaled as per the following equation:

$$Scaled\ KW = \frac{maximum\ average\ load}{load\ at\ every\ hour} \quad (2.1)$$

It is observed that consumption is highest during summer months. Later in this context, we will investigate the load composition that shaped this behavior. Moreover, the daily, weekly, monthly and seasonal residential load profile is shown in Figures.2.3, 2.4, 2.5 and 2.6. From Figure 2.4, we observe the difference in load between the AM and PM time. The residential loads in the AM time are not as high as PM time due to sleeping time. So most of the manually operated loads (i.e., oven, vacuum cleaner, and

TV) in this period are idle while the automatically and semi-automatically operated loads (i.e., refrigerator and air conditioner) are less affected by the factor of time. Figure 2.6 shows the monthly average and peak load of residential costumers. It is noted that the average load is approximately 86% of the peak load in most months. The effect of weather is clear in the summer period from late May to early September where AC loads spike the electricity usage to more than 130% between February and June. To address the acute effect of temperature, Figure 2.5 depicts the hourly load in four different days that resemble four different seasons: June the 28th, December the 30th, September the 25th and April the 1st corresponding to summer, winter, fall, and spring respectively. The effect of extreme weather conditions, where summer days can reach a temperature of 55° and -10° in winters, in Saudi Arabia is observable in Figure 2.5. Air conditioning, the absence of thermal insulation and heating loads in summer and winter respectively caused the increased power consumption in these seasons relative to spring and fall.

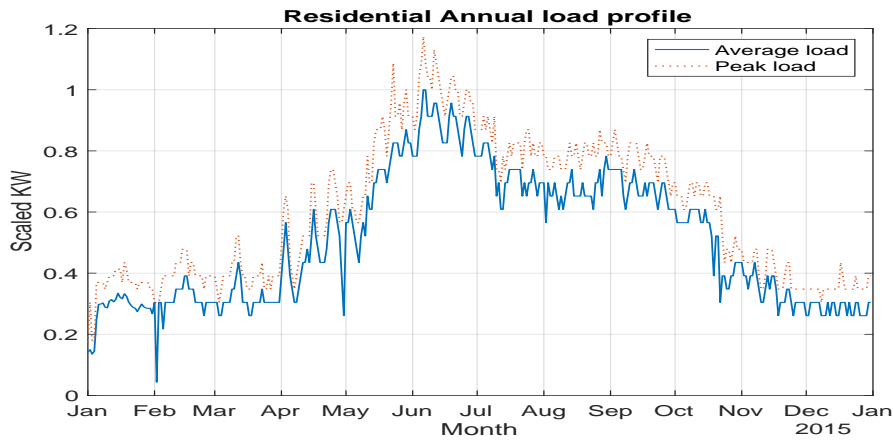


Figure 2.3: Residential annual load profile.

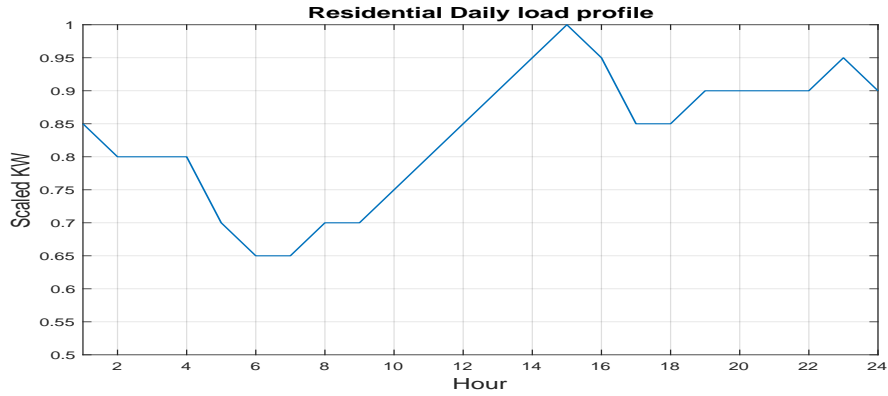


Figure 2.4: Residential hourly load profile.

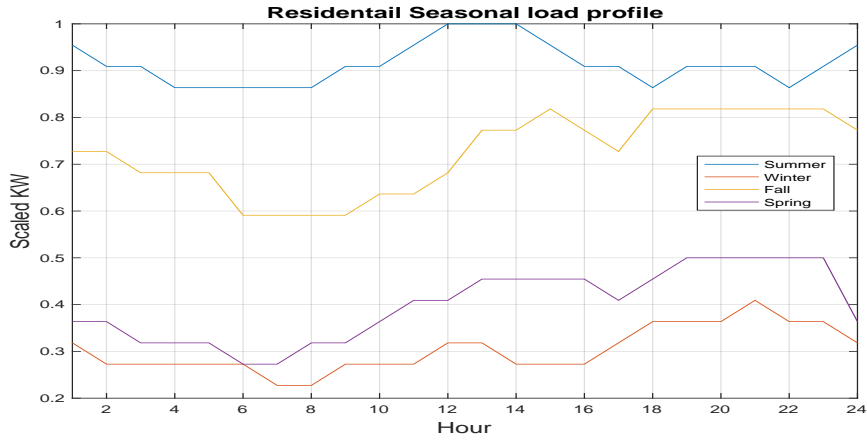


Figure 2.5: Residential seasonal load profile.

Typical Structure and Composition of Residential Loads

To apply demand side management, a precise specification of the load composition is important in order to know the contribution percentage of every device to the overall load profile. Data taken by the Saudi Arabian General Authority for Statistics (GAS) in 2016, shows the usage hours of different home appliances and devices per day [17] (Table 2.4). After applying the bottom-up approach by finding the rating and time of use for every home activity, we will now back-project these findings into the consumption that we got from the top-bottom approach that is from the substation

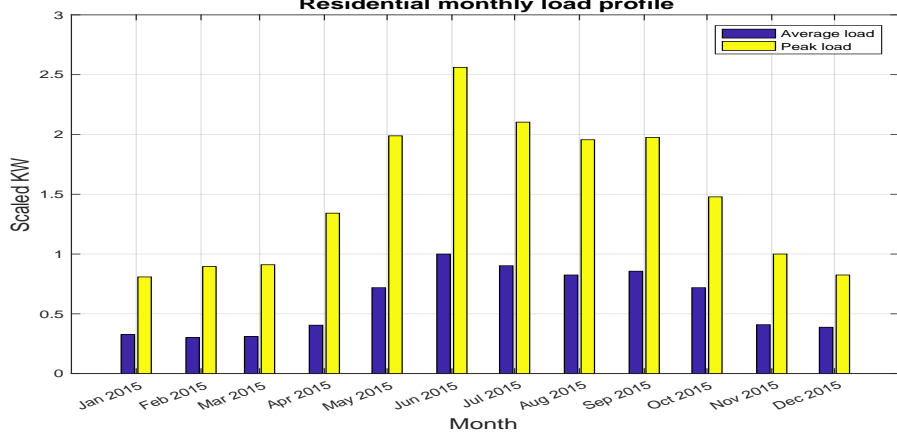


Figure 2.6: Residential monthly load profile.

to the load point. Using Table 2.4, equation 2.2 was applied to acquire the average summer and winter consumption.

$$E^d(s) = TOU^d(s) * q^d(s) * (W_R^d * x_R^d(s) + W_I^d * x_I^d(s)), s = 0, 1 \quad (2.2)$$

where 0 and 1 resembles winter and summer respectively. d is the device considered and TOU is the time of use in hours. x_R and x_I are the percentage of run-time and idle-time of the machine respectively. Similarly W_R and W_I are the wattage consumption in run-mode and idle-mode respectively. Lastly, q is the number of units of that appliance in a household.

After applying the preceding equation, we acquire the consumption of each load activity in summer and winter seasons (Table 2.5). The months from October to February will be considered as winter and the rest are considered as summer. In other words, the data were proved using both the top-bottom and bottom-up approaches. Interestingly the pie-charts in Figure 2.7 and Figure 2.8 show the percentage share

Table 2.4: Household activities and calculation parameters

Activity	TOU (winter)	TOU (summer)	number of units (winter)	number of units (summer)	Rating (W)	Idle rating (W)	Operation	Run-time (%)	Idle-time (%)
Heating (oil-filled)	8	1.5	2	1	1500	0	Semi Auto	0.5	0
Air conditioning	3	10	2	5	1800	100	Semi Auto	0.6	0.4
Water heating	14	4.7	3	1	1500	30	Auto	0.3	0.7
Water coolers	10	17	1	1	250	10	Auto	0.5	0.5
Water Bump (Dynamo)	1.5	2.1	1	1	250	0	Auto	1	0
Washing & Drying	1.3	1.9	2	2	2000	0	Semi Auto	1	0
Ironing	1	1.8	1	1	1000	0	Manual	1	0
Vacuum cleaning	1	1.3	1	1	1000	0	Manual	1	0
Cooking	1.6	1.4	1	1	2150	0	Semi Auto	1	0
Electric kettle	1.3	2	1	1	1800	0	Manual	1	0
Lighting	7.3	7.5	50	50	10	0	Manual	1	0
Food preservation	24	24	2	2	100	0	Auto	1	0
TV	5.3	5.9	1	2	120	13	Manual	1	0
PC	2.1	2.6	2	2	150	7.5	Manual	1	0
Gaming devices	2.6	3	4	4	30	7.5	Manual	1	0

of each home activity during summer and winter months. From Figure 2.8, it is observed that Air-conditioning (AC) loads sums up to 62% of the total load in summer months. This finding is proven as SEC announced a similar percentage on their reports [1]. AC loads shrink to only 11% in winter as the temperature goes down, thus the heating loads rise, and we found that water and ambient heating constitutes to 50% of the monthly winter demand. As an indicator of the accuracy of the composition percentages, we observe that lighting in winter represented 6% of the profile, while it was 4% in summer. The reason is that at winter the evening time is longer and even the day time is cloudy sometimes; therefore, lighting usage in the winter is higher than summer. Other activities such as washing/drying, ironing, and cleaning are pretty much similar. It is worth mentioning, that social behavior and psychological studies can also utilize these findings to investigate for example why in general people

are cooking in winters more than summer. These findings are the cornerstones of another contribution of this thesis, which is applying DSM.

Table 2.5: Summer and winter energy consumption per activity

Activity	Winter Energy Consumption (Wh/day)	Summer Energy Consumption (Wh/day)
Heating (oil-filled)	12000	1125
Air conditioning	6720	56000
Water heating	19782	2213.7
Water coolers	1300	2210
Water Bumb (Dynamo)	375	525
Washing & Drying	5200	7600
Ironing	1000	1800
Vacuum cleaning	1000	1300
Cooking	3440	3010
Electric kettle	2340	3600
Lighting	3650	3750
Food preservation	4800	4800
TV	636	1416
PC	630	780
Gaming devices	312	360
Total (KWh/month)	1895.55	2714.69

2.2.2 Commercial Load Modeling

Commercial loads such as shopping malls, restaurants, and multi-storey buildings are larger in scale than domestic loads. Due to the opening and closing times and the decreased intervention of human factors, commercial loads have a flatter profile which makes the tracing of the load behavior easier and more predictable. The commercial load profile simulated from real load data is shown in the following figures (Figures.2.9 - 2.11). From Figure 2.9, we notice that the commercial load profile is very similar

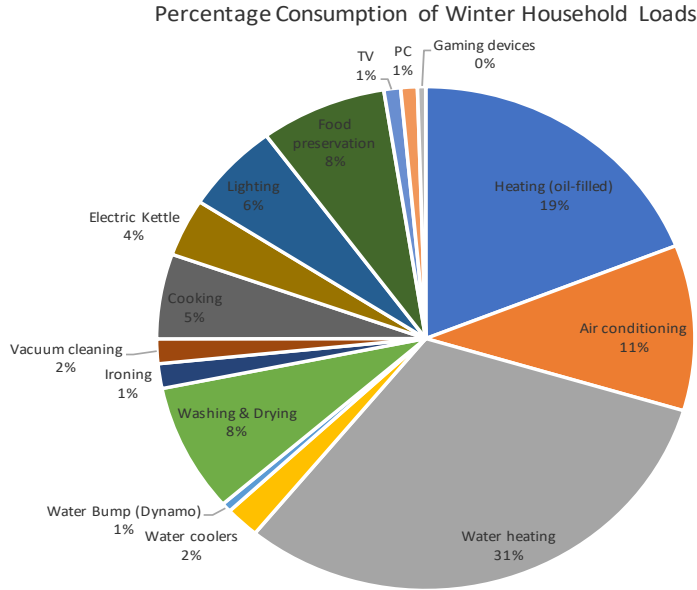


Figure 2.7: Percentage of household appliances in winter.

to the residential one in the sense that the hourly variations are high. The daily load profile, Figure 2.10, shows an interesting feature of commercial loads. The load from 11 PM to 6 AM is much less than the consumption during the rest of the day. This is obviously due to operating hours of shops, restaurants, and supermarkets. The curve suddenly increases after 6 AM and the steeply decreases after 10 PM. Again, the effect of seasons is clearly shown in Figure 2.12 and Figure 2.11, where the difference between summer and winter demand is huge which plays a major rule in effecting the utilities in terms of generation installation. This is one of the driving reasons for the consideration of demand-side management by power system operators which attempts to shift or shut some of the loads during the day to peak shave the demand curve and thus mitigating the need of building new generation units. The percentage increase in summer demand over winter is shown in equation 2.3 and it is presented that summer demands are 172% higher than winter demands.

Percentage Consumption of Summer Household Loads

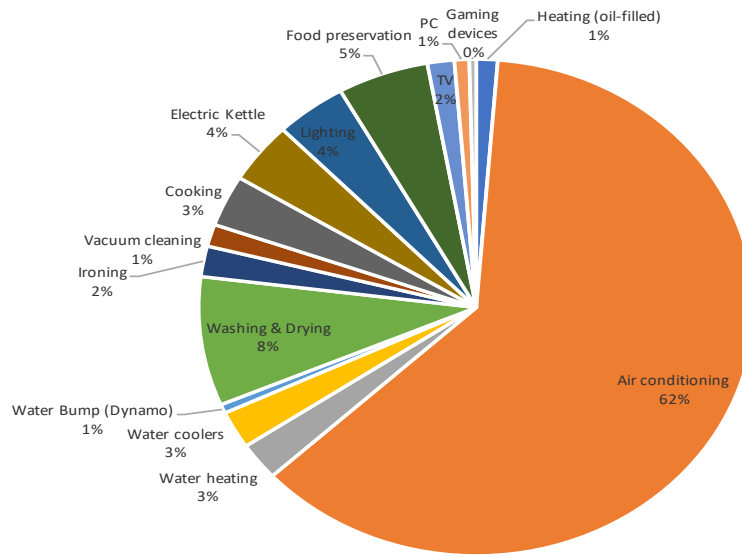


Figure 2.8: Percentage of household appliances in summer.

$$\begin{aligned}
 \text{Summer demand percentage increase} &= \frac{\text{Summer avg demand} - \text{Winter avg demand}}{\text{Winter avg demand}} \% \\
 &\approx \frac{60 - 22}{22} \approx 172\% \quad (2.3)
 \end{aligned}$$

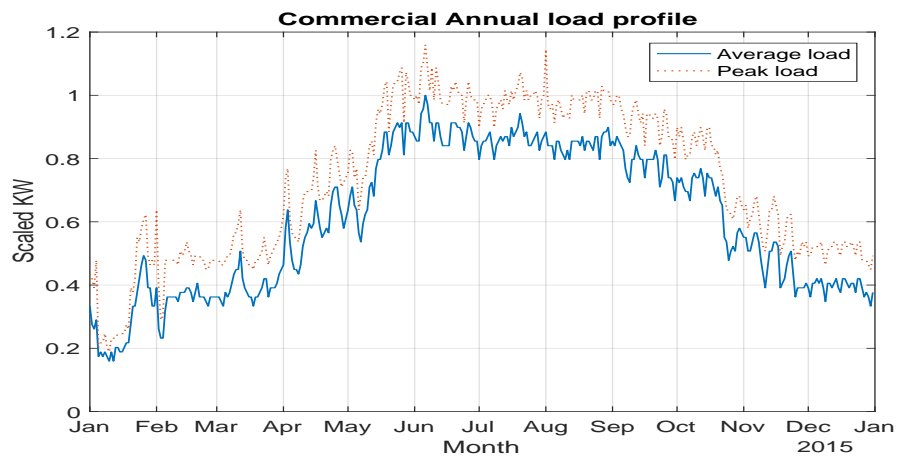


Figure 2.9: Commercial annual peak and average load profile.

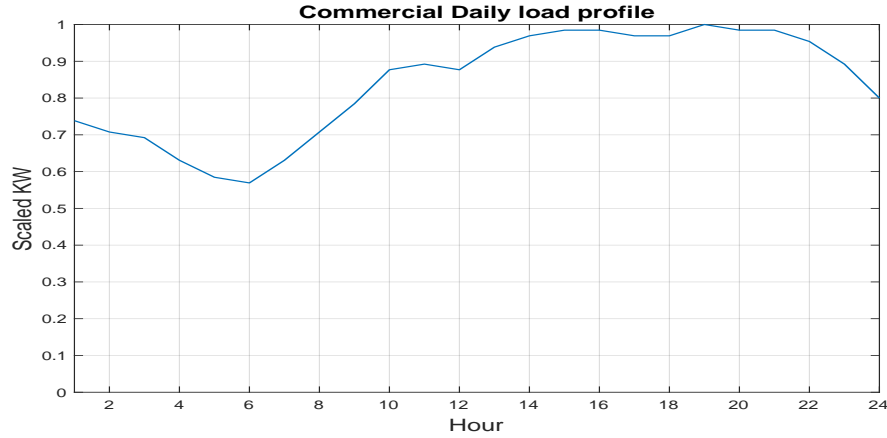


Figure 2.10: Commercial hourly load profile.

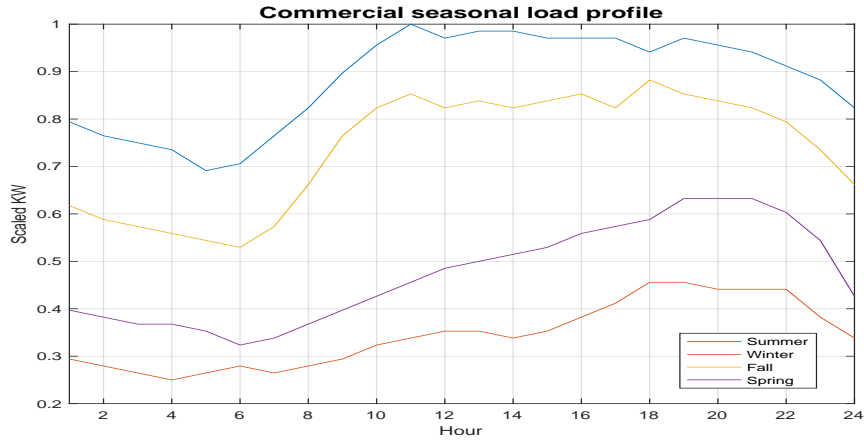


Figure 2.11: Commercial seasonal load profile.

2.2.3 Industrial Load Modeling

Most of today’s research about microgrid considers only the residential costumers which are not the real case and thus limiting the practicality of a microgrid study. However, for our proposed MG in Figure 1.1 we will assume that we have four load sectors. In this part, the industrial loads will be analyzed. The data is taken from the first industrial city in Dhahran, Saudi Arabia. Active and reactive power annual, monthly, seasonal and daily consumption is shown in the following figures (Figure 2.13 - 2.17). Figure 2.13, shows the annual active power consumption profile, respectively.

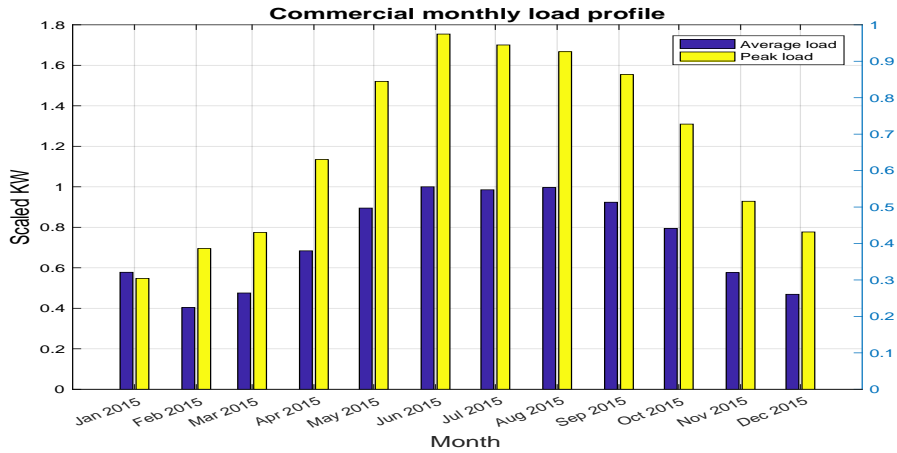


Figure 2.12: Commercial monthly load profile.

It is evident from the figure how industrial loads don't change much during the year. This is simply because the operation of industries is planned and scheduled during the day and on the long run during the year. Also, the factor of human interference is minimal and the operation is usually automated. Figure 2.15, shows how the seasonal factor diminished in the case of industrial loads. The summer consumption is higher by only 18% than the winter load. Reactive loads are considered in industrial loads because they have an effect on the overall load profile. The consumption of VARs is usually in the range of 25-45% of the consumption of the real load. Figure 2.14 shows the hourly active and reactive load profiles of industrial loads. Observe that the curve in the period from 1 AM to 6 AM is generally lower than the rest of the day where most industries are run. The monthly load profile in Figure 2.16 shows again how the effect of seasonal variation is minimal in industrial demands. Figure 2.17 shows the Power Factor (PF) of the industrial customers. From the PF figure, we observe that the power factor is in the range of 0.85 and it is usually higher than that in other load types such as residential and commercial, but for industrial loads and due to

the many induction machines, furnaces and other heat producing machines the power factor was affected.

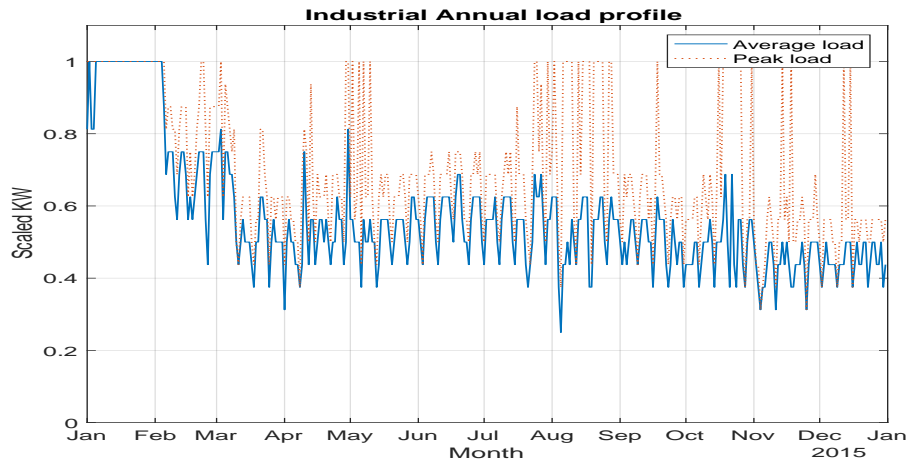


Figure 2.13: Industrial annual active power load profile.

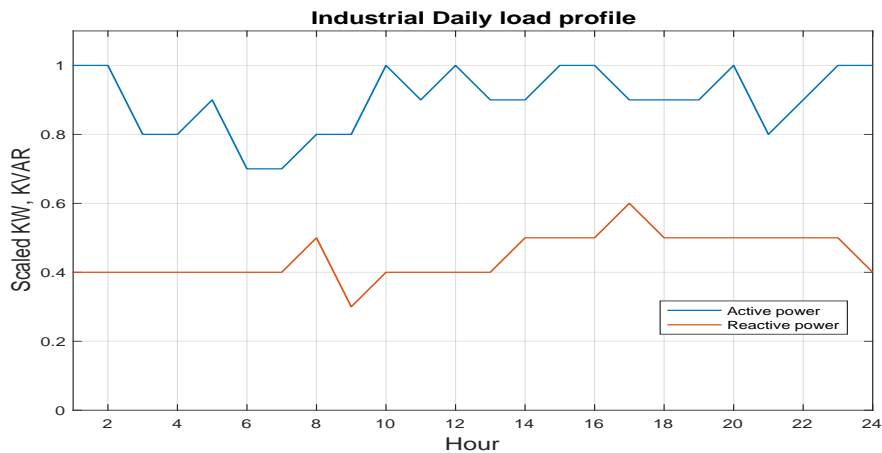


Figure 2.14: Industrial daily active and reactive power load profile.

2.2.4 Hospital Load Modeling

Our proposed microgrid testbed aims to increase the practicality of the microgrid concept by introducing different load types with different criticality levels. A local hospital data in the eastern province will be used in this study. The following figures

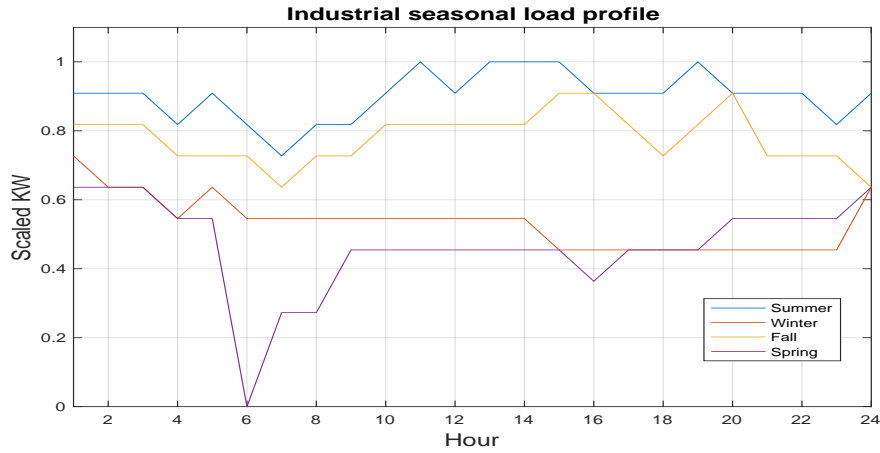


Figure 2.15: Industrial seasonal active power load profile.

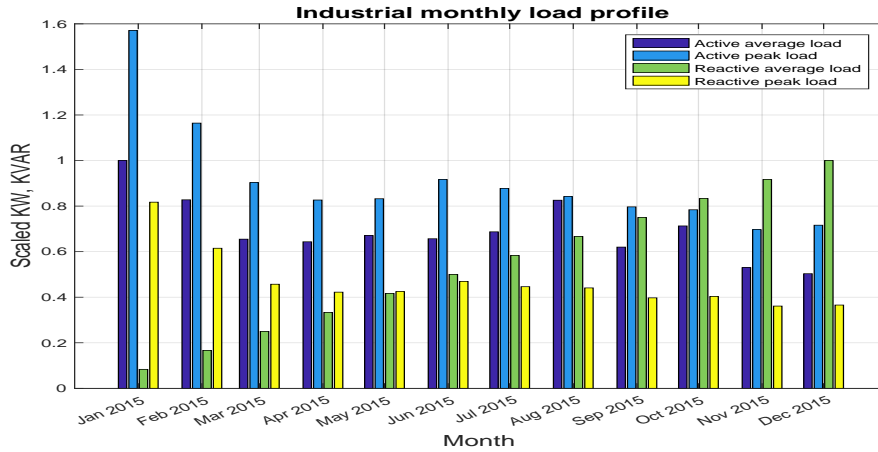


Figure 2.16: Industrial monthly active and reactive consumption load profile.

show the load profile of this governmental hospital (Figure 2.18 - 2.20). Figure 2.18, shows that there is a small difference between average and peak loads in hospitals and this is simply because hospitals are usually fully operated that they are less subjected to individual activities. It is also observed from Figure 2.18 that the load profile in hospitals is much flatter than commercial and residential loads. Figure 2.19, shows how small are the variations of the hospital load during the day. This is attributed to the fact that hospitals operate on a 24 hour shift, where the load at late night is not of a much different than the load in the daytime. The effect of seasons is shown

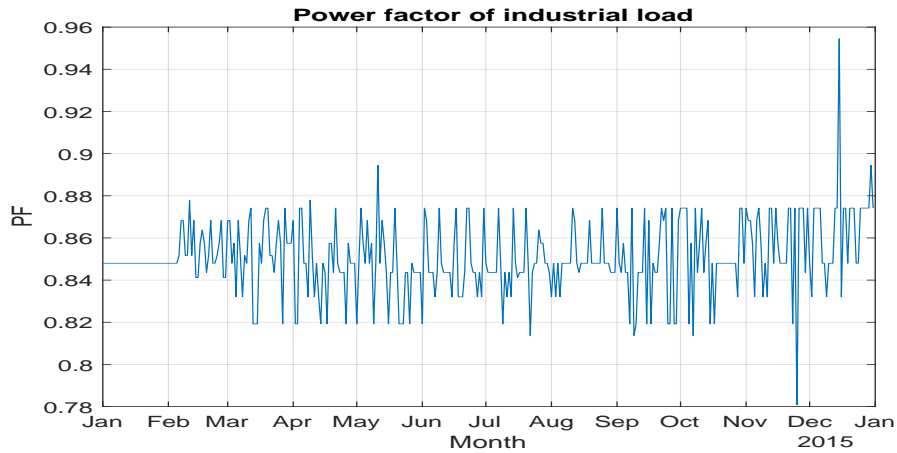


Figure 2.17: Power factor of Industrial load.

in Figure 2.21 and 2.20 where again summers, late May to early September, have the highest power consumption and this is due to cooling loads, particularly ACs.

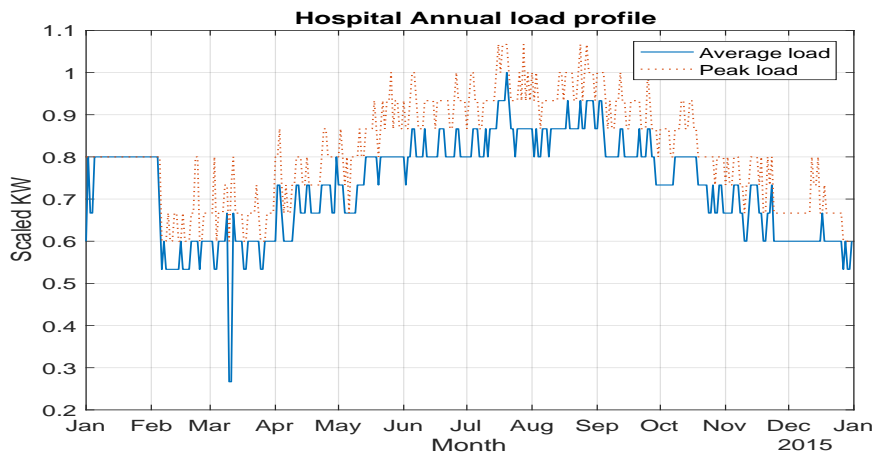


Figure 2.18: Hospital annual peak and average load profile.

2.2.5 Load Factor of All Load Types

The load factor or sometimes referred to as the utilization factor is a very important indicator. Power companies are always eager to improve their load factor. A higher load factor is in fact beneficial for both customers and utilities. The utility will not stress their network and their load profiles will be less varying, which increases the

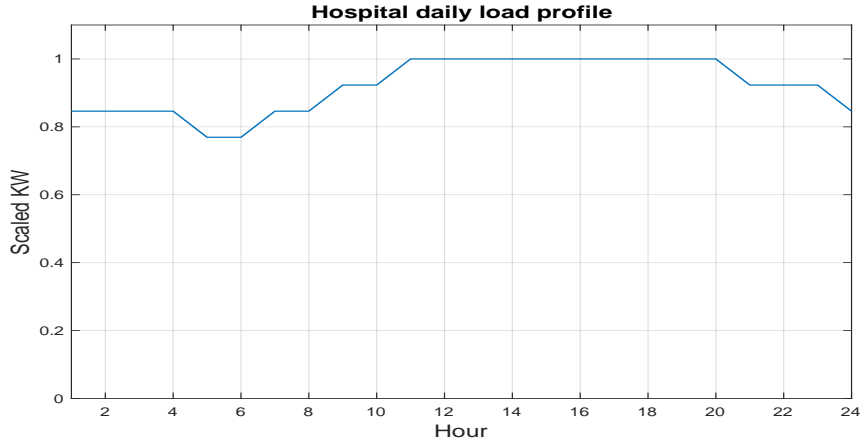


Figure 2.19: Hospital daily load profile.

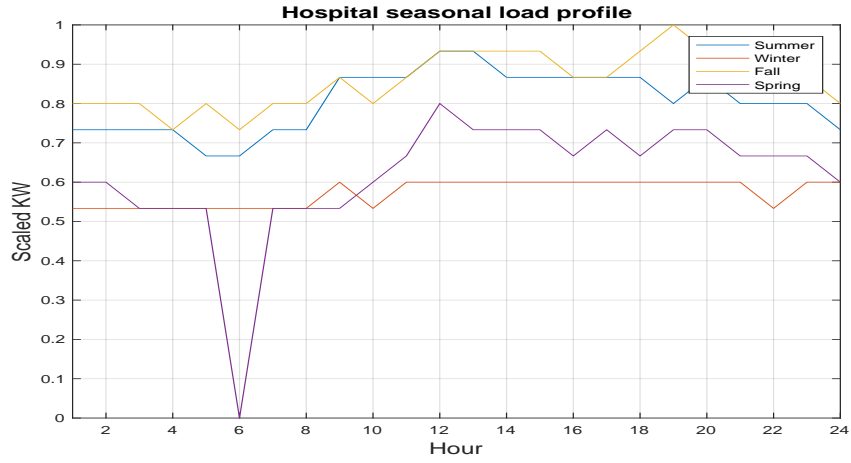


Figure 2.20: Hospital seasonal load profile.

overall efficiency and power factor. While for the consumers, a higher load factor means less average unit cost of energy for the same maximum consumption. The load factor in general is:

$$Load\ Factor(\%) = \left(\frac{Average\ load}{Peak\ load} \right) \times 100 \quad (2.4)$$

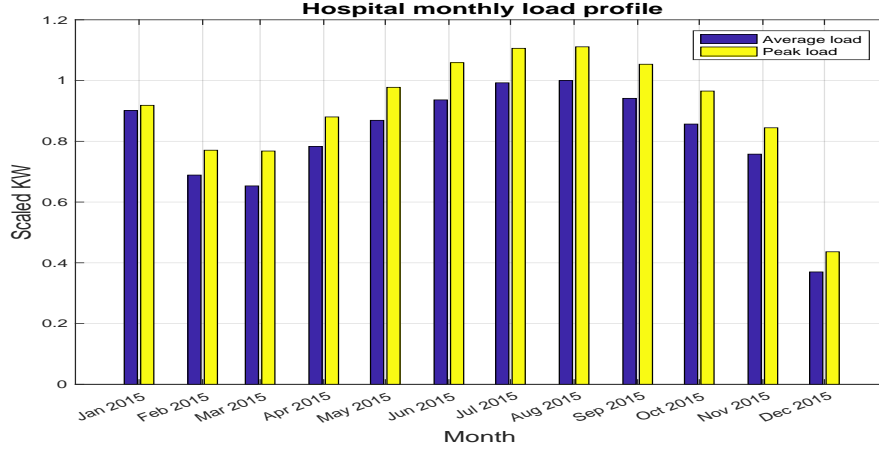


Figure 2.21: Hospital monthly load profile.

Therefore, the monthly load factor can be obtained using the following equation:

$$Monthly\ Load\ Factor(\%) = \frac{\sum_{t=1}^{t=720} P_t}{MAX(\sum_{t=1}^{t=720} P_t) \times 720} \times 100 \quad (2.5)$$

where P_t is the power (KW) at hour t . The monthly demand factor of the four load types is shown in Figure 2.22. From the load factor figure, we can conclude that the hospital load is highly utilized and the variations are small during the day and during the month. The residential load has a good factor during the month but a low load factor during the day.

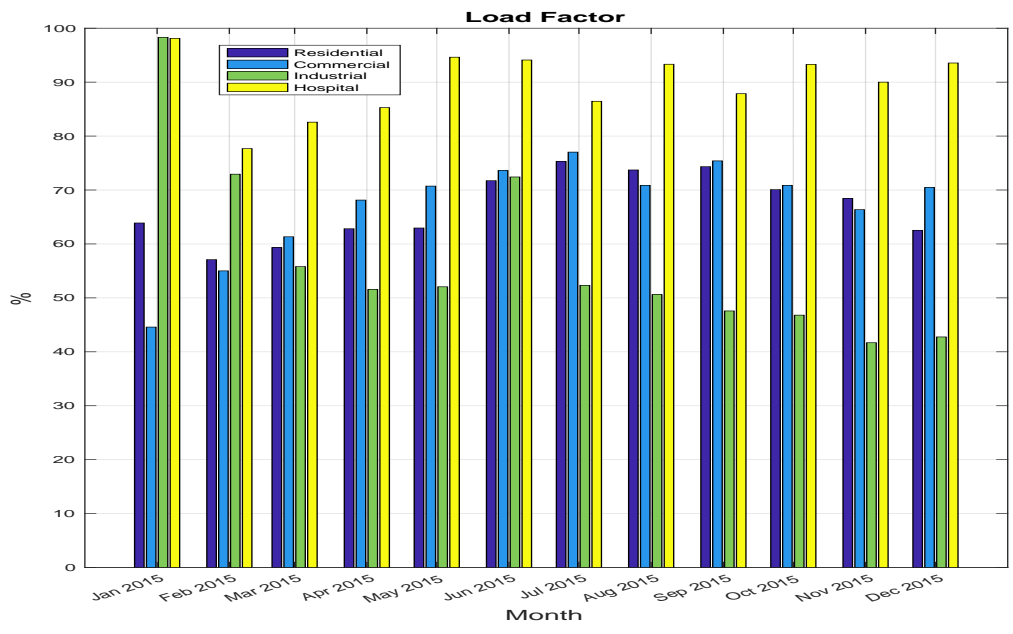


Figure 2.22: Monthly demand factor.

CHAPTER 3

MODELING OF DISTRIBUTED ENERGY RESOURCES

Although finite energy resources such as fossil fuels are cheap, highly dispatchable and capable of load following, current power systems all over the world witnessed a significant growth of renewable energy resources. The importance of solar photovoltaic, wind energy and battery energy storage systems in modern power systems cannot be overemphasized with the ever rising concerns about carbon dioxide levels and the resulted global warming, which propelled the research about RES. Renewable generation constituted up to 70% of the newly installed capacities in the world in 2017 [82]. The fact that they have zero or minimal emissions in addition to having zero fuel cost made them famous. Yet there are several obstacles facing the proliferation of renewable energy technologies. Renewables such as PV and wind are intermittent by nature meaning that their output is variable and uncontrollable. Furthermore, RES are non-dispatchable unless costly storage is accompanying them. Given the

decentralized nature of DER which are mostly RES, the issue of system integration and energy management has to be solved. One of the critical drivers for employing microgrids is their capabilities to address most of these issues, as was discussed in section.1.1.

In addition to DG, Energy Storage Systems (ESS) are essential components of any microgrid. Most DERs in microgrids are renewable based resources; thus the factor of intermittency and non-dispatchability is always of concern. ESS such as batteries, supercapacitors, flywheels and EVs help in smoothing the varying power output of the renewables. Also, ESS help in balancing the generation and demand, given their fast response rate and immediate dispatchability.

The proposed microgrid testbed will have two of the most commonly used RES, that is PV and wind energy, and it will include a BESS, which will smooth the variations of renewables output as well as supplying enough energy when there is a shortage in the generation (Figure 3.1). The irradiance, temperature, wind speed and direction data that will be used to extract the PV and wind is thankfully provided by the Research Institute (RI) at King Fahd University of Petroleum and Minerals (KFUPM). In this chapter, a literature review about the sizing and integratability of the energy sources to the microgrid will be presented. Then the modeling of PV, wind and the battery will take place in three different sections.

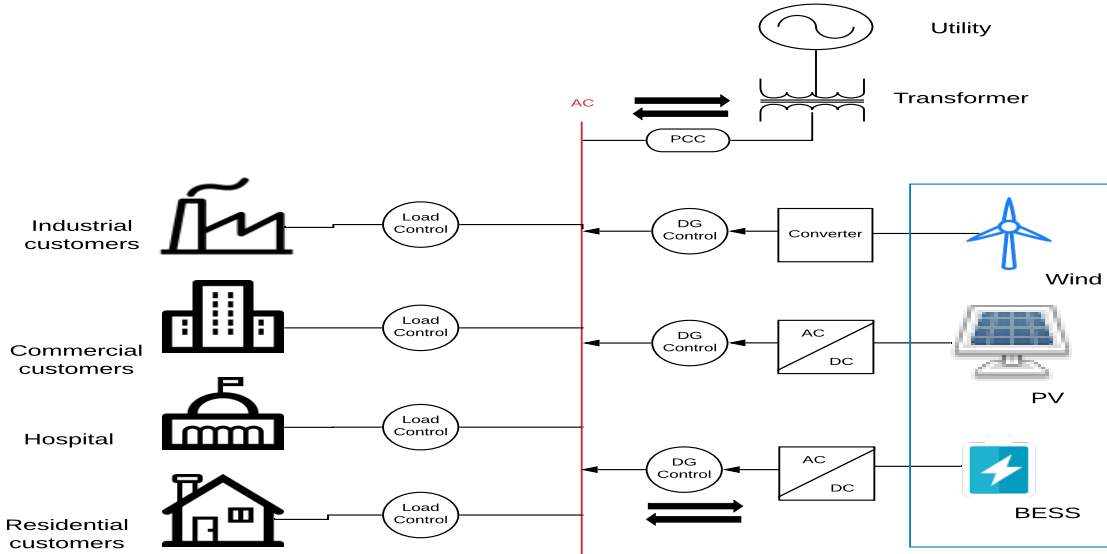


Figure 3.1: Microgrid configuration with DERs in the rectangular.

3.1 Literature Review

Powering small and rural communities has been easier since the RES took place. Microgrids efficiently deploy and integrates small-scale DGs, which are most of time renewable-based sources. In [83], the authors modeled four energy sources: PV, EV employing V2G and G2V, CHP and energy storage system. Loads of their microgrid was also controllable. The authors studied the potential of microgrid having the DGs, ESS and the controllable loads. They concluded that by running the microgrid different times in grid-connected and islanded-mode, the perfect sizing of all resources could be determined. The authors in [84] introduce an algorithm to optimize the sizing of PV, wind, and battery when the microgrid is islanded and does not have a connection to the primary power system. The objective function of the optimization problem is to minimize the cost of the system subjected to the constraint that generation must always meet demand. The proposed sizing algorithm was tested and evaluated in the

Zhoushan island in China. In [85], another optimization method for PV, wind, and battery is proposed. The objective function is similar to the one proposed in [84]; however, the number of wind turbine generators, photovoltaic modules and batteries were all incorporated in the optimization function. Also, a factor was added to the optimization problem which is the loss of power probability (LPSP), defined as the time event when total demand in the system is higher than the total supply. The proposed method was tested as a case study and then compared with some iterative algorithms. Reference [86] proposed an intelligent MPPT controller that uses neural network and differential evolution to track and yield the maximum power from the PV array. An extended literature review about the two renewable sources (PV, wind) and batteries can be found in Section.1.4.

3.2 PV Energy Modeling

With the Saudi economic reforms to move from oil-dependent country to a more diversified economy, many sectors in the government are pushing toward achieving the vision, one of which is the energy sector. The bill of energy is increased to reduce the losses of oil consumption. Thus, renewable energy can present a solution to help in reducing energy consumption furthermore. Photovoltaics (PV) cell energy is becoming a primary source of energy in many countries, and Saudi Arabia lies in the so-called sun-belt where the number of sunshine hours during the year is very high. The monthly average sunshine hours in Saudi Arabia is tabulated in Table 3.1. Being one of the top manufacturers of the solar cell, China comes the first in top PV power generating

country. The advantages of PV include but not limited to:

- No fuel cost. As PV converts the sunlight energy into electricity.
- Minor maintenance cost, as PV, is a stationary electricity generator and thus less maintenance is required.
- An environmentally friendly source. PV produces zero carbon emission, and it has a noiseless operation.
- Scalability. PV output can be simply increased by connecting more modules in parallel or in series.
- Accessibility. Unlike hydro or geothermal sources, sunlight energy can be captured almost everywhere.

There are however some disadvantages for PV such as cell efficiency, power, and cost of manufacturing. In this section, the PV energy output will be modeled to use it later in the microgrid testbed.

The rated output power of PV panel ($P_{PV, rated}$) is calculated by [87][88][89] as the following:

$$P_{PV, rated} = \eta_r * IRR * A * L_M * L_R * L_S * L_D * L_A * L_C * L_T \quad (3.1)$$

where, $L_M, L_R, L_S, L_D, L_A, L_C$ and L_T are the mismatch, DC rating, soiling, shading, aging, diodes and sun-tracking derating factors, respectively. A is the area occupied by the generator (m^2). IRR is the solar radiation incident on PV which can be calculated

Table 3.1: Saudi Arabia daily sunshine hours.

Month	Hours
JAN	7.4
FEB	8.5
MAR	8.5
APR	7.8
MAY	9.2
JUN	10.7
JUL	10.6
AUG	10.5
SEP	10.1
OCT	10.0
NOV	8.3
DEC	7.8

by

$$IRR = \frac{GHI \sin(\nu + \rho)}{\sin(\nu)} \quad (3.2)$$

where GHI is the global horizontal solar irradiance [W/m^2] and ρ is the tilted angle.

ν is:

$$\nu = 90^\circ - \sigma + \delta \quad (3.3)$$

where σ is the latitude and δ is given by:

$$\delta = 23.45^\circ \sin\left(\frac{360}{365}(284 + day)\right) \quad (3.4)$$

The actual solar output power (P_{PV}) at time(t) of PV panel is calculated using the rated solar output power ($P_{PV,rated}$) by:

$$P_{PV}(t) = \begin{cases} P_{PV,rated}(t) \times \frac{S}{S_r}, & 0 \leq S \leq S_r \\ P_{PV,rated}(t), & S_r \leq S \end{cases} \quad (3.5)$$

where, S_r is the standard solar irradiance [1000W/m²]

Panasonic HIT 330W 96 cell solar panels will be used in this study. It was chosen because it has an outstanding performance in a high-temperature environment with a low-temperature coefficient (P_{MPP}) of -0.2580%. The characteristics of the solar panels are listed in Table 3.2. Having the cell temperature coefficient, the output power of the PV panel will vary according to the efficiency which is directly affected by the ambient temperature. At time t , the actual solar output power after the temperature effect ($\omega_{s,T}$) can be modeled as:

$$P_{PV,T}(t) = P_{PV}(t) - P_{MPP} \times P_{PV}(t)(T(t) - T_{STC}) \quad (3.6)$$

where T is the temperature at hour(t) in Celsius(C°) and T_{STC} is the temperature at standard testing conditions, which is usually 25 C° .

Table 3.2: Panasonic solar panel specifications.

Manufacturer	Panasonic
Product name	HIT N330
Cells per module	96
Module watts (STC)	330
Max power voltage and current	58V, 5.7A
V_{oc}, I_{sc}	69.7V, 6.07A
Module efficiency	19.7%
Temperature coefficient P_{mpp}	-0.2580%

The local irradiance data used to find the PV output is shown in Figure 3.2. Notice that the summer months; July, June, and August have the highest irradiance levels. Also, we observe the effect of summer and winter on the length of day and evening times. The span of the December or January curve on the time axis, for example, is

narrower than June or July. Accordingly the temperature data in Dhahran is shown in Figures.3.3 and 3.4. The effect of seasons is clear in Figure 3.3, the data was hourly sampled throughout the whole year. In months 6, 7 and 8 the curve reaches the highest levels around 46 C° and the least temperature is around 5 C° . The histogram in Figure 3.4, shows the temperature in three months which lies in three different seasons: January, July, and October.

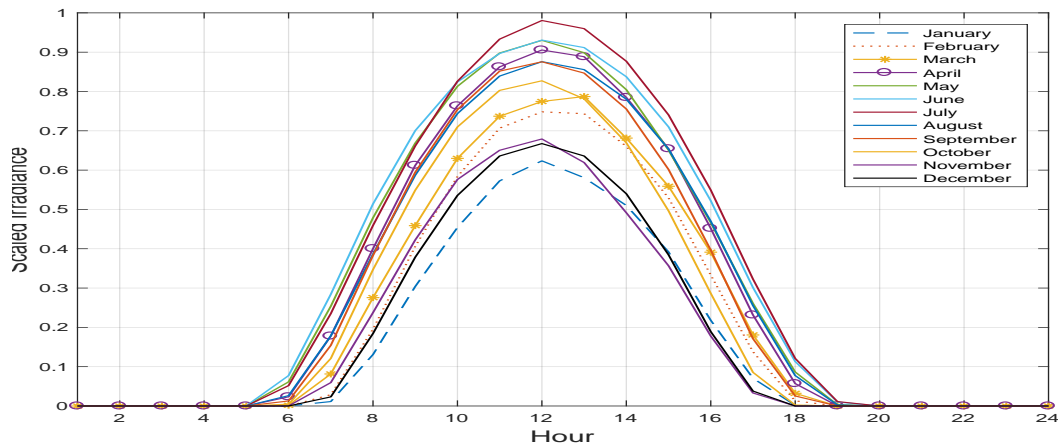


Figure 3.2: Average hourly Scaled irradiance per month.

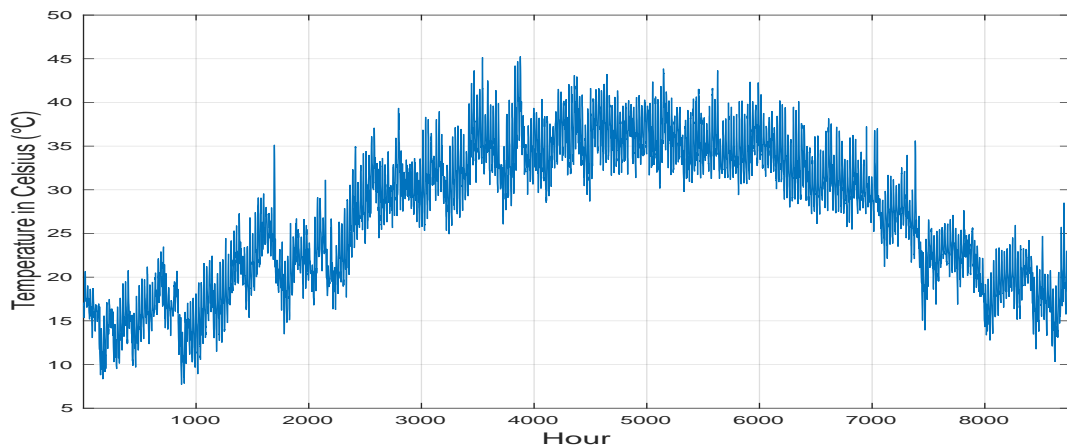


Figure 3.3: Annual Temperature in Dhahran.

After simulating all necessary data for PV modeling, the PV energy output is found utilizing the previous equations as shown in Figure 3.5. The maximum PV output

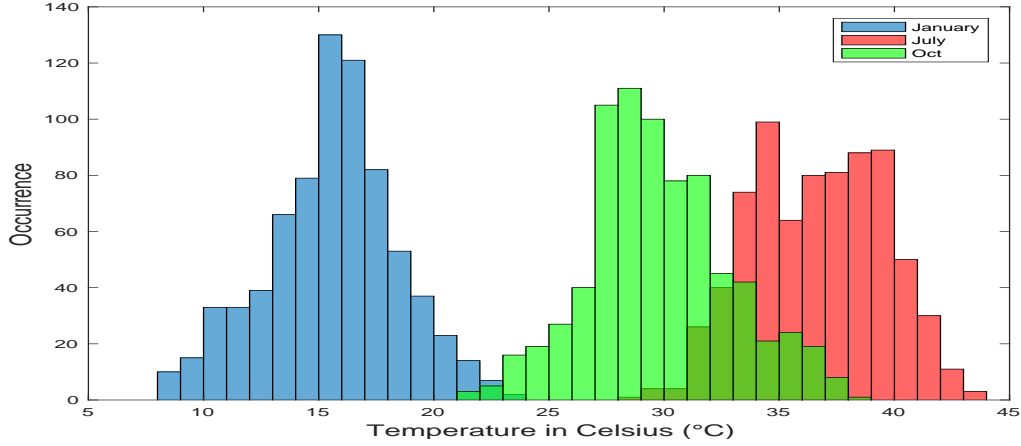


Figure 3.4: Temperature histogram of three different months.

occurs in July with a total energy of 160 KWh, however it should be observed that after including the temperature effect the total energy reduced to around 155 KWh and this is due to the fact that in July the temperature is most of the time higher than the STC temperature which is 25 C°, which in turn reduces the efficiency of the panel. The opposite happens in cold months such as January, where the temperature was usually below 25 C°, and thus output energy was higher after we considered the temperature factor. This output energy will feed the four types of loads later when the microgrid test-bed is designed. The total monthly energy was found on an hourly basis as in the following equation:

$$E_{PV}(t) = \sum_{t=1}^{720} P_{PV}(t) \quad (3.7)$$

where 720 indicates the hours in one month.

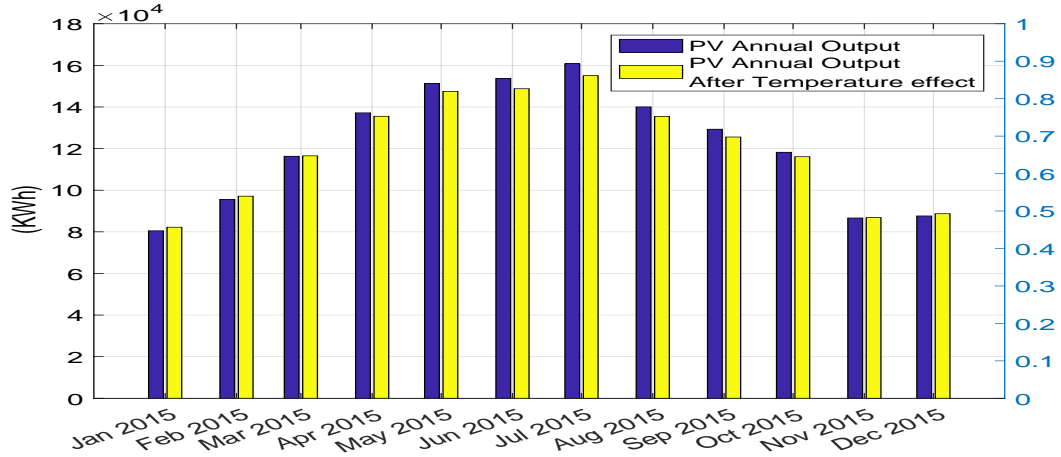


Figure 3.5: Monthly PV energy output with and without the effect of temperature.

3.3 Wind Energy Modeling

Wind energy will be also used another distributed generation source in our microgrid test-bed. Wind is a green energy resource that utilizes the wind energy to rotate a generator that is mounted on a turbine. Like PV, wind is a free and unlimited source. The capital cost of wind is less than PV, but the maintenance cost is higher as wind relies on moving parts, generators, to produce electricity. Wind power generators are not totally environmentally friendly as it is witnessed that wind farms impact birds wildlife. Also, wind turbines can be noisy, and they tend to affect the natural wind current and wind speed of the location. However, if wind farms are located in remote locations such as the sea, they can provide a reliable, safe and carbon-free energy.

The power curve of a wind turbine is shown in Figure 3.6, where ν_c , ν_r and ν_f are the cut-in, rated and cut-off speeds, respectively. The wind turbine will start generating electricity when the wind speed is higher than its cut-in speed, and it will give the rated power when the wind speed is higher or equal to the rated speed of the turbine. When the wind speed is higher than the cut-off limit, the brakes will take

action, and the blades will stop rotating.

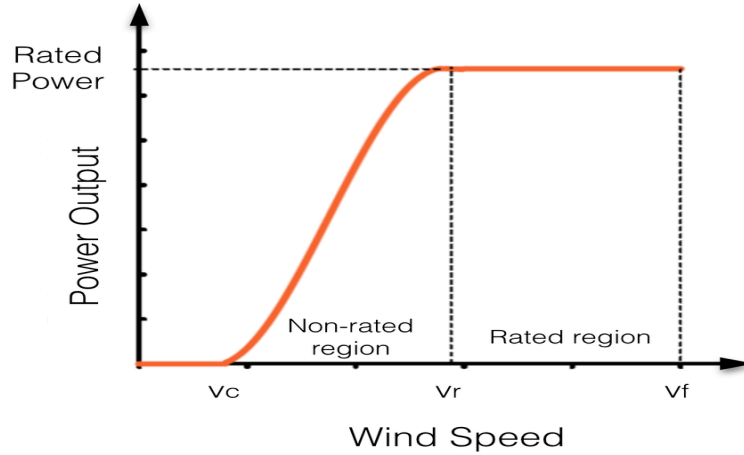


Figure 3.6: Wind turbine power curve [4].

The wind data that will be used for our system is taken from Dhahran area at a 5m high mounted anemometer. The relation between wind speed and the rated wind output power ($P_{wind,rated}$) is raised to the power 3, as shown in the following equation:

$$P_{wind,rated} = \frac{1}{2} C_P \rho A \nu^3 \quad (3.8)$$

where C_P is the maximum power coefficient, ranging from 0.25 to 0.45, dimensionless (theoretical maximum = 0.59). ρ is air density $1.225 [Kg/m^3]$, A is rotor swept area $[m^2]$ and ν is the wind speed $[m/s]$.

To estimate the capacity of the wind generator, the annual consumption load and the average wind speed must be known. To extract the wind speed at different height from the height of the anemometer original measurement, an extrapolation process will be done between the old and new heights using a specific wind shear model. The measured variation in wind speed with height at the site is defined by using the power law shear exponent known as the Hellman exponential law:

$$\frac{V1_{H1}}{V2_{H1}} = \left(\frac{H1}{H2} \right)^\alpha \quad (3.9)$$

Where α is the power law wind shear exponent, H is the height reference to ground, and V is the mean wind speed. The value of the wind shear exponent depends on the nature and roughness of the terrain, and the nature of wind in that area. These values have been determined in the literature. In this context, since Dhahran is located by mountainous terrain, α is set to 0.25 (Table 3.3).

The output wind power of the wind turbine is given as the following:

$$P_{wind}(\nu) = \begin{cases} 0, & 0 \leq \nu \leq \nu_c \text{ or } \nu_f \leq \nu \\ P_{wind,rated} \times \frac{\nu - \nu_c}{\nu_r - \nu_c}, & \nu_c \leq \nu \leq \nu_r \\ P_{wind,rated}, & \nu_r \leq \nu \leq \nu_f \end{cases} \quad (3.10)$$

Table 3.3: Wind shear exponent based on terrain [2]

Terrain	Wind shear exponent (α)
Open water	0.1
Smooth area	0.15
Low bushes with a few trees	0.20
Heavy trees	0.25
Hilly, mountainous terrain	0.25

The wind speed at different altitudes was computed and simulated in MATLAB on an hourly basis and the resulting wind roses at different heights are shown in Figures.3.8-3.10. Zero indicates the direction of the north. The monthly average wind speed is shown in Figure 3.11. Our considered wind turbine is 50m height and thus the output wind power will be calculated based on the 50m altitude wind data. The

characteristics of the consider wind turbine are shown in Table 3.4 and its power curve is shown in Figure 3.7.

Table 3.4: Wind turbine specifications

Manufacturer	Vestas
Product name	V47-700
Hub height	50 m
Rated power	700 KW
Generator type	Induction
Cut-in speed (ν_c)	4.0 m/s
Rated wind speed (ν_r)	16.0 m/s
Cut-off speed (ν_f)	25.0 m/s
Survival wind speed	59.5 m/s

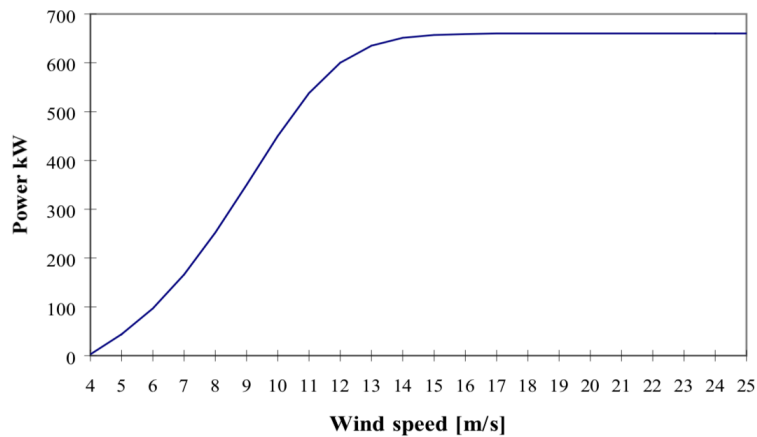


Figure 3.7: Vestas wind turbine power curve [5]

The resulting monthly wind energy output is shown in Figure 3.12. It can be clearly observed that June and July have the highest wind energy output of around 250 KWh, while the lowest average energy output occurs in September with 140 KWh.

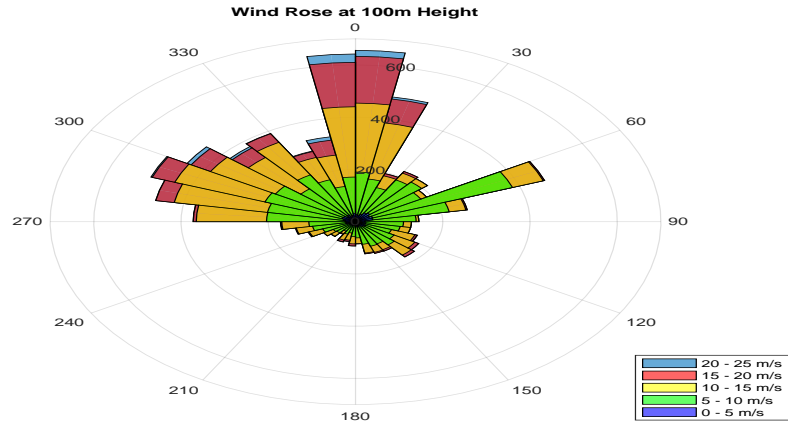


Figure 3.8: Wind speed and direction at 100m altitude.

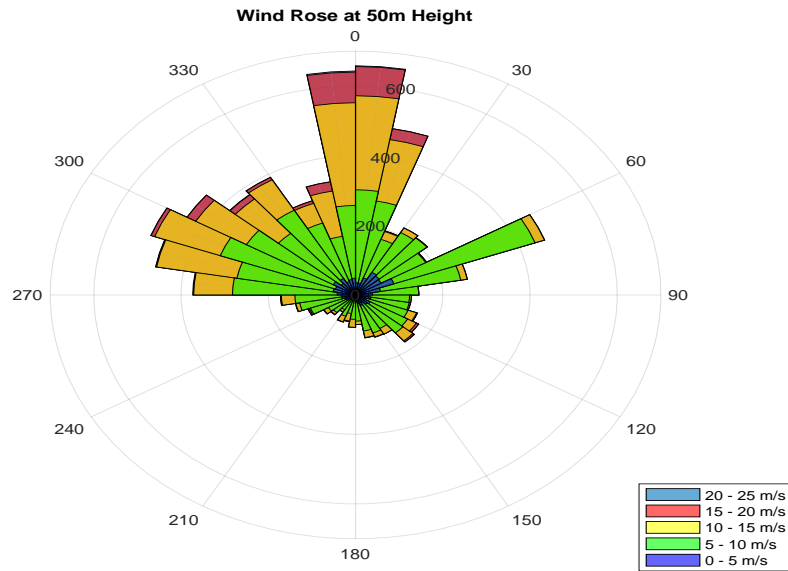


Figure 3.9: Wind speed and direction at 50m altitude.

3.4 Battery Energy Storage System Modeling

Enhanced reliability and energy security are two major advantages of microgrid networks. The large integration of renewable sources can make the system vulnerable to energy unbalance issues, resulting in failures. In microgrids, for some time periods, the supply from DG is higher than the total demand. These are the periods where

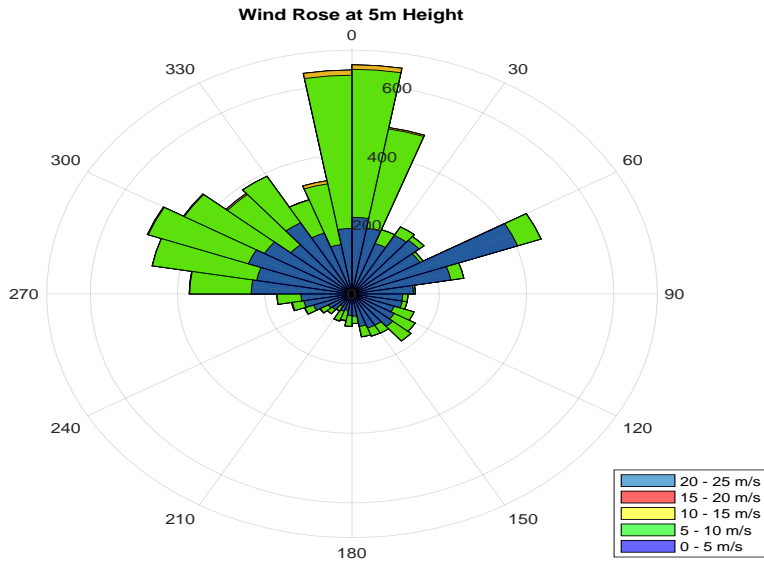


Figure 3.10: Wind speed and direction at 5m altitude.

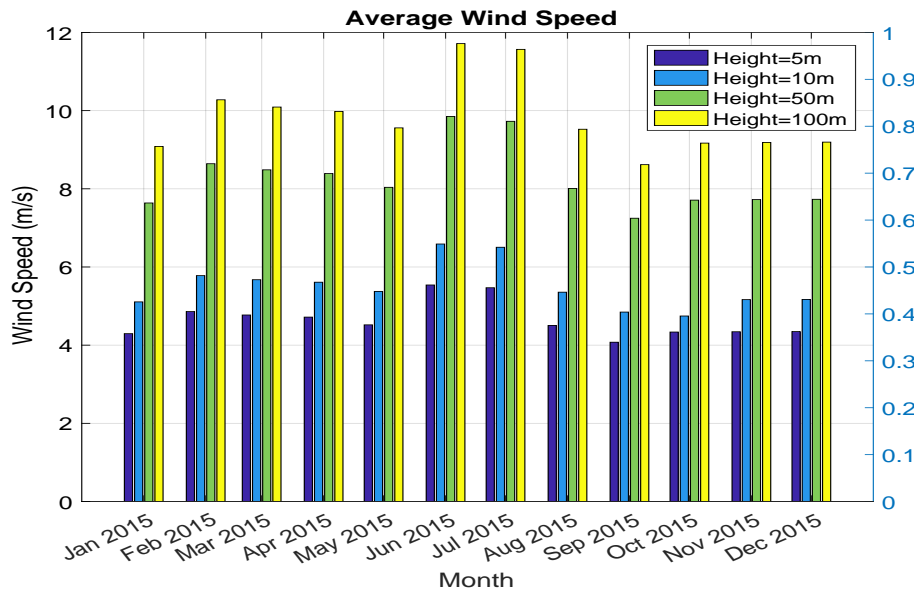


Figure 3.11: Average monthly wind speed at different altitudes.

the excess power is sent to the battery for it to be charged. On the contrary, when the load is higher than generation then the microgrid will have a certain deficit, which should be satisfied using the battery discharge. The battery also will take quick action in response to the renewable generation capricious variations throughout the day. If

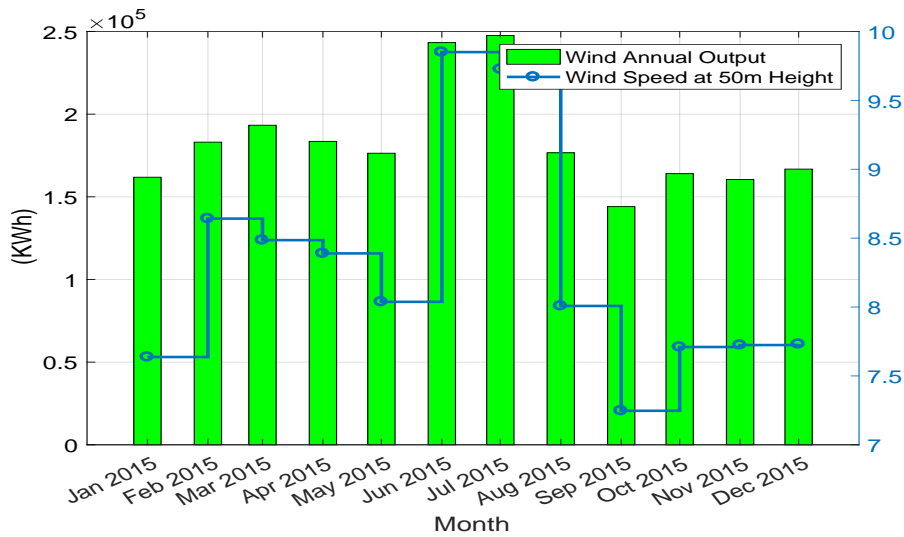


Figure 3.12: Monthly wind energy output.

the battery cannot completely satisfy that deficit then the difference will be compensated from the main grid. There are basically two classifications of battery based on the nature of storage:

1. Direct energy storage technology

Storage systems using this technology stores the electricity directly without changing it to an alternative form of energy. Examples include super-capacitors energy storage (SCES) and superconducting magnetic energy storage (SMES).

2. Indirect energy storage technology

This type is more common, and it involves converting the electricity into another form of energy. For example, BESS converting electricity in chemical energy. Pumped hydroelectric energy storage (PHES) and flywheel energy storage (FES), which both convert the electrical energy into some form of mechanical energy.

As for the applications of microgrid entailing energy management, a high energy density system is required. Lithium-ion BESS will be considered for this study due to their safe operation and relatively long life cycle.

One important battery variable that is necessary for the proper performance and management of the microgrid is the State of Charge (SoC). The State of Charge (SoC) of a battery at a certain time t is formulated as:

$$SoC(t) = \frac{E_b(t)}{C_b} * 100 \quad (3.11)$$

where $E_b(t)$ is the stored energy in the battery at time t [KWh], while C_b is the capacity of the battery. The SoC is constrained by a maximum and minimum value depending on the battery type and expected life cycle:

$$SoC_{min} \leq SoC \leq SoC_{max} \quad (3.12)$$

With the charging and discharging behavior of the battery the SoC will vary as the following:

$$SoC(t_T) = SoC(t_0) + \left(\frac{P_b^{charge} \times \eta^{charge} - P_b^{discharge} \times \eta^{discharge}}{C_b} \right) \times \Delta T \times 100 \quad (3.13)$$

where P_b^{charge} , $P_b^{discharge}$, η^{charge} and $\eta^{discharge}$ are the charging and discharging power [KW] and efficiency [%], respectively. ΔT is the time spent in charging or discharging [hour]. The charging and discharging power of the battery are usually the same but in opposite flowing direction and they are governed by a certain limit in which the

battery cannot exceed as the following:

$$- P_b^{discharge} \leq P_b^{charge,discharge} \leq P_b^{charge} \quad (3.14)$$

So if the battery has a maximum $P_b^{charge} = P_b^{discharge} = 150KW$ then the inequality will be as follows:

$$- 150KW \leq P_b^{charge,discharge} \leq 150KW \quad (3.15)$$

Meaning that the battery will either be charging itself with a range of 0 to 150KW power or discharging itself with the same amount.

CHAPTER 4

MICROGRID TEST SYSTEM DESIGN

Microgrids, as the Department of Energy (DoE) defines them ” A microgrid is a group of interconnected loads and distributed energy resources within clearly defined electrical boundaries that acts as a single controllable entity with respect to the grid. A microgrid can connect and disconnect from the grid to enable it to operate in both grid-connected or island-mode. ” [90]. The number of microgrids in real applications is growing especially in areas that are isolated from the main grid, for example, Santa Rita jail, Fort Carson, Isle of Eigg and Fort Collins. Fewer grid-tied microgrids have been established due to the added complexity of the design caused by the direct interaction with the utility. Microgrids add tremendous values to its costumers including the utility. The microgrid has to be economically smart, meaning that it will feed its load from local generation as possible and it will take from the storage if generation is not available. The microgrid will implement an energy transaction with the grid

when there is not enough power from the DGs and ESS to feed the loads. With the same concept, the microgrid will sell electricity to the grid if there is excess power. Our microgrid test system should be able to achieve these transactions. In addition to that, our microgrid will be incorporated later with a flexible, intelligent load priority list, which will order the loads based on their importance based on a given time, available energy and reliability indices. Furthermore, the proposed microgrid will be subjected later to a priority list incorporated Demand Side Management (DSM) programs to test the effectivity of each scheme and verify the microgrid operation under each case. The microgrid is designed for study purposes, and its data will be available on a web-page.

In the previous chapters, we modeled the four load types that will be now part of our microgrid design. Furthermore, two renewable generation sources have been considered and modeled; PV and Wind. A Battery Energy Storage System (BESS) was designed and optimized to ensure a right balance between the microgrid local generation and demand. All of the previously modeled data were taken from Dhahran city, east of Saudi Arabia. Our MG test-bed will be studied over a 24 hours period, that day is 28th of June, 2015 (Figure 4.1).

In the next sections, a literature review about MG test-beds will be introduced. Then, the light will be shed on our proposed MG test-bed to explain its connections, control and operation principle.

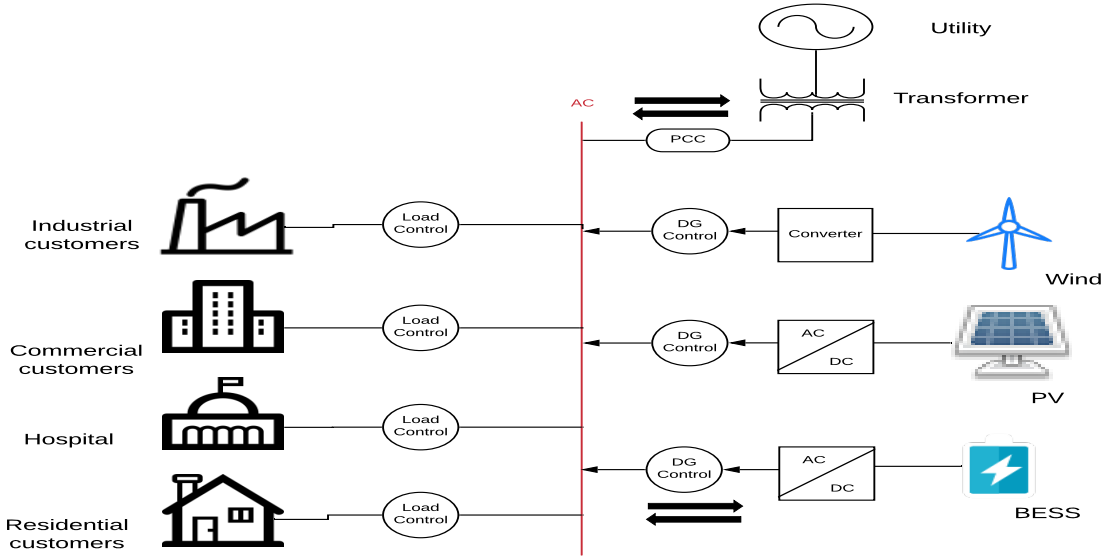


Figure 4.1: Configuration of the proposed microgrid test-bed.

4.1 Literature Review

The research about microgrid increased rapidly in the previous decade. Though, few microgrid test-beds exist in the literature. The significance of a MG test-bed is that it will enable researchers to benchmark their ideas on the same platform. Thus, comparisons and knowledge trading can be easily conducted. CERTS 13.2KV/480V MG test-bed is one of the earliest systems established, and many studies have been done on it [91]. An excellent overview of all existing microgrid test-beds is shown in [92]. Different MG connection types have been studied:

- AC microgrid, which is the one proposed in this context.
- DC microgrid [93],[13].
- Hybrid AC/DC microgrid, which is investigated in Chapter.7.
- High frequency AC (HFAC) microgrid, which was studied by CERTS [94].

4.2 Description of The Test System

The test system that we are proposing integrates four load categories and two renewable energy resources; PV and wind. A BESS is also integrated to the system to balance the supply and demand in case of a deficit. The test-bed is a single-phase 60 HZ AC power network with a secondary voltage of 400V. Some specifications about our proposed microgrid are shown in Table 4.1.

Table 4.1: Classifications of the proposed microgrid test-bed

Classification	Utility microgrid
Operational mode	Grid-tie mode
Integration level	High
Connection type	AC, 60HZ
Distributed generation	Wind, PV
Energy Storage	Battery
Load types	Residential, commercial industrial, hospital
Features	High power quality, DSM load priority, stability and robustness, successful transaction with the grid

4.2.1 Test-bed's Renewable Energy Resources and Storage

As discussed, the microgrid has two local distributed generation sources and a battery storage system. The solar power generation maximum power output happens in summer with a 710KW while the average generation throughout the year is 295.5 KW. The wind turbine maximum output is 700KW with an annual average of 251KW. Thus the maximum total power generated from the renewable sources is 1.41MW. Both wind and PV power output profile was shown in Chapter.3, but most of our case studies on the system will be done over a 24 hour period, explicitly 28th of June,

thus the PV and wind generation profile of that day are shown in Figures.4.2,4.3. A battery-based storage system is also installed to take action and feed the loads when there is a shortage in the generation. When there is excess in generation the battery will be charged. The maximum battery output power is approximately 20KW. The battery has 25800Ah capacity with a SoC operation region between 90% to 20%.

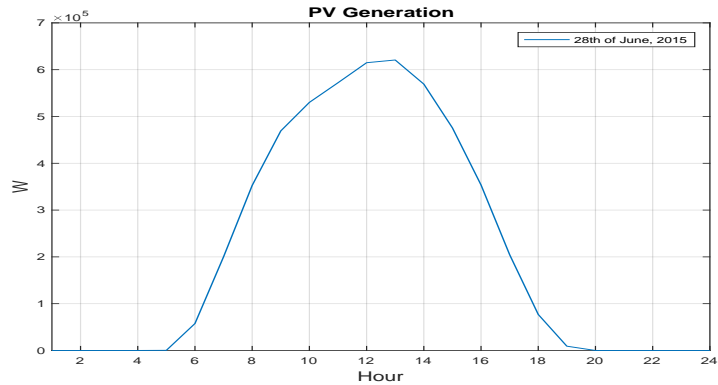


Figure 4.2: PV hourly generation on 28th of June.

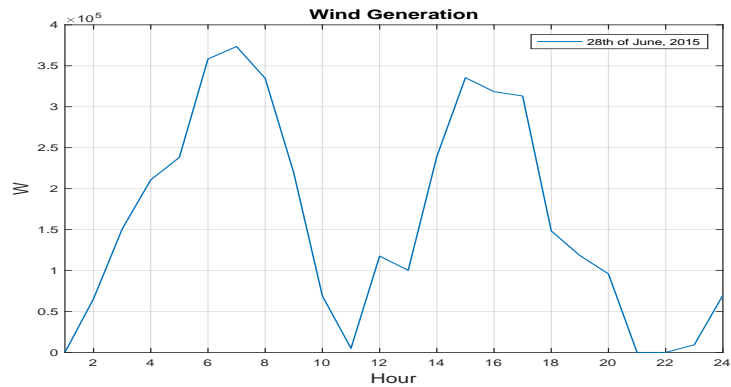


Figure 4.3: Wind hourly generation on 28th of June.

4.2.2 Test-bed's Demand

The test-bed feeds power to four single costumers with four different load types; residential, commercial, industrial and a hospital. The peak of the residential load occur

in the summer for a few hours with a power consumption of 5.6 KW. The commercial and hospital load peaks are 7.2 KW and 21 KW, respectively. The industrial has the highest peak of around 1 MW. The maximum MG load is 1.034 MW. Industrial loads usually are much higher than other loads and since their load profile is almost flat as was shown in Chapter.2, they will flatten the load profile of the aggregated loads due to its size compared to other load types. The four load types and the aggregated load of the day 28th of June are presented in Figure 4.4. The aggregated loads and generations profiles on that day are displayed in Figure 4.5. In fact, the renewable generation sometimes is zero or very close to zero as witnessed in hours 1, 21, 22 and 23. The annual day by day renewable generation and demand curves for the microgrid test-bed are shown in Figure 4.6.

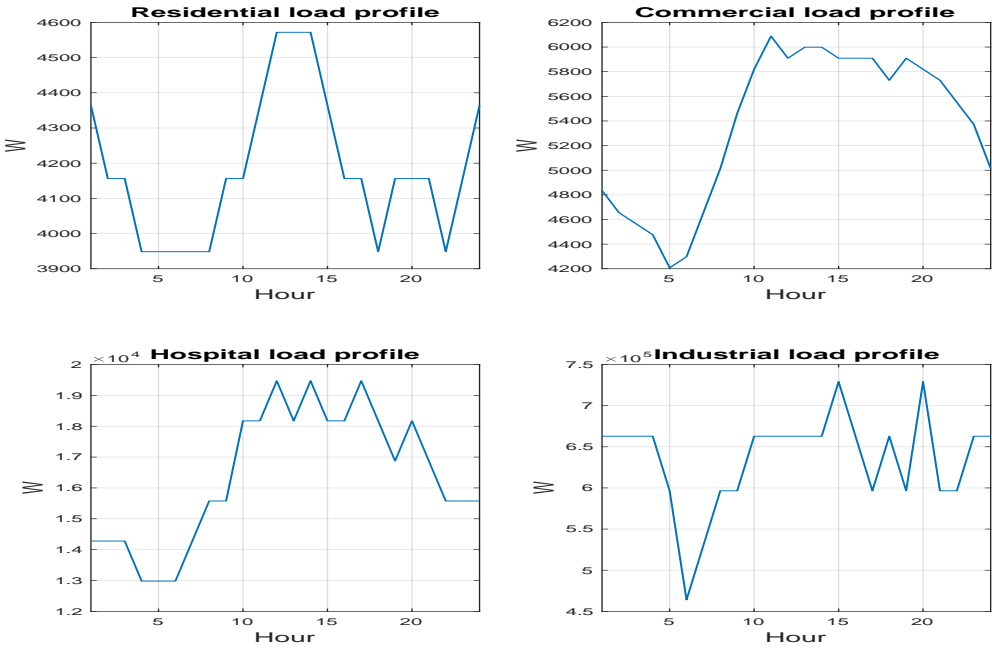


Figure 4.4: Hourly load profiles on 28th of June.

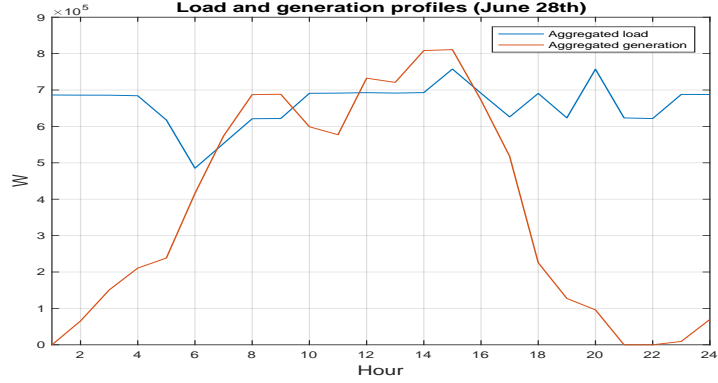


Figure 4.5: Aggregated hourly load and generation of the MG test-bed on 28th of June.

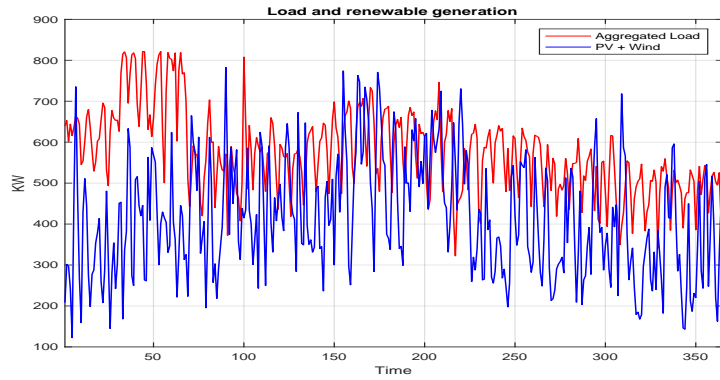


Figure 4.6: Aggregated annual day by day load and generation of the MG test-bed.

4.2.3 Configuration of The Test-bed

The microgrid is a single phase 400 V_{RMS} , 60 HZ power network. Two renewable energy resources; PV (bus1) and wind (bus2) are considered as distributed generation. Their data such as temperature, irradiance and wind speed are updated on an hourly basis. A battery storage system is also connected to smooth the variations of the RES. Four types of loads; residential, commercial, industrial and hospital are connected and subjected to ANN based load priority list. Loads are categorized into critical (C) and non-critical (NC) loads. The hospital is considered as critical, and the rest of the load categories vary on criticality level depending on the given time and the available

energy. A single-pole mounted transformer links the microgrid and the main grid. The step-down transformer has 1.6 MVA rating and a primary voltage of 6.6 KV with a secondary voltage of 400 V. To simulate the main grid, a swing type three-phase 33 KV voltage source is connected. The voltage is then stepped down using a three-phase Y-Y transformer from 33 KV to 6.6 KV. A 1 KM long transmission line transmits the power to the microgrid three winding transformer. A table listing the maximum and average generation and load capacities throughout the year are presented in Table 4.2. A one-line diagram of the test-bed is depicted in Figure 4.7.

Table 4.2: Maximum and average generation and load capacities of the MG test-bed

Maximum renewable generation capacity (KW)			Maximum load capacity (KW)					
Generator	$P_{RES,i}^{max}$	$P_{RES,i}^{avg}$	Load type	$P_{load,i}^{max}$	$P_{load,i}^{avg}$	Load type	$P_{load,i}^{max}$	$P_{load,i}^{avg}$
PV	710	295.46	Residential	5.611	2.431	Industrial	994.30	553.297
Wind	700	251.26	Commercial	7.163	3.748	Hospital	20.77	14.212
$\sum_{i=1}^2 P_{RES,i}$	1381.89	415.11	$\sum_{i=1}^4 P_{load,i}$	1022.7	573.69	-	-	-

4.3 Operation of The Test System

Unlike many commodities, electrical energy is a unique case in the sense that once power is generated, it must be consumed somewhere else. Any unbalance in this equation can lead to brown-outs or eventually blackouts. Microgrids relief the main grid's congestion and help increase the reliability and energy security of its network and neighboring networks; the utility. The idea of a microgrid is that it is able, most of the time, to locally feed its load. However, when the generation in the microgrid is less than the demand, the utility will play a role in supplying the deficit to the microgrid and balancing the microgrid again. On the contrary, when the microgrid's

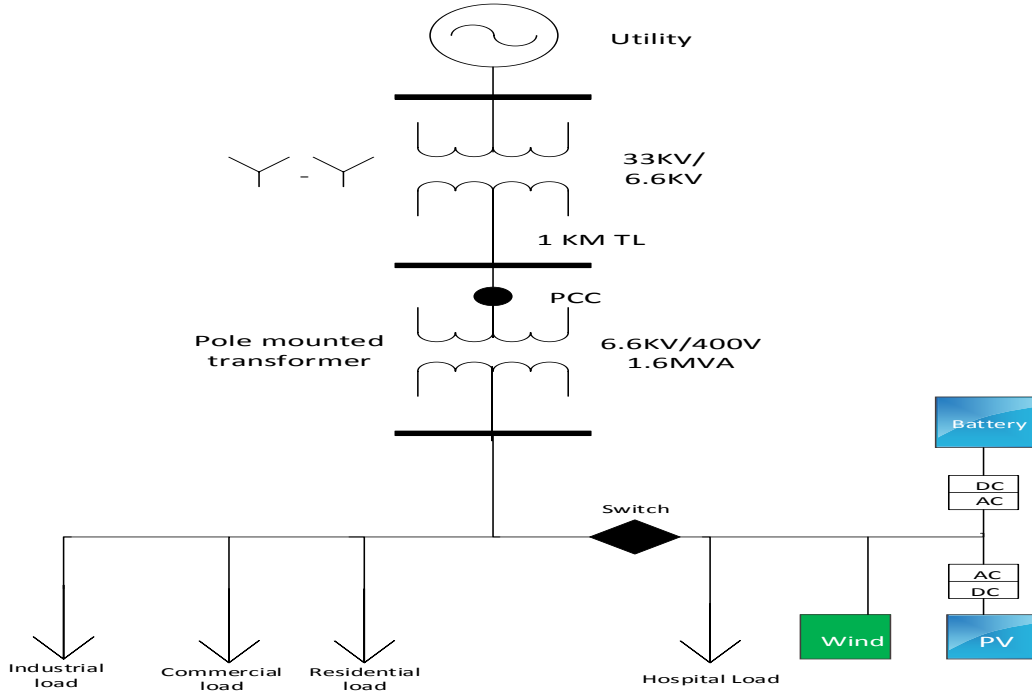


Figure 4.7: One line diagram of the MG test-bed.

local generation is higher than its demand the extra power will be transmitted to the main grid. The energy balance equation of our microgrid that will govern its operation is shown below:

$$P_{PV}(t) + P_{wind}(t) + P_{battery}(t) + P_{utility}(t) \geq P_{load}(t) \quad (4.1)$$

Where, P_{PV} is the photovoltaics power output, P_{Wind} is the wind turbine power output, $P_{Battery}$ is the battery energy output and $P_{Utility}$ is the main grid output. The load power $P_{Load}(t)$ at certain time t is defined as:

$$P_{Load}(t) = P_{RES}(t) + P_{COMM}(t) + P_{IND}(t) + P_{HOS}(t) \quad (4.2)$$

Where $P_{RES}(t)$, $P_{COMM}(t)$, $P_{IND}(t)$ and $P_{HOS}(t)$ are the residential, commercial, industrial and hospital loads at time t , respectively.

The operation principle of the microgrid at hour t is as follows:

1. The microgrid's centralized controller will gather the raw generation and load data from MATLAB m.file.
2. The PV, wind and load will be calculated and acquired based on that hour t .
3. The modeled generation and load is subjected to Equation.4.1.
4. If $P_{PV}(t) + P_{wind}(t) \geq P_{load}(t)$ then:
 - 4.1. Charge the battery if its SoC is less than 90%.
 - 4.2. Send the extra power to the utility, otherwise.
5. If $P_{PV}(t) + P_{wind}(t) \leq P_{load}(t)$ then:
 - 5.1. Discharge the battery if its SoC is greater than 90%.
 - 5.2. Take the deficit power from the utility, otherwise.
6. Update t and repeat the steps again.

A detailed flowchart of the microgrid test-bed operating principle is illustrated in Figure 4.8.

4.4 Microgrid Testbed Case Studies

Eight case studies will be implemented to test the operation of the microgrid. All of the case studies will be run for the date 28th of June 2015. The battery sizing is

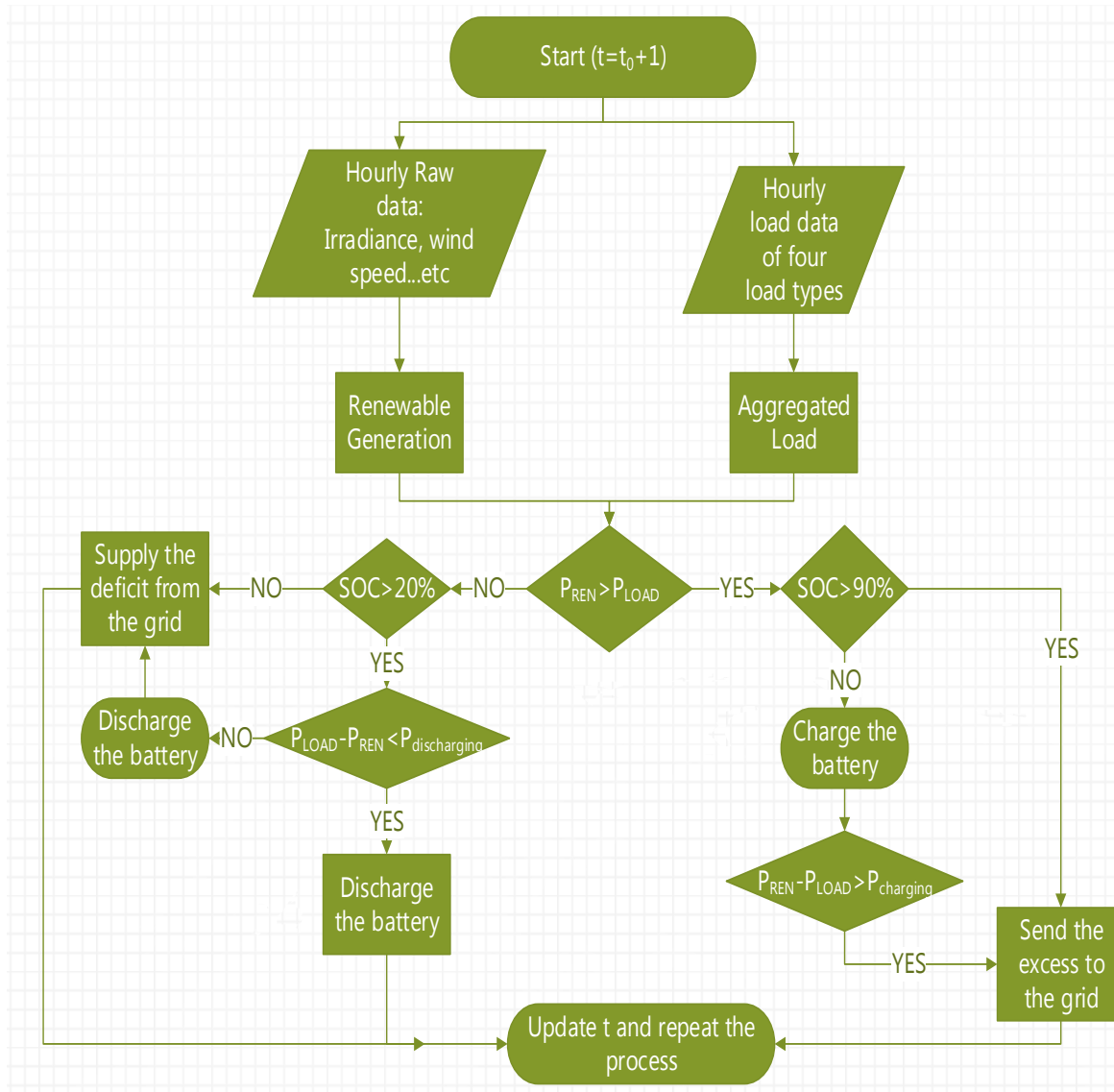


Figure 4.8: Flowchart of MG test-bed operating principle.

3000 AH with charging and discharging power of 35 KW. The battery was assumed to be 80% charged at the beginning of the simulation. The considered case studies are explained in Tables.4.3-4.4.

Table 4.3: Microgrid test system case studies.

Case	PV	Wind	Battery	Load	Comments
1	N.O	N.O	N.O	N.O	
2	Shading (t=12)	N.O	N.O	N.O	*All cases are run based on the 28 th of June data. *N.O: Normal Operation * $t_1 - t_2$ indicates that the fault happened for an hour from $t_1 - t_2$
3	N.O	N.O	Sizing change	N.O	
4	Shading (t=12)	N.O	N.O	Fault at industrial bus (t=3)	
5	N.O	N.O	Fault at battery bus (t=10-16)	N.O	

Table 4.4: Microgrid test system case studies with different dates

Case	PV	Wind	Battery	Load	Date
6	N.O	N.O	N.O	N.O	28 th -29 th of June
7	N.O	N.O	N.O	N.O	25 th of December
8	N.O	N.O	Sizing change	N.O	25 th to 31 st of December

4.4.1 Case 1: Normal MG operation

The first case study as shown in the table is the when all connected elements are in normal operation. P_{PV} , P_{Wind} , $P_{utility}$ and P_{load} are shown in Figures.4.9. The battery power [W] and its SoC [%] are shown in Figure 4.10. Notice that at hour 9, the PV and wind generation was higher than P_{load} and excess power was sent to the battery and to the utility ($-P_{utility}$, $-P_{battery}$). In the period from hours 1 to 6, the load was higher than the generation and thus both battery and the grid took action to meet the deficit. In the $P_{battery}$ curve, observe that before at hour 12, the excess load was only enough to charge the battery and hence no power was sent to the main grid.

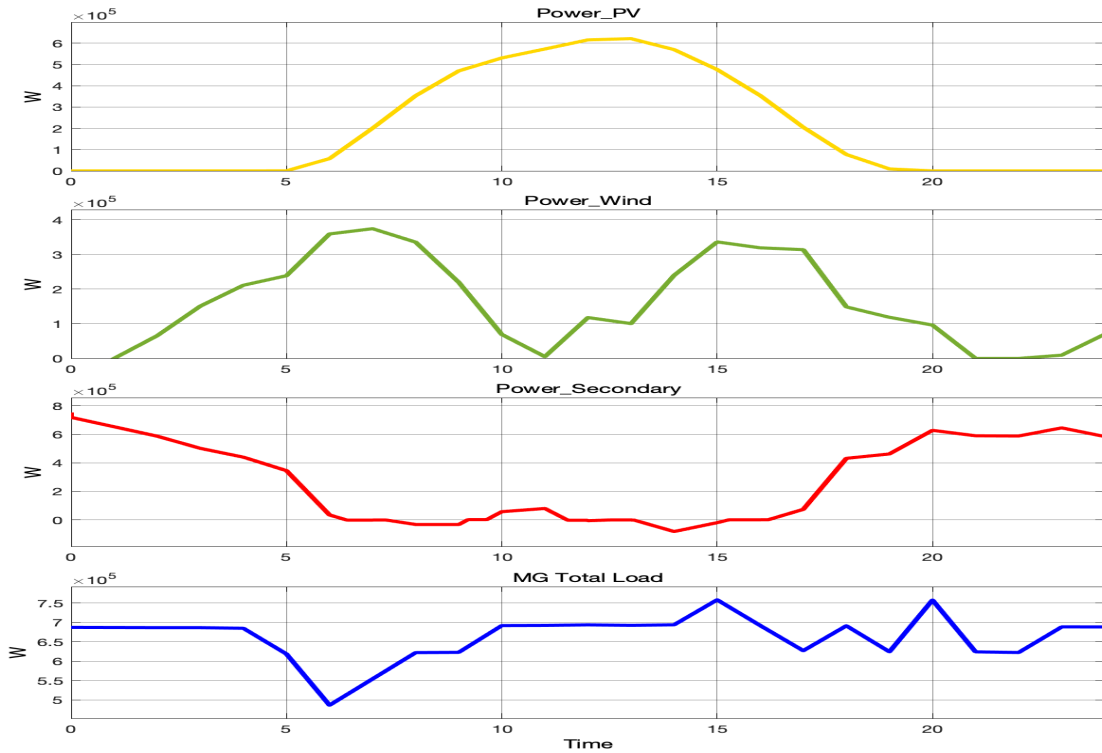


Figure 4.9: Running of case 1.

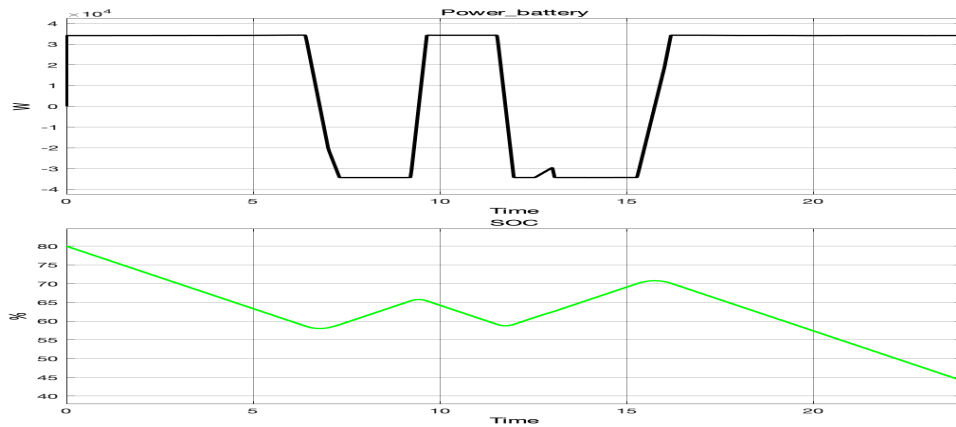


Figure 4.10: Running of case 1, battery response.

4.4.2 Case 2: Shading Effect

This case shows the effect of shading, which might happen due to clouds, dust or simply any human or animal causing that shade. A shading effect at hour 12 that lasted for approximately 20 minutes and caused a 40% reduction on the PV output

was introduced. From Figures.4.11-4.12, one can notice the fast response from the battery to substitute for the sudden reduction in generation caused by the shading effect. A small disturbance is seen in the utility voltage at the beginning and end of that incident.

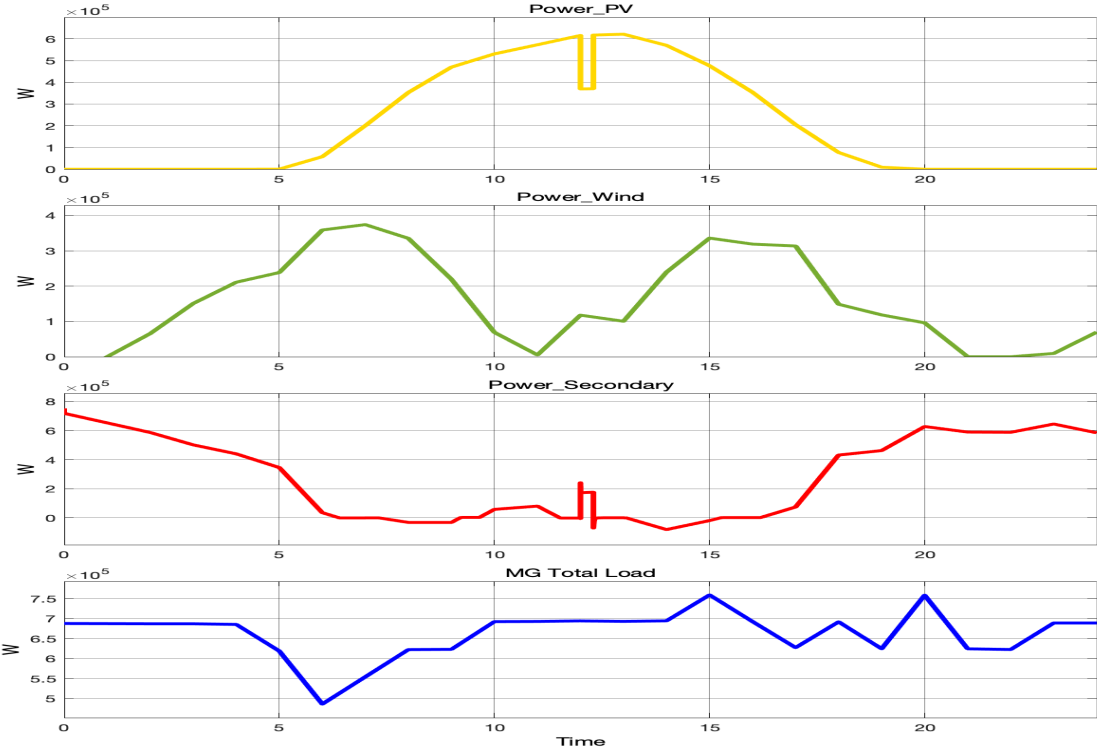


Figure 4.11: Running of case 2.

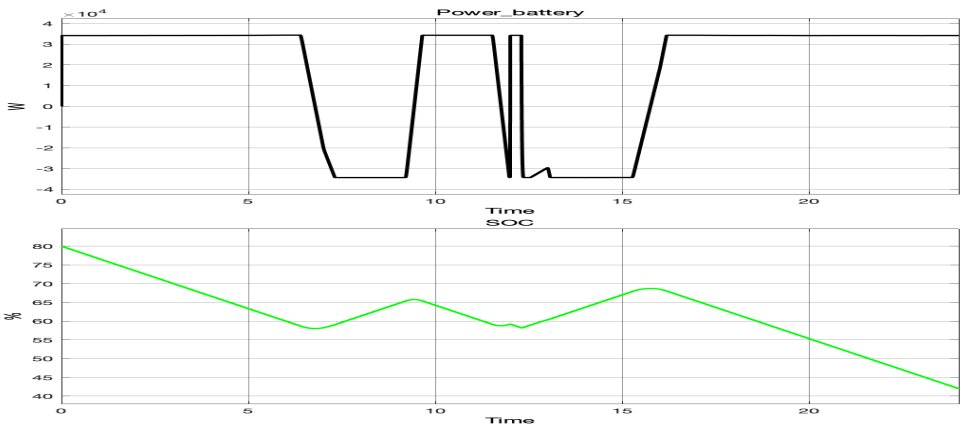


Figure 4.12: Running of case 2, battery response.

4.4.3 Case 3: Battery Sizing change

In this case, the sizing of the battery was changed from 3000 AH to 1000 AH without modifying the battery charging and discharging maximum power. Figures.4.13-4.14 displays the system's response. It is worth mentioning that between hours 1 to 6, the battery storage was fully consumed due to the high demand and the low AH capacity. At hour 6 the battery's SoC reached the pre-specified minimum; 20%, thus the battery was automatically disabled, and its output power was zero. When renewable generation became higher than the load at hour 7, the battery was charged.

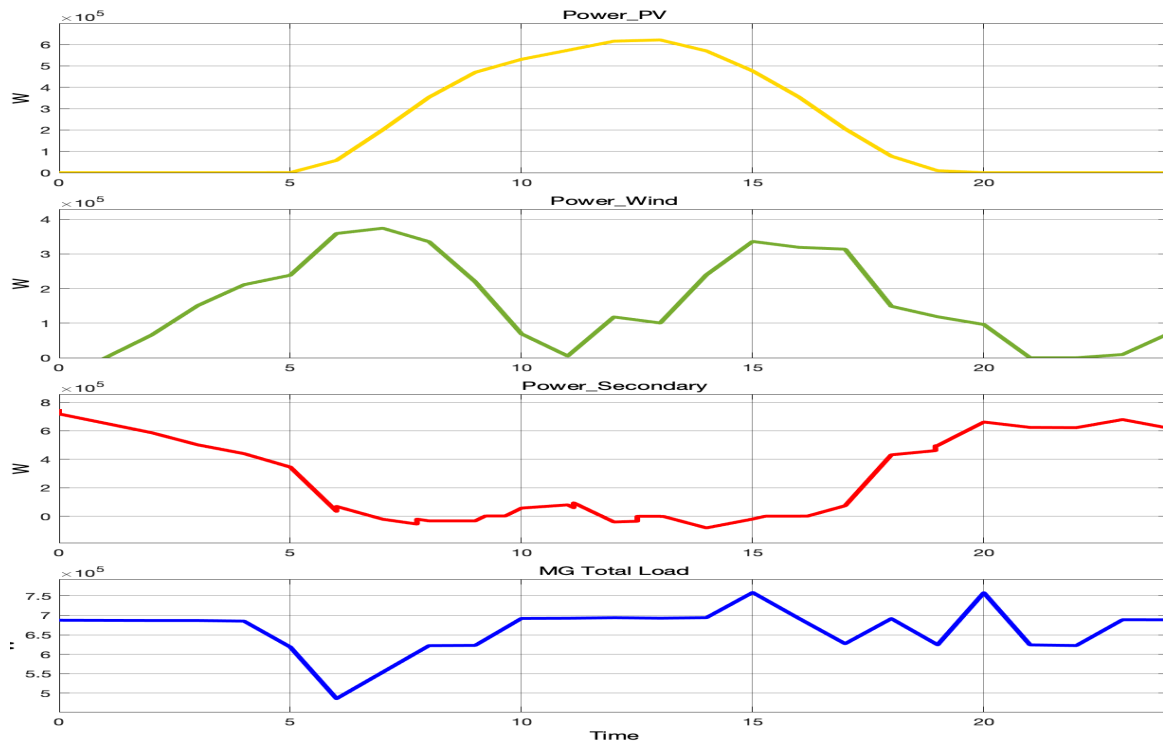


Figure 4.13: Running of case 3.

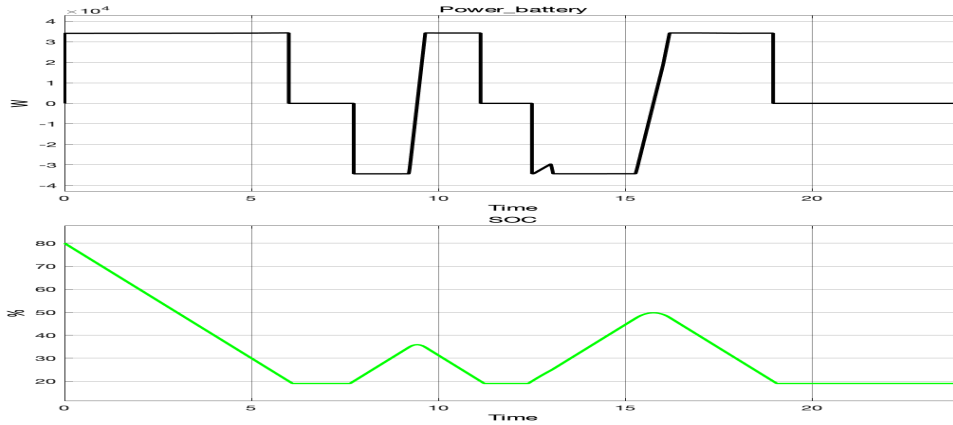


Figure 4.14: Running of case 3, battery response.

4.4.4 Case 4: Fault At Industrial Bus and Shading

In this case, two disturbances were introduced: a) A shading effect similar to the one in Case.2, b) a fault at the industrial load bus at hour 3 causing it to be totally disconnected from the microgrid. The industrial load is the biggest in our microgrid, the effect of that disturbance is clearly observed on the big reduction of the power coming from the grid and from the battery. Actually at that instant, the renewable generation, basically wind, was higher than the load (Figures.4.15-4.17).

4.4.5 Case 5: Fault at Battery Bus

Lastly, in this case, the battery was out for the period from 9 AM to 4 PM. In Figure 4.19, it is visible that because the battery was disconnected there was no charging nor discharging during that period. While Figure 4.18 shows that the grid bear alone all responsibility to balance the supply and the demand.

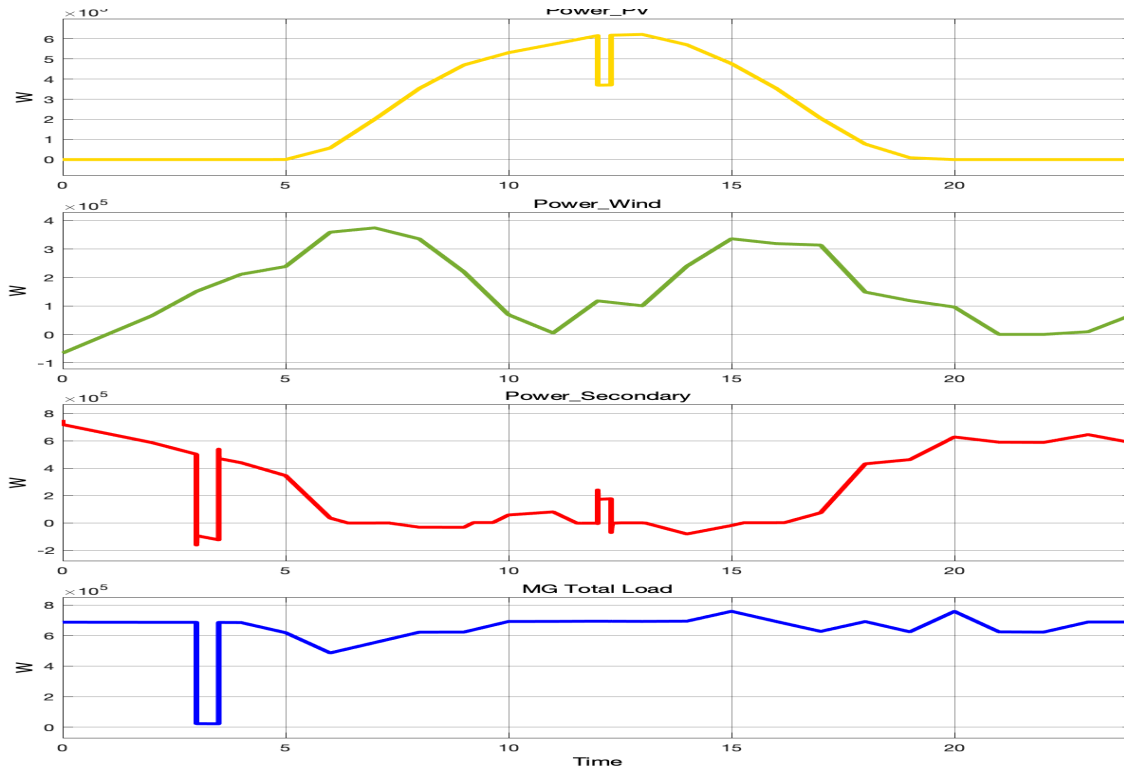


Figure 4.15: Running of case 4.

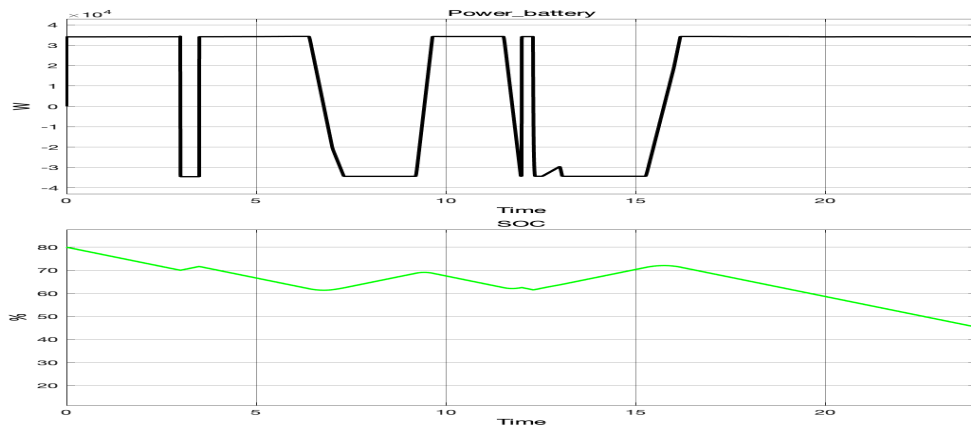


Figure 4.16: Running of case 4, battery response.

4.4.6 Case 6: MG Run for Two Simultaneous Days

This case is very similar to case 1 but the only difference is that now we will run the simulation for two consecutive days that is from 28th to 29th of June. Notice that the x-axis now spans from 1 to 48. The microgrid behavior and the battery response are

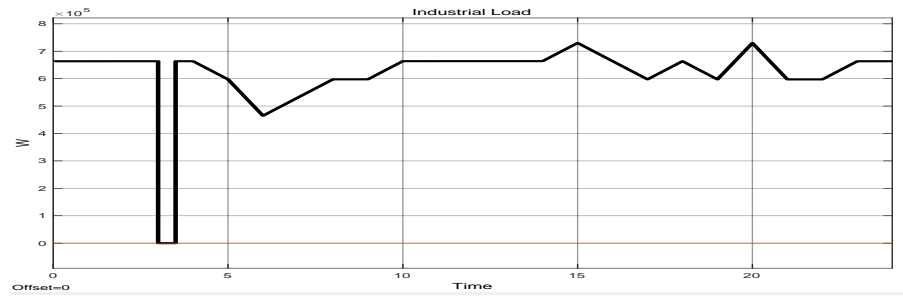


Figure 4.17: Running of case 4, industrial load.

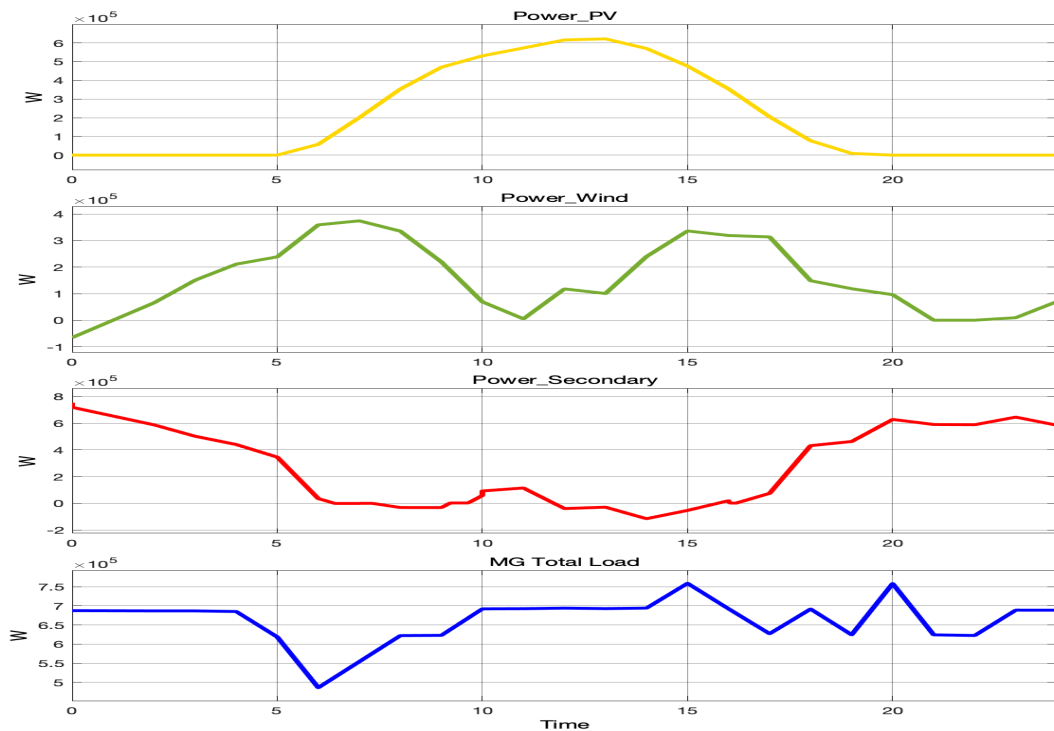


Figure 4.18: Running of case 5.

depicted in Figures.4.20-4.21.

4.4.7 Case 7: MG Run on Winter Day

All of the previous simulations were done in summer. In this case, a normal winter day was simulated, which is December the 25th. As can be seen from Figure 4.22, the

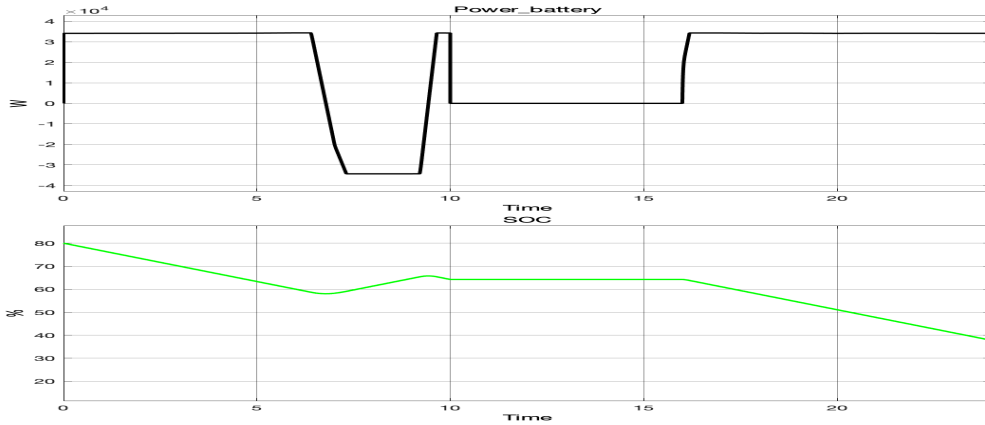


Figure 4.19: Running of case 5, battery response.

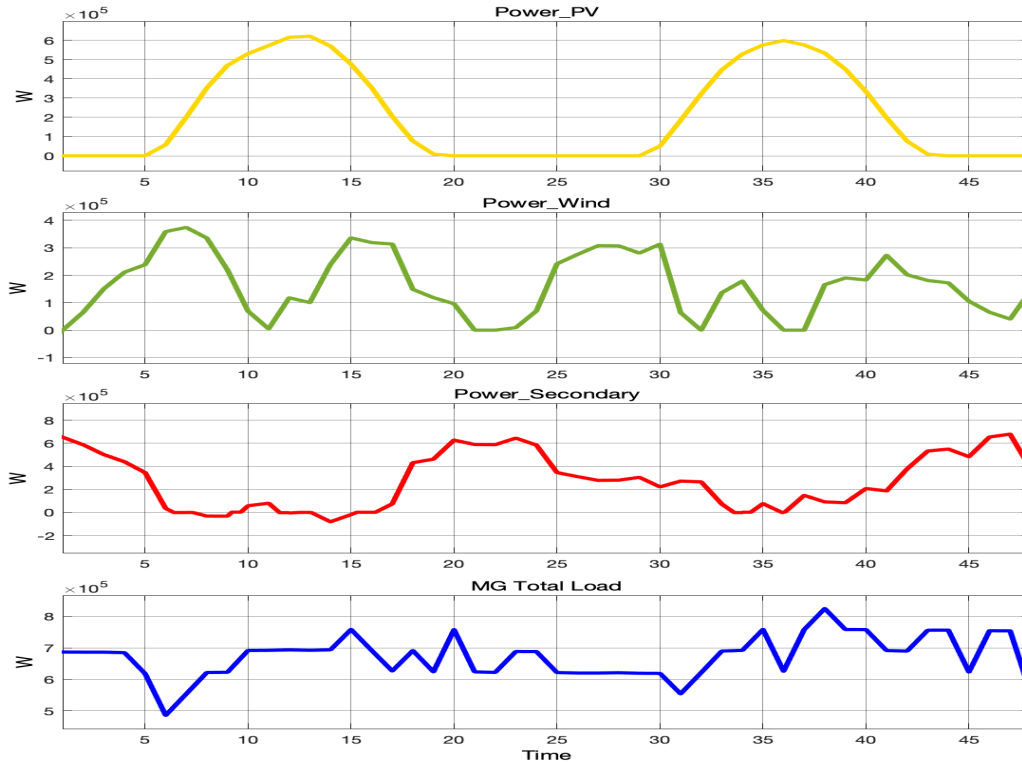


Figure 4.20: Running of case 6.

aggregated microgrid load is much less than the summer case, and the peak load no longer occurs at noon, where it is clear that now the curve is a bit smoother and the demand peaks in the evening particularly 8:00 PM. Furthermore, we should observe that PV generation is much less than the summer season which is expected due to the

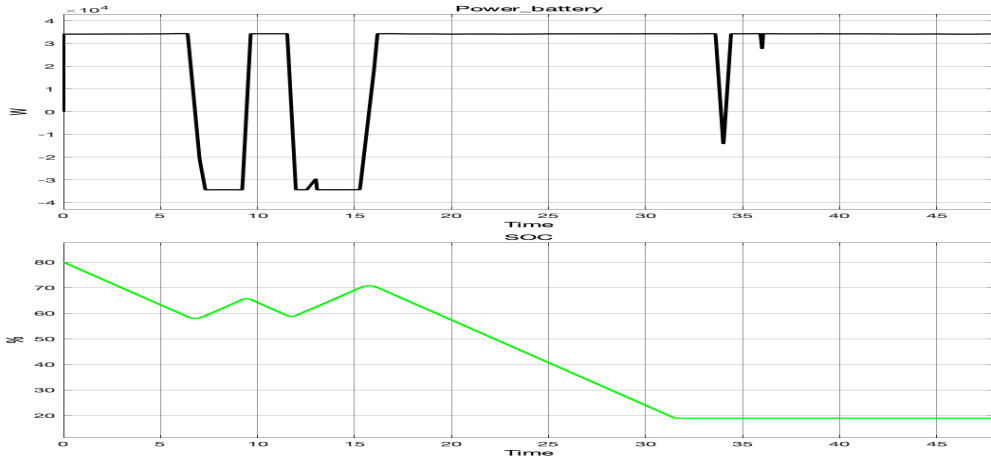


Figure 4.21: Running of case 6, battery response.

fallen irradiance in winter. The battery response is shown in Fig.4.23.

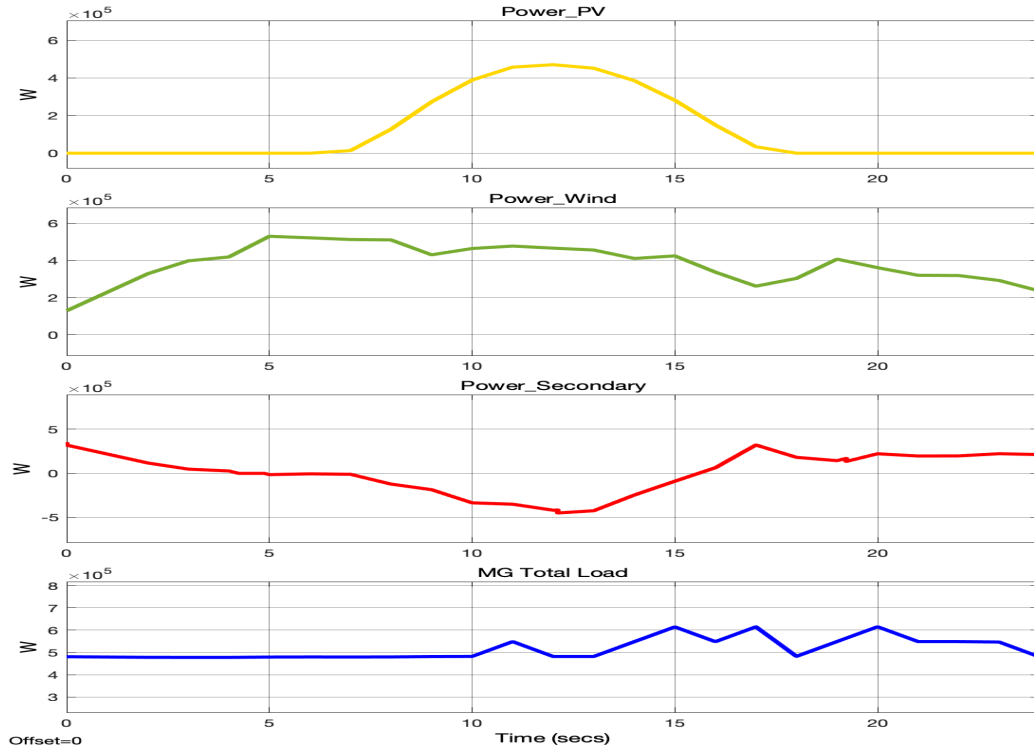


Figure 4.22: Running of case 7.

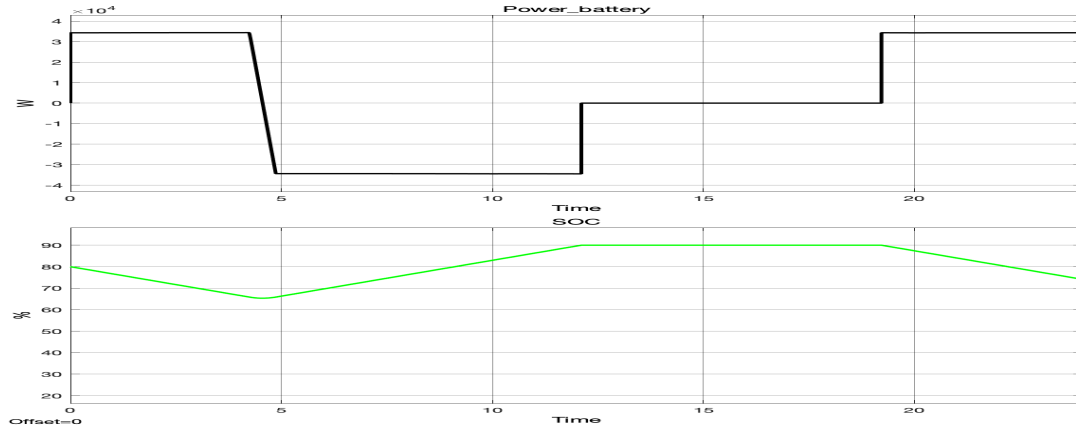


Figure 4.23: Running of case 7, battery response.

4.4.8 Case 8: One Week Run

In this case, a one-week simulation run was tested. The battery size has been changed to 20000 AH. Notice that now the x-axis elongates for the span of 168 hours (Figure 4.24). In this curve, we can observe how cyclic is the demand and PV generation. The wind is a bit varying and highly unexpected, notice the period from 60 to 90, that is more than one day, the wind output was very close to zero for most of the time. The battery response in Figure 4.25 presents many spikes and it is supplying power for almost 65% of the time, which means that extra generation units have to be installed in order to recharge the battery properly.

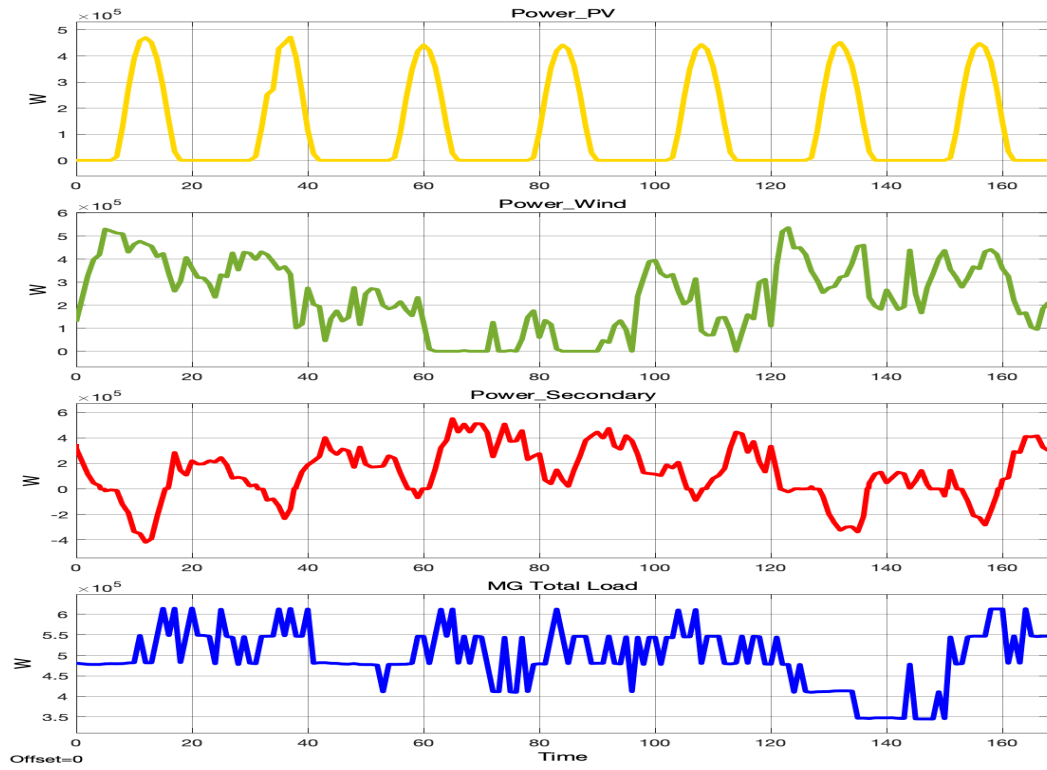


Figure 4.24: Running of case 8.

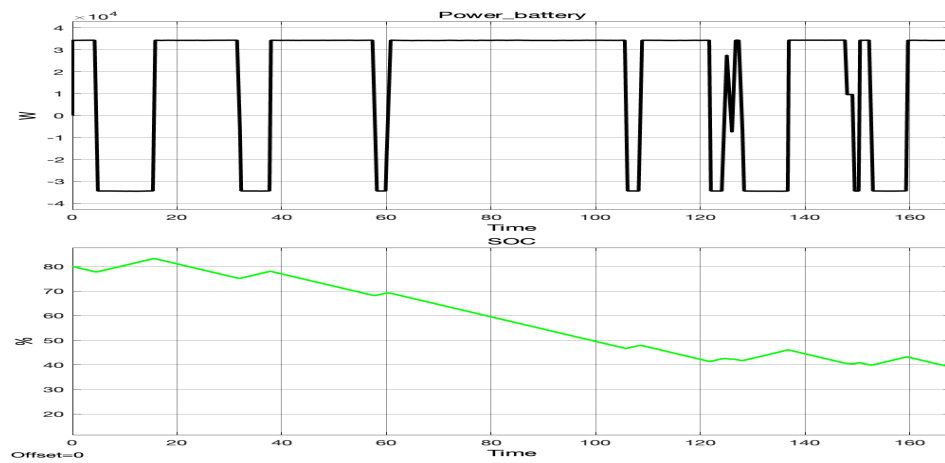


Figure 4.25: Running of case 8, battery response.

CHAPTER 5

INTELLIGENT LOAD PRIORITY LIST

In previous chapters, the load, renewable generation and energy storage systems were modeled and sized. Then, a microgrid test system was proposed to incorporate the different load types and DERs. In the current chapter and the one after it, an improvement in our test-bed will be made. All of the studies will be back-projected and synced applied to our proposed microgrid to enhance its performance. In the present conventional power systems, most failures are occurring at the distribution level. The concept of the microgrid is considered to be a solution to this issue. Microgrids should achieve smart and robust load restoration, in which a decision is made on which load should be supplied first and what are the loads that follow. Faults can occur due to several reasons, starting from natural disasters and equipment failures to human errors and lack of safety measurements. After the occurrence of an outage, the power has to be rapidly restored. One of the aspects of smart restoration is to dynamically

rank the loads to be restored based on many factors. For example, between 1 AM to 6 AM residential loads should be restored prior to the commercial loads, since most shops, restaurants, gyms are closing at that time. Thus, time would be an essential input to determine the criticality of each load at that time. Other inputs are SAIFI, SAIDI, and energy not supplied.

In this chapter, a smart dynamic load priority list (LPL) will be modeled using artificial neural network (ANN), where different categories of loads such as residential, commercial, industrial and hospital will be prioritized for restoration and Demand Side Management (DSM) based on the given time, reliability indices and amount of available energy. The resultant time varying LPL will be used as an input for the DSM studies in the next chapter. A literature review about LPL and ANN will be given in the next section. Then, an introductory material to better understand the deep learning networks is presented. The problem formulation and modeling followed by the results will take place in different sections too.

5.1 Literature Review

Many papers in the literature tackled service restoration in terms of restoration speed [95], minimization of out-of-service loads [96], cost reduction [97] and the possibility of reaching the pre-fault state promptly [98]. However, and to the best of our knowledge, nobody is considering the dynamic LPL that will rank all types of existing loads according to their criticality level. Until now, the LPL is judged based on predefined human decisions. Some system operators try to restore as many loads as possible

without looking into the importance of each load and the time when the fault occurs. Customers who may be ranked top priority include hospitals fire stations, data centers, and police departments. Loads that would be ranked at the bottom of the LPL are for example schools and offices during off-school and off-office hours periods. Therefore, given that the load is dynamic in nature, the LPL should also be fully dynamic.

In [99], Artificial Neural Network (ANN) was used to figure out the optimal reconfiguration of a Radial Distribution System which will minimize the power losses. The authors tested the proposed technique on a 16 bus system and showed that the information about the configuration that will yield the minimum loss could be acquired using the algorithm. In [100], economical, reliability and criticality factors were considered for the service restoration of the distribution network. However, the ranking was fixed, and the concept of dynamical LPL was not discussed. The authors in [101], developed a software planner which helps the system planners and operators to select the next transformer to be repaired when several transformers are due for repair and are out of service. The transformers are prioritized based on the risk reduction that may arise from such replacement; The risk reduction is defined as the minimum number of customers that will be out of supply when such transformer is eventually replaced. Each transformer is ranked based on its risk reduction index, and the program is then run to optimize the restoration of these out of service transformers given stated objective function. A key point of notice is that this work relied on the system loading and reliability data for its modeling formulations.

The authors in [102] proposed a multi-objective evolutionary algorithm (MOEA) to prioritize the switching and restoration of distribution networks [2, 6]. Their work

further entails remote prioritization switching, sequence restoration of the first three priority customers and switching sequence for a vast network. The problem is divided into three stages; In stage 1, they obtained an optimized solution to service restoration using the MOEA where customers and switches are ranked. In phase 2 one of these candidate solutions is selected considering several constraints and is provided to the distribution operator, and in step 3, it finally determines an admissible switching sequence for implementing the chosen solution. The nobility of this methodology is its applicability to vast network without the need for network reduction in short time. In [103], the authors determine the switching sequence of service restoration (SR) in distribution systems using MEAN-MH+ES incorporated with a heuristic optimization technique. This enables them to generate a feasible sequence of switching operation (FSSO) and SR plan (SRP) given the associated constraints. For its analysis, they considered voltage drop and substations loading as relaxed constraints; however, these quantities are only considered if they pose no harm to the network equipment and customers. The algorithm performed well when tested on the real and large-scale DS of Londrina city. It was noted that the relaxed constraint utilized in this algorithm enables a large number of customers to be restored at ones consequently reducing the overall restoration time.

In [104], the author used the Exhaustive Search (ES) approach as a preceding stage before using the Meta-heuristic multi-objective Evolutionary Algorithm with Node-depth encoding (MEAN-MH) to find the optimal solution of service restoration problems. They were able to apply their methods to real large distribution networks. The paper did not take into account the available energy or the various power con-

sumed by individual consumers. The paper in [105] utilizes the quantum-inspired differential evolutionary algorithm to solve power restoration prioritization problem in the smart grid using the permutation-based combinatorial optimization problem to find the maximum load that can be restored at a particular time. It also prioritizes the load and ranks the network generators based on their capacities. This work is shifted more to the generation and transmission side rather than what goes on at the transmitting end.

5.2 Artificial Neural Network

The Artificial Neural Networks (ANN) has been adopted in many physical problems having a relationship between inputs and outputs because the ANN can learn and generalize from a set of input data called the training set or data. A neural network (NN) has network architecture consisting of neurons, connecting strength, nodes properties and updating rules [106]. The NN records fair success if it can accurately learn well and generalized as much as it can. The learning style of the ANN is classified into three; supervised, unsupervised and reinforcement learning styles [106]. In supervised learning, the training sets' input and output are known, and the network learns from this information to form a pattern or model. Reinforcement learning is a particular type of supervised learning where the output of the NN is feedback to the input neurons to influence the learning process. In unsupervised learning, the output of the training set is unknown, and hence the training process is such that network neurons must compete, and the best neurons emerge [107]. This process then determines what

the outputs will be.

Our problem adopts the method of supervised learning since the inputs and output training data are available. We incorporated the algorithm of feed-forward computational topology where the output is not fed back to the input. Unlike the recurrent topology where the output from some nodes of the neurons is fed back as an input to other neurons.

Figure 5.1, shows the architectural layout of the feed-forward topology with multiple inputs, multiple outputs and two hidden layers as used in this work. The letters m and n denote the numbers of output, input neurons corresponding to the training input sets. While i, j and k denote number layers in the input, hidden and output respectively. In this work, the values of $[i, j, k]$ are chosen as $[1, 3, 1]$ for the training set, the n^{th} training input must correspond to the m^{th} training output. The number of neurons in the j^{th} layer is not necessarily equal to the number of neurons in the $(j + 1)^{th}$ layer.

Furthermore, the selection of the number of neurons in the hidden layer is important, and has a direct impact on the learning rate. This could be set using a trial and error method. The other parameter of the ANN that needs to be chosen and properly adjusted are initial weights, learning rate and activation function which can either be linear, sigmoid, signum, sigmoid derivative, etc. Most of these functions are already modeled in MATLAB software tool. The NN toolbox can choose the training error, number of neurons for input and output data sets. It can also by default divide the input data into training sets, validation sets and test set. However, these values can be customized according to the user's application. In this work, we chose (80%,

10%, and 10%) for training sets, validation sets and test sets respectively. Another parameter which can be set or be chosen by default in the NN toolbox is the number of epochs which is the number of times we want the learning to take place.

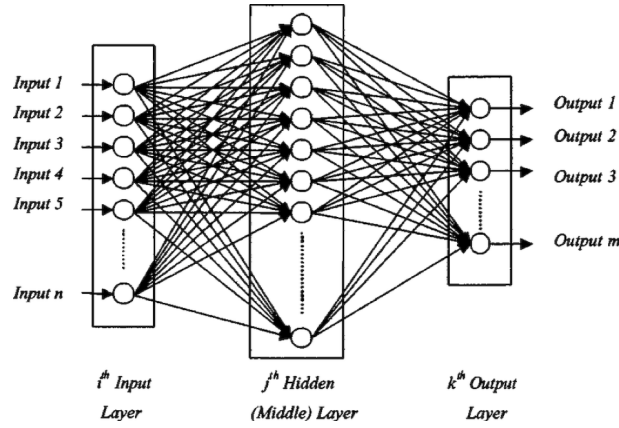


Figure 5.1: Multiple input, multiple output two layers feed-forward computational topology.

5.3 Load Priority List Problem Formulation

After laying out the concept behind ANN, now the neural networks will be used to formulate an intelligent, flexible LPL for reconfiguration and management of micro-grid demands. The list is dynamic in nature, in which the priority of loads changes with time and amount of available energy. However, some loads will always be given the highest priority, for example, hospitals, data centers, fire and police stations. A multi-layered artificial neural network will be used to train the algorithm on the proposed priority scheme. After a long training process, the ANN will be able to take decisions based on the current time, available energy and the status of reliability indices. Figure 5.2 shows the flow of the proposed method. Firstly, after the occurrence of the fault, the time, available energy and reliability indices are inputted. Then, the

ANN processes the inputs and outputs of the proposed LPL for that certain hour. The LPL is dynamic and will change according to the change in the input sets.

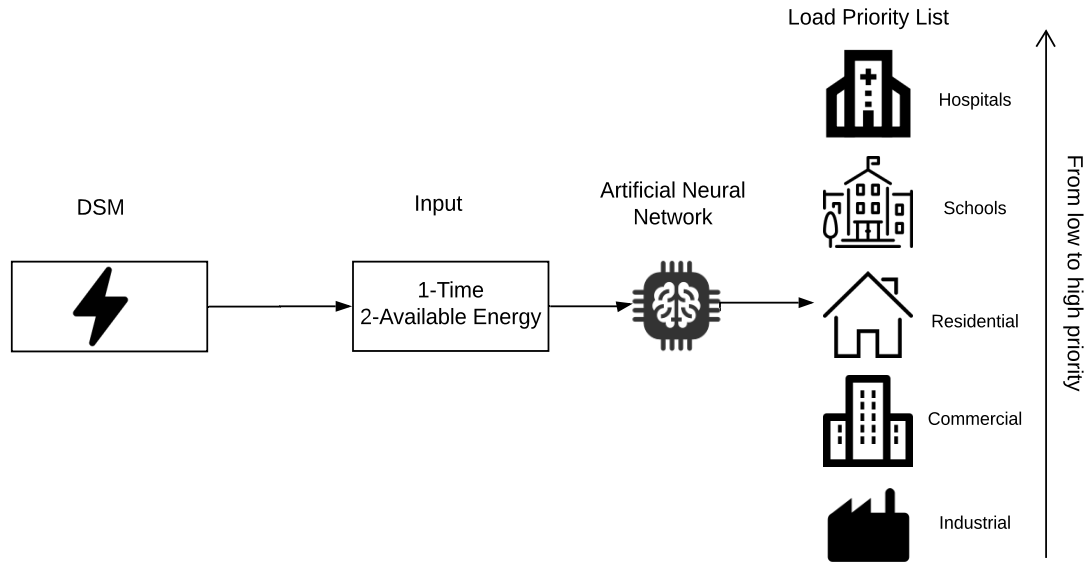


Figure 5.2: Flowchart of the proposed flexible LPL.

The training input consists of four vectors which include: time in hours, System Average Interruption Duration Index (SAIDI), System Average Interruption Frequency Index (SAIFI) and Average maximum load available at each hour for five categories of loads. The same loads of modeled in Chapter.2, and offices and schools loads were taken as a ratio of the commercial load category. Each load category is made of three vectors; SAIFI, SAIDI and average capacities of load consumed by each load corresponding to every hour. Therefore, the total number of training inputs (n) becomes 17. There are five outputs, the order of which correspond to the priority listing. These outputs are the different load categories which include hospital, commercial, industrial, residential, schools and offices. These outputs are encoded with integers 0, 1 2, 3 and 4, as summarized in Table 5.1. It should be noted that this number of coding is only for load representation and doesn't indicate the priority. The reliability indices

Table 5.1: Load categories and corresponding numerical code

Load Category	Assigned Number	Comments
Schools & offices	4	Essential load Schools, offices
Hospitals & fire stations	3	Critical load, always prioritized
Industrial	2	Factories, workshops etc..
Residential	1	Homes, apartments, compounds etc..
Commercial	0	Shops, restaurants, gyms etc..

inputted are System Average Interruption Frequency Index (SAIFI), System Average Interruption Duration Index (SAIDI) and Customer Average Interruption Duration Index (CAIDI). They are formulated in the following equations:

$$SAIFI = \frac{\textit{Total number of all interruptions}}{\textit{Total number of connected costumers}} \quad (5.1)$$

$$SAIDI = \frac{\textit{Total duration of all interruptions}}{\textit{Total number of connected costumers}} \quad (5.2)$$

$$CAIDI = \frac{SAIDI}{SAIFI} = \frac{\textit{Total duration of all interruptions}}{\textit{Total number of all interruptions}} \quad (5.3)$$

The training inputs are formulated as follows:

$$X = [x_1 \ x_2 \ x_3 \ \dots \ x_n] \quad (5.4)$$

Where n is the total number of inputs, 17 in our case (Table 5.2). The variables x_i that form the input elements for the training input and are such that x_1 denotes the hours, and x_{17} denotes the total available energy at that hour. These inputs order are presented in Table 5.2.

Table 5.2: Training input sets

Training input	Load category				
	Industrial	Residential	Commercial	Hospital	Schools and Offices
Load	x_2	x_5	x_8	x_{11}	x_{14}
SAIDI	x_3	x_6	x_9	x_{12}	x_{15}
SAIFI	x_4	x_7	x_{10}	x_{13}	x_{16}

Also, the inputs:

$$x_1 = Time \quad (5.5)$$

$$x_{17} = Total\ Available\ Load\ at\ Hour\ x_1 \quad (5.6)$$

The training output is formulated as follows:

$$Y = [y_1\ y_2\ y_3\ y_4\ y_5] \quad (5.7)$$

The inputs must be totally made with the hours which is the first input. The number of entries corresponds to the number of hours. The used training set is for one month period, corresponding to 720 hours. The detailed annual, seasonal, monthly and daily energy data for all load categories are presented in chapter.2.

5.4 Simulation Results and Discussion

At this stage, each load category has been assigned a certain number. The order of the numbers does not represent the criticality level. The assigned numbers and the corresponding load categories are shown in Table 5.1. The general criticality structure as assumed is shown in Table 5.3. According to the table, hospitals will always be

Table 5.3: Load criticality levels

Criticality levels	Examples
High	Hospitals, fire station
Medium high	Schools and offices (working hours)
Medium	Industrial, commercial and residential
Low	Schools, offices and commercial (off hours)

given the highest priority independent of time. This will be reflected on the results later, where hospitals will always appear on the top of the LPL. Schools and offices are given higher priority during working hours than all other loads, but of course less priority than the hospital. All other loads, i.e., residential, commercial and hospital have a medium priority that is also affected by the time of the day and the time of the week. The ANN deals with the hourly load, that is for every hour a LPL will be generated. Thus, for example, June has 720 hours, and hence the LPL will be created 720 times to provide the system operator with an hour by hour list that will facilitate taking actions in case of load management or restoration.

The results of the network showing the LPL at different times are shown below. Figure 5.3, shows the proposed LPL for restoration. Note that $t=15$ is Saturday, the first day of the month at 3 PM, which is a working day in Saudi Arabia. It is observable that hospitals have the highest priority followed by schools & offices then commercial, industrial and residential respectively. This makes sense, as this hour is considered a working hour and thus schools & offices were given higher importance than other loads. Figure 5.4, shows the LPL for hour 60 which is Monday 12 at noon. Although it is a different hour on a different day, but the characteristics of that day and hour are similar. By similar, we mean that it is working hours and it is not

a weekend. On the hour 136 for example, Figure 5.5, residential loads gained the second highest importance after hospitals, whereas schools and offices had the least importance level. The reason is that, although hour 136 is at 4 PM which is considered working hours but it is on Thursday, which is a weekend in Saudi Arabia and thus the ANN learned that on weekends schools and offices should not be prioritized. An interesting behavior occurred at hour 156, which is noon of Friday (Figure 5.6). Since it is Friday prayer time in Saudi Arabia and all shops freeze between 10 AM to 1 PM at that time the commercial load category was given very low importance alongside with the schools & offices category. However, at hour 160 which is 4 PM on the same day, the commercial load sector regained importance and jumped to the third level instead of fourth. In other words, the commercial load retrieved its original position before the interruption of the Friday prayer. The residential was of high priority at that hour because it is a weekend at that time. The structure of our neural network is shown in Figure 5.8. Four layers were used in the network, and a different number of hidden neurons is assigned to each layer. The first and last layers are the inputs and outputs, respectively and the rest of layers are hidden between the first and the second layer. The gradient and validation checks of the network are shown in Figure 5.9. The regression plot of the training, testing and validation process are shown in Figure 5.10. The regression shows how close the validation is to the real inputted data and the presented network shows an excellent regression. The performance of training, testing and validation process is plotted in Figure 5.11. The Mean Square Error (MSE) of the validation function achieved is 0.6616.

All in all, an intelligent flexible LPL is proposed for smarter load restoration.

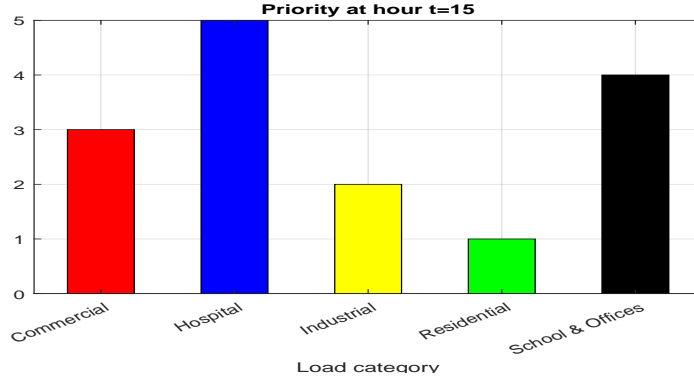


Figure 5.3: Priority list when $t = 15$

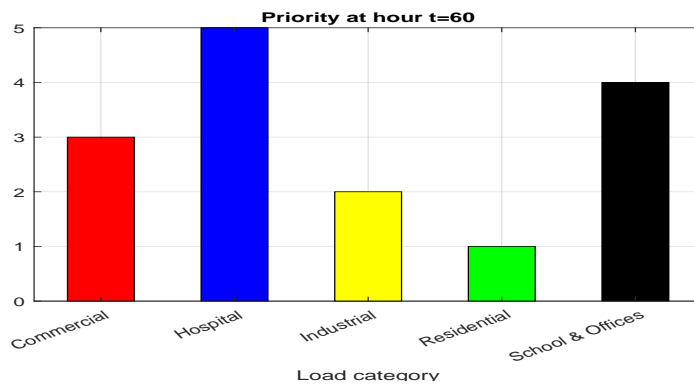


Figure 5.4: Priority list when $t = 60$

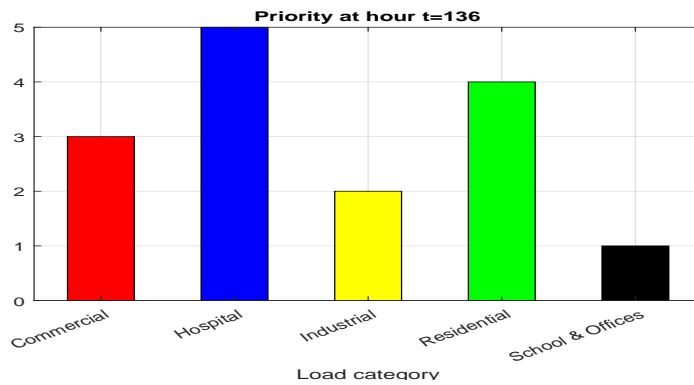


Figure 5.5: Priority list when $t = 136$

Artificial Neural Network (ANN) is used to extract the model of the system according to the given inputs and outputs. Multiple inputs were considered such as reliability indices SAIDI, SAIFI and CAIDI. Time and available energy to feed the system at that time were inputs too. The output was the LPL, which dictates the prioritization

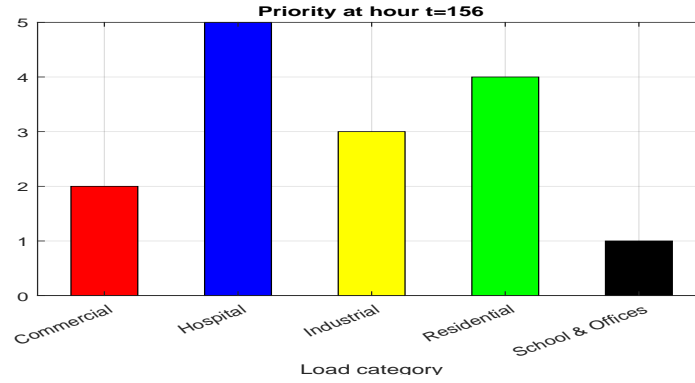


Figure 5.6: Priority list when $t = 156$

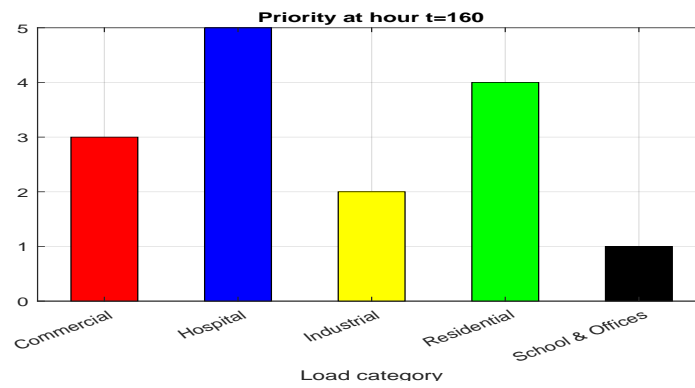


Figure 5.7: Priority list when $t = 160$

of supplying the different load categories according to the given inputs. From the results, it is shown how the list is flexible in the sense that it assigns high priority to some loads at certain times and lower priority at another. The list was tested under different hours and days conditions, and the results of different cases were thoroughly discussed. The technique is tested and validated showing a very small Mean Square Error (MSE).

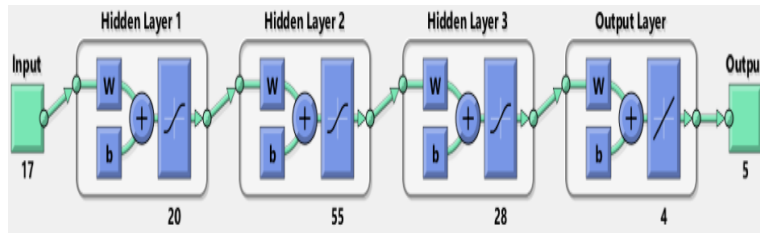


Figure 5.8: Network Layers

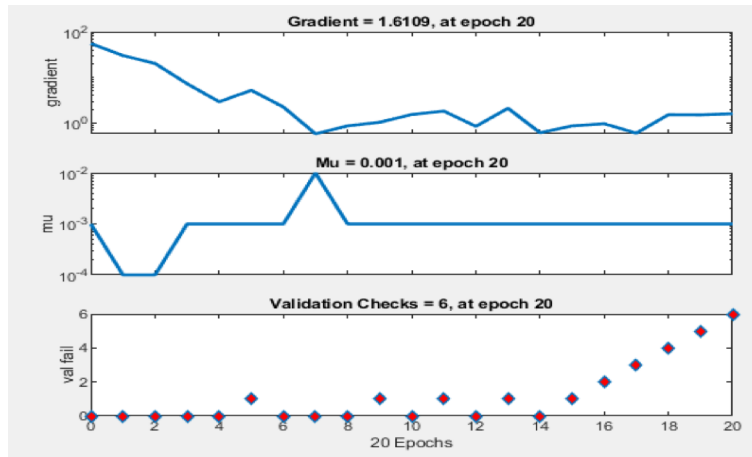


Figure 5.9: Gradient of the neural network

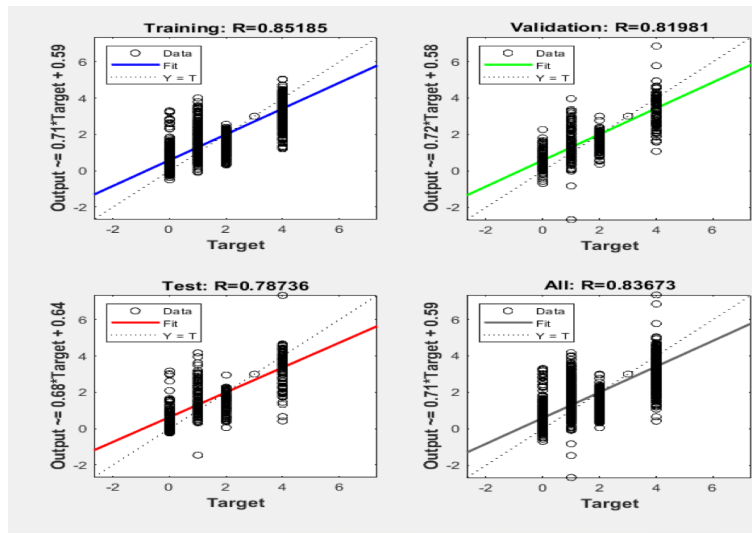


Figure 5.10: Regression of the neural network

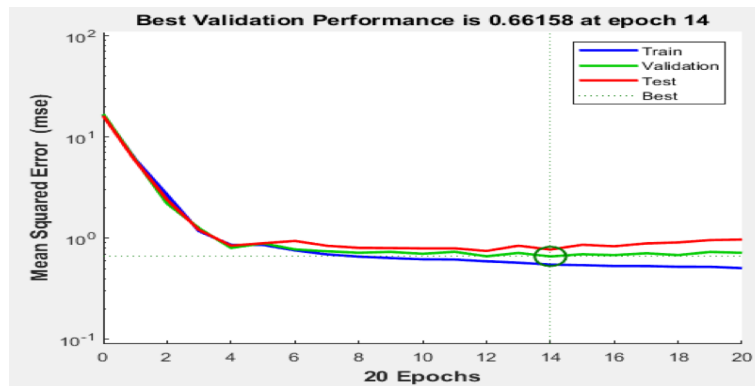


Figure 5.11: Performance of the neural network

CHAPTER 6

DEMAND SIDE MANAGEMENT SCHEMES

Usually, the installed capacity is sized based on the peak demand, which occurs only for a very brief period during the year. Thus, a considerable amount of the generation capacity is not fully utilized when under commissioning, which causes expenses to the utility even if these generators are not running. Therefore, the concept of Demand Side Management (DSM), Demand Response (DR) came to address the issue of this variability. DSM is the process of encouraging electricity costumers to shift or reduce their energy usage according to the utilities instructions and preferences. It is beneficial to both costumes and utilities. On the user side, they can eventually overcome their electricity bill by enrolling to the DSM scheme enforced by the retailer, which is usually incentivized. On the utility side, peak loads can be shifted, and the valleys of the load profile can be filled to smooth the demand curve which will turn increase the efficiency and reliability of the system (Figures.6.1, 6.2 & 6.3). In fact, advanced

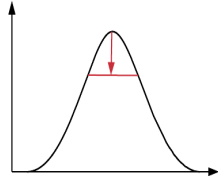


Figure 6.1: Peak shaving

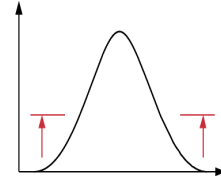


Figure 6.2: Valley filling

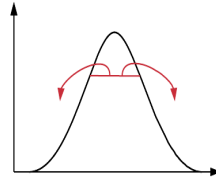


Figure 6.3: Peak shifting

metering infrastructure (AMI) have had made it possible for utilities to acquire precise information about energy use on the customer side. Thus, pre-programmed devices can perform specific steps to shed and mitigate loads when there is a sudden increase in demand or a contingency in generating units. Ergo, assisting utilities not to bear the costly investments such as building generation plants, buying from the spot market or call options. According to [108], the application of DSM by 459 utilities in the USA saved them 50.6 billion kilowatt hours (kWh). There are many other advantages for adopting DSM such as increased reliability, reduced cost, improved market, and higher efficiency.

In this chapter, different DSM schemes will be formulated. The microgrid test-bed will run every case to see the effect of the DSM on the overall system performance. An energy balance based DSM will be firstly implemented, then the LPL acquired previously will be used as an input for the DR decisions. After that, peak shaving and valley filling DSM will be applied and tested using the test system designed previously.

A detailed literature survey about DSM was introduced in Section.1.4. Introductory material about FL will be provided in the next section followed by case studies of different DSM schemes.

6.1 Fuzzy Inference Systems (FIS)

Fuzzy logic is a method to match a set of input and output data. The rules for that matching can be imprecise, maybe not in the form of numbers such as linguistic variables. Thus, a rigid systematic for the method is not needed as this method will handle the semi-truth and uncertain matching to attain a low cost and robust solution. FL was firstly introduced by Lotfi Zadeh in 1965. The operation principle is as follows: for each fuzzy variable a number of Membership Function (MF) on its x-axis will be formulated, referred to as universe of discourse, the range of MF is from 0 to 1, which is the y-axis. Different shapes of the MFs exist: Gaussian, z-shaped, sigmoidal and trapezoidal and the type should be chosen based on the user's application. A mathematical representation of FL can be modeled as follows:

$$L = \{(x, \mu_L(x)) | x \in X\} \quad (6.1)$$

where L is the fuzzy set, $\mu_L(x)$ is the membership function and X is the universe of discourse. Based on the MFs a set of if-then rules are applied to link the input and the output as follows:

$$If < (antecedent) > Then < (consequent) > \quad (6.2)$$

Thus the process of FL involves: 1) fuzzifying the inputs and applying the fuzzy operators (and, or, or not), 2) Applying the result to the consequent.

By applying the previous concept to our problem, the list of inputs and outputs has to be determined. In most case studies that will be done in the coming sections, our inputs will be time, the energy balance equation as shown in Eq.4.1 and the LPL result that was formulated and acquired in Chapter.5. All of these inputs are sent to a black box and later mapped with the output, which is in our case; the amount of load curtailed and from which load type the curtailment should be implemented (Figure 6.4).

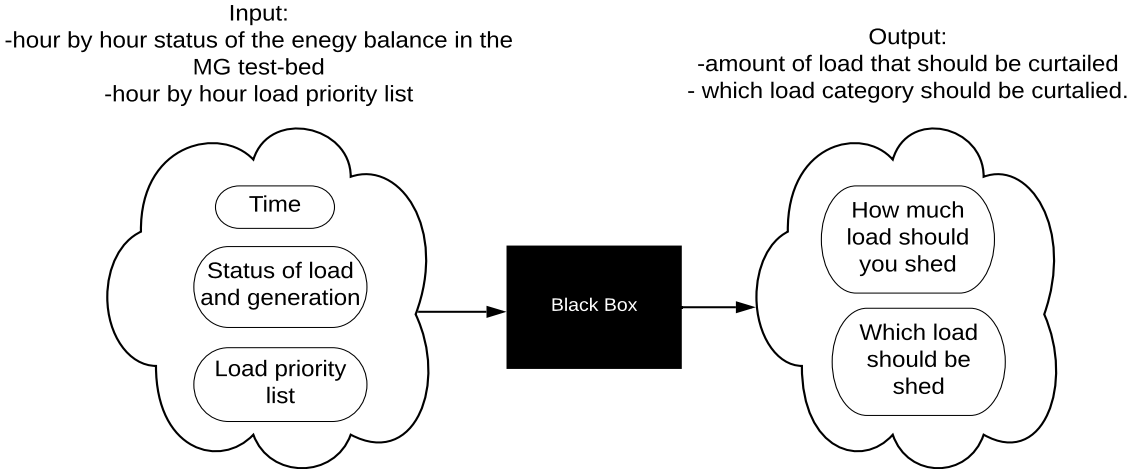


Figure 6.4: FL mapping of input and output spaces.

6.2 Implementation and Evaluation of Demand Side Management Schemes

Load and renewable generation are changing continuously. Microgrids must be able to supply the loads at all times and under all conditions. Different actions can be taken to ensure a safe and adequate flow of energy to the consumer. Sometimes it is very expensive to install a generation reserve which will run only for a few hours when the demand peaks. The proposed microgrid test-bed can incorporate any study. An intelligent, flexible LPL was integrated as an additional feature to enhance the system and make it smarter. The hourly changing intelligent priority list will let the decision maker know which loads are interruptible and which are not. In this section, an extra study will be performed in the system, which is developing and testing different DSM programs for the sake of increasing energy security and ensuring an improved load factor. Due to the existence of multi-variables in this problem which are the time of the day, energy balance and load LPL, a FL controller based model will be formulated to achieve DSM. FL will be used in three cases out of the upcoming six cases. All of the case studies are implemented on one-day time span, 24 hours, and that day is 28th of June. The following table summarizes the examined cases (Table 6.1).

Table 6.1: DSM case studies

Case	DSM	Load priority list	Fuzzz logic
1	Energy Balance	NO	YES
2	Energy Balance	YES	YES
3	Peak shaving of each load	YES	NO
4	Peak shifting	YES	NO
5	Peak shaving of aggregated load	YES	NO
6	Residential AC	NO	YES

6.2.1 Energy Balance Based DSM

The microgrid should be able to independently supply its loads, however, sometimes it is just not feasible to install new generation capacities which will only be utilized for a few hours in the year. Thus, the microgrid utilizes its coupling with the utility to buy electricity in case of any discrepancies. It will also supply electricity to the utility if the local generation is higher than the current demand. As observed from the behavior of our demand modeled in Chapter.2 is that it usually peaks in the middle of the day and it is higher between 4-11 than it is from 12 to 7 AM and the main reason is because of air-conditioning loads. As a result, the price of energy at peak times is certainly higher than low demand periods. The energy balance based DSM model that we are proposing aims to reduce the amount of power bought from the utility by

shedding some of its unimportant loads. The amount of shedding will be more severe for the high priced tariff periods and will be more relaxed for cheaper ones. The tariff of buying from the utility is illustrated as follows:

$$C_{utility} = \begin{cases} E(t) \times T_{low}, & 0 \leq t < 10 \\ E(t) \times T_{high}, & 10 \leq t \leq 16 \\ E(t) \times T_{medium}, & 16 < t < 24 \end{cases} \quad (6.3)$$

where t is the time in hours, $C_{utility}$ is the cost of buying power from the utility. E is the energy bought and T_{low} , T_{medium} and T_{high} are the low, medium and high electricity tariff, respectively, based on the time of the day. The difference equation that will determine the load-supply situation and the percentage difference is:

$$P_{difference}(t) = \frac{P_{load}(t) - P_{DER}(t)}{P_{load}(t)} \times 100 \quad (6.4)$$

where $P_{load}(t)$ is the load power at time t defined in Eq.4.2 and $P_{DER}(t)$ is total power generated in the microgrid at time t , defined as:

$$P_{DER}(t) = P_{PV}(t) + P_{Wind}(t) + P_{battery}(t) \quad (6.5)$$

Hence, if $P_{difference}(t)$ is positive, then the demand is higher than the total load at that time, and it is negative when the load is higher.

Having the idea and the goal laid out, the fuzzy system was designed to decide the amount of shedding needed to reduce the total expensive power bought from the

utility. The inputs and outputs of the FL are shown, alongside with the membership functions (Figure 6.5-6.7). The load and generation of the microgrid before and after DSM is shown in Figure 6.8. An interesting results are observed in this case, where approximately at the period from 9:30 to 11 (period 2 (P_2)) the MG load was higher than the supply, the system rapidly spotted that increase and reacted with a load shedding of about 15% to let the local generation cover the total demand preventing the incident of buying from the grid at this critical time. Load shedding was also done in periods 1 (P_1) and 3 (P_3), but the severity of the shedding is relaxed; however, it is stronger in P_3 than in P_1 although the imbalance of supply and demand is almost the same. The percentage of curtailment at each hour is shown in Figure 6.10 and the load before and after the shedding is shown in Figure 6.9. The 3-D surface of the FL rules is a good window to understand the general mapping of the inputs and output (Figure 6.11). It shall be mentioned that in this case, we are shedding the loads as bulk without going into the details of each load category (Table 6.2). The energy sum bought from the utility decreased from 6.28 MWh to 3.7 MWh and the power bought during the most expensive period was minimized. The detailed fuzzy rules are listed in Appendix.B. The microgrid response is shown in Figures.6.12-6.13.

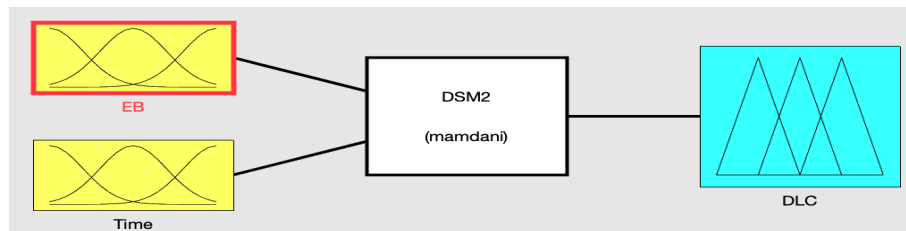


Figure 6.5: Case 1: FL input and output variables.

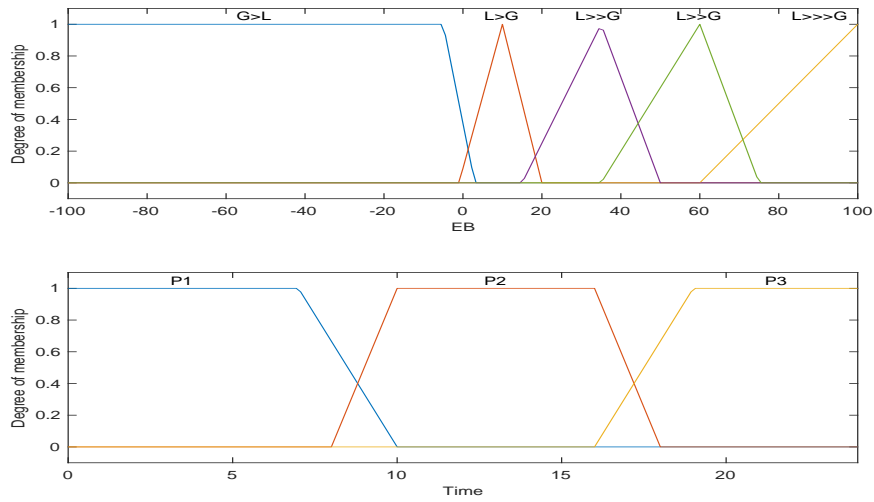


Figure 6.6: Case 1: Membership functions of the FL input.

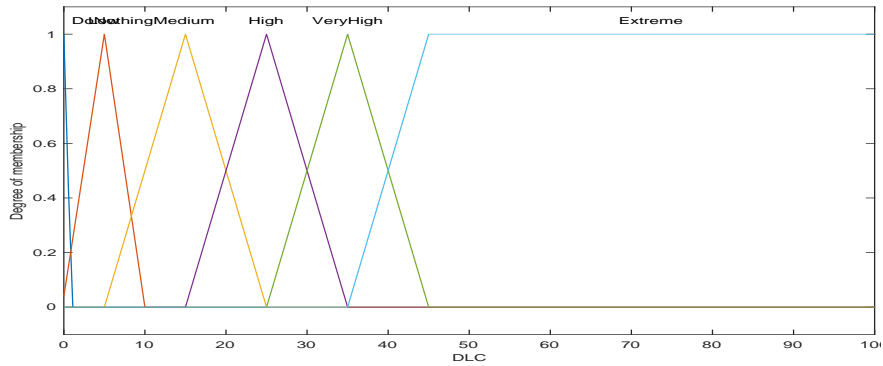


Figure 6.7: Case 1: Membership function of the FL output.

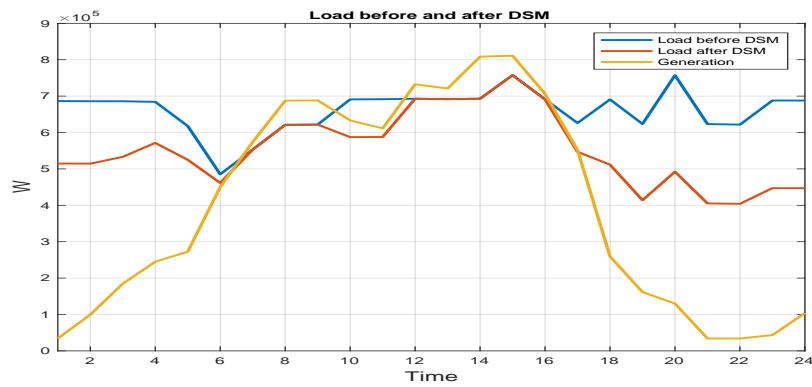


Figure 6.8: Case 1: MG Load and generation before and after DR.

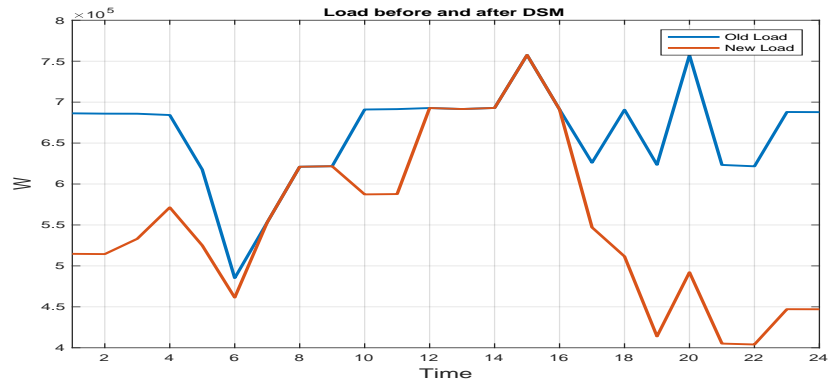


Figure 6.9: Case 1: MG Loads before and after DR

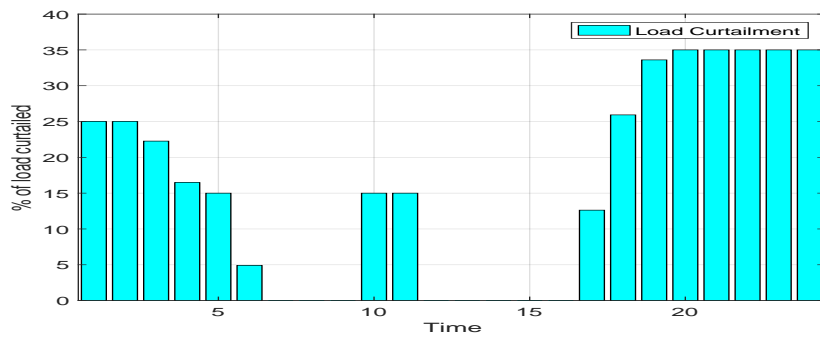


Figure 6.10: Case 1: Percentage of curtailment.

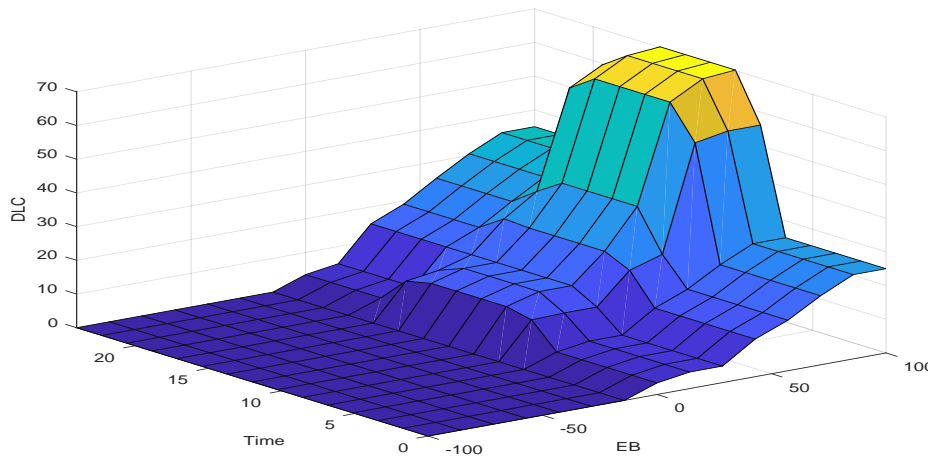


Figure 6.11: Case 1: Surface of the FL rules.

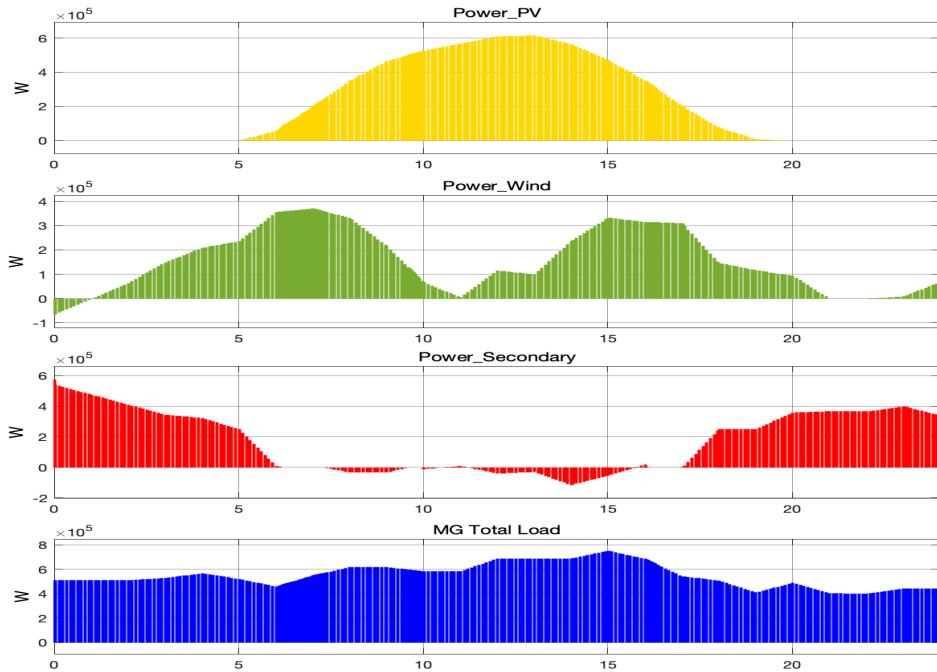


Figure 6.12: Case 1: MG test-bed response to the DSM.

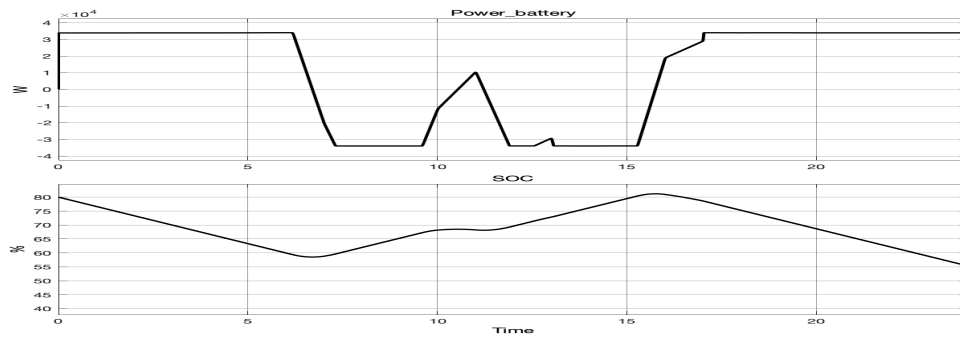


Figure 6.13: Case 1: MG test-bed battery response to the DSM.

6.2.2 Energy balance Based DSM Incorporated With LPL

In this case, the same formulation as the previous case will be considered, provided that an extra input will be added which is the LPL and thus now our output will be shedding the loads according to their situation in the LPL, hence four outputs will be considered; one for each load type (Figure 6.14-6.16). The number assigned to each load category is found in Table 5.1. The model succeeded to eliminate the

Table 6.2: Inputs and outputs of energy balance based DSM

Inputs to the FL system		Output of the FL system	
Hour	$P_{difference}(\%)$	Period	Curtailement (%)
1	95.03	P1	25
2	85.47	P1	25
3	73.07	P1	22.27
4	64.21	P1	16.48
5	55.87	P1	15
6	7.23	P1	4.91
7	-3.73	P1	0
8	-10.68	P1, P2	0
9	-10.71	P1, P2	0
10	8.36	P1, P2	15
11	11.59	P2	15
12	-5.74	P2	0
13	-4.25	P2	0
14	-16.67	P2	0
15	-7.06	P2	0
16	-2.19	P2, P3	0
17	11.83	P2, P3	12.63
18	62.42	P2, P3	25.93
19	74.08	P3	33.61
20	82.83	P3	35
21	94.52	P3	35
22	94.51	P3	35
23	93.69	P3	35
24	84.89	P3	35

power bought from the utility at P_2 , while applying the LPL which is shedding only the interruptible loads (Figure 6.17). Notice that the shedding occurred between 9:30 and 11 AM was done by reducing the residential load by 22% and the industrial and commercial loads by 10%. The reason is that at that hour the residential was the least in priority and thus the curtailment of it was the highest. Conversely, from 20 to 23 shedding occurred to the industrial by 60% and to the commercial by 45% and the reason why the shedding was severe is because of the high difference between demand and supply (Figure 6.18-6.20). Some periods has no curtailment at all and

the reason is that the demand falls within the generation range. Referring to Figure 6.21, we shall observe that the hospital load profile before and after DSM was the same and the reason that it was always at the top of load LPL. The shedding in industrial load was higher in P_3 than in P_2 and in P_2 than in P_1 and the main reason is its order in the LPL. The 3-D surfaces of the FL rules are shown in figures.6.22-6.23. To easily track the energy difference, the curtailment and the priority of each load category refer to Table 6.3. The energy sum bought from the utility decreased from 6.28 MWh to 1.9 MWh and the power bought during the most expensive period was minimized. Priority 1 indicates that the priority order is: hospital, residential, industrial then commercial, while priority 2 means: hospital, commercial, industrial then residential. Priority 3 is hospital, residential, commercial then industrial, while priority 4 is hospital, commercial, residential then industrial. The microgrid response is shown in Figures.6.24-6.25. The detailed fuzzy rules are listed in Appendix.B.

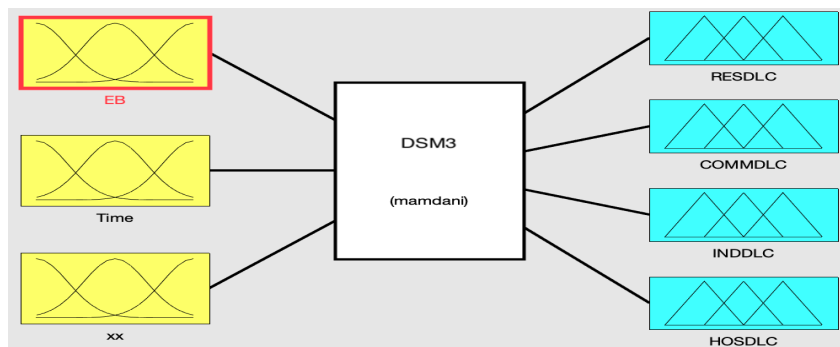


Figure 6.14: Case 2: FL input and output variables.

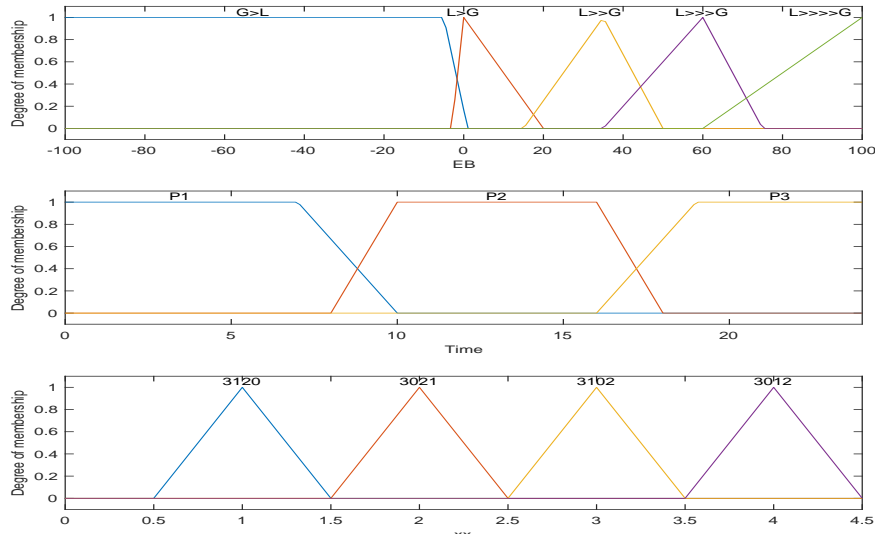


Figure 6.15: Case 2: Membership functions of the FL input.

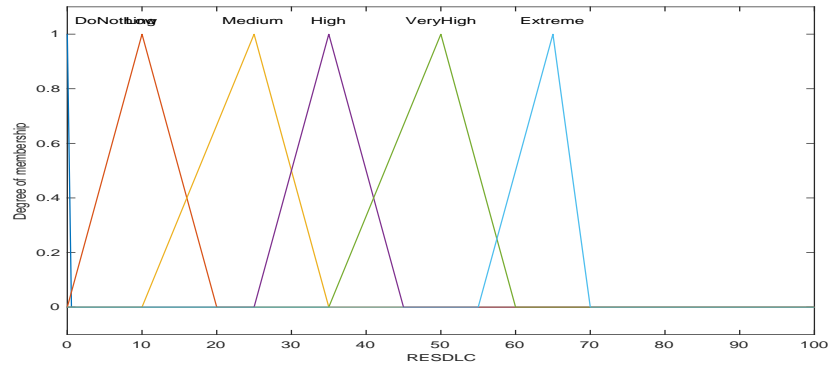


Figure 6.16: Case 2: Membership functions of the FL output.

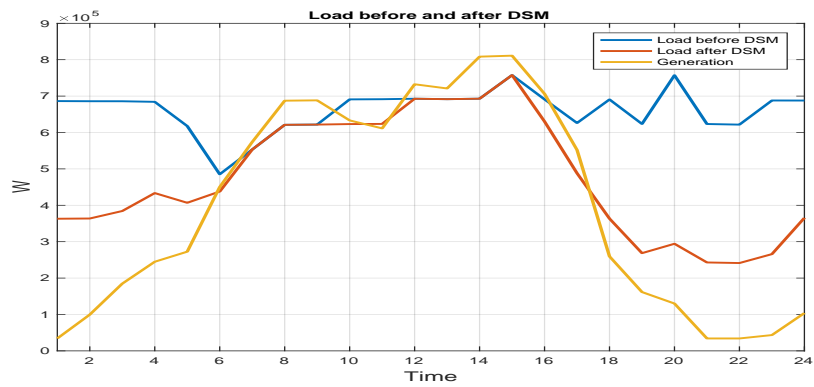


Figure 6.17: Case 2: MG Load and generation before and after DR.

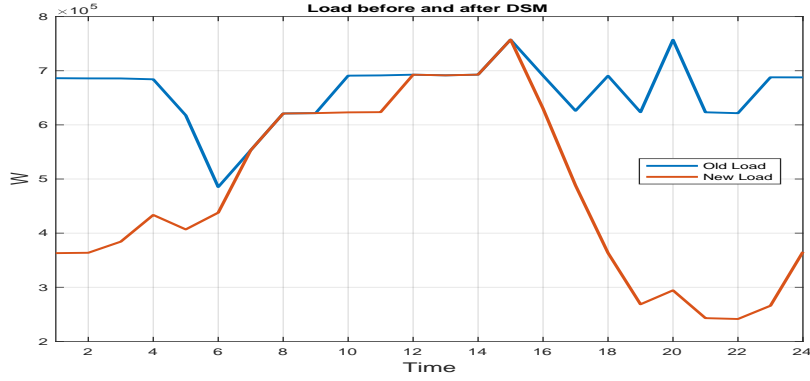


Figure 6.18: Case 2: MG Loads before and after DR

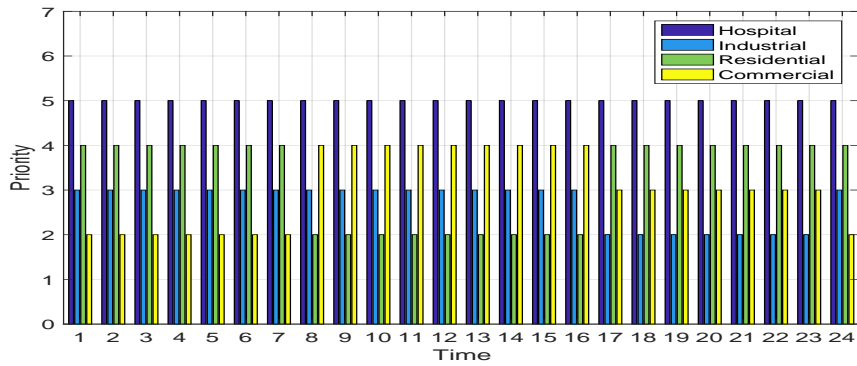


Figure 6.19: Case 2: Priority of each load category.

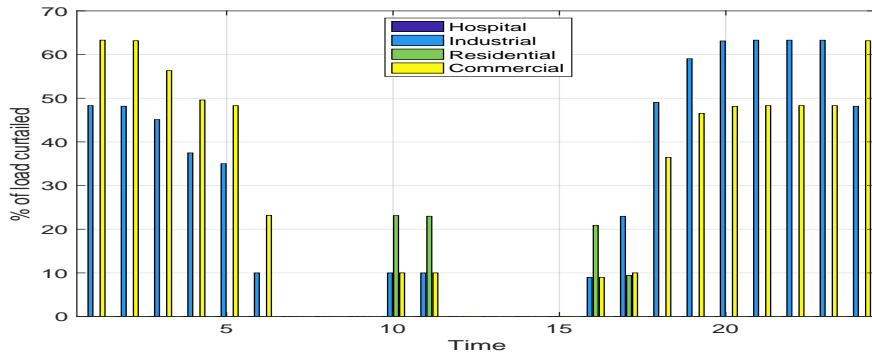


Figure 6.20: Case 2: Percentage of curtailment of each load category.

6.2.3 Peak Shaving LPL based DSM on Each Load Category

In this case, the peak of each load type will be clipped (Figure 6.1). The clipping amount is subjected to the load priority list. That is, if the peak of a certain load

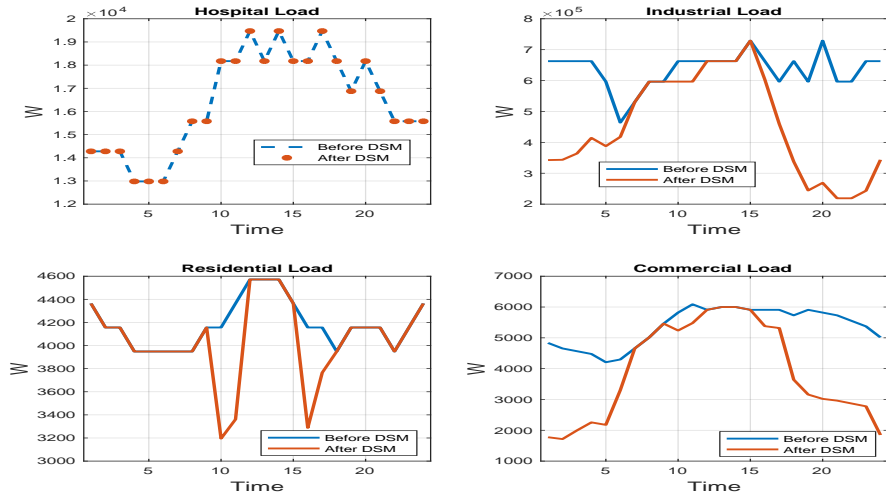


Figure 6.21: Case 2: Load profile of the four load types before and after DSM.

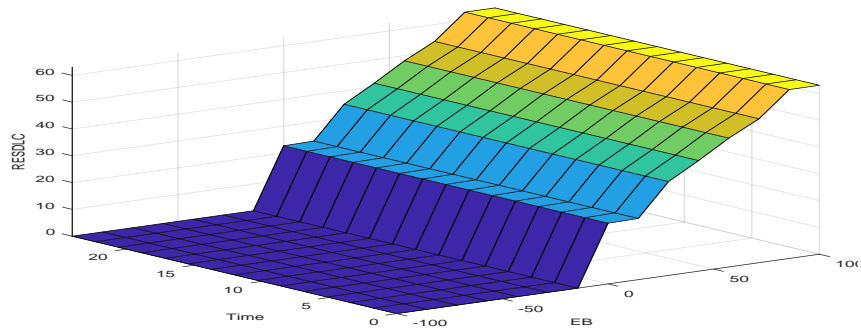


Figure 6.22: Case 2: Surface of the FL rules with time as x-axis.

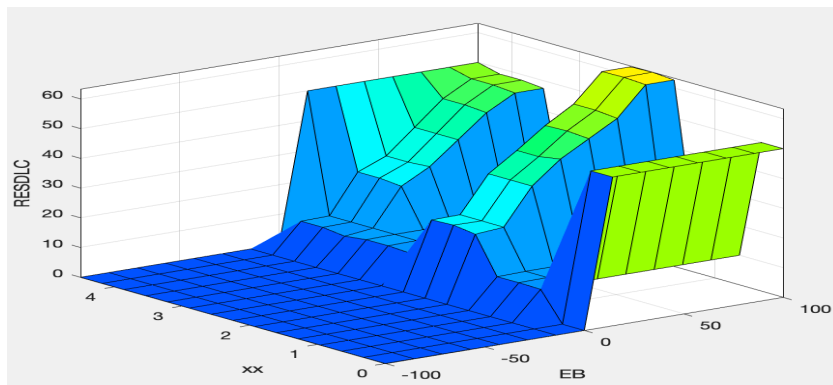


Figure 6.23: Case 2: Surface of the FL rules with priority as x-axis.

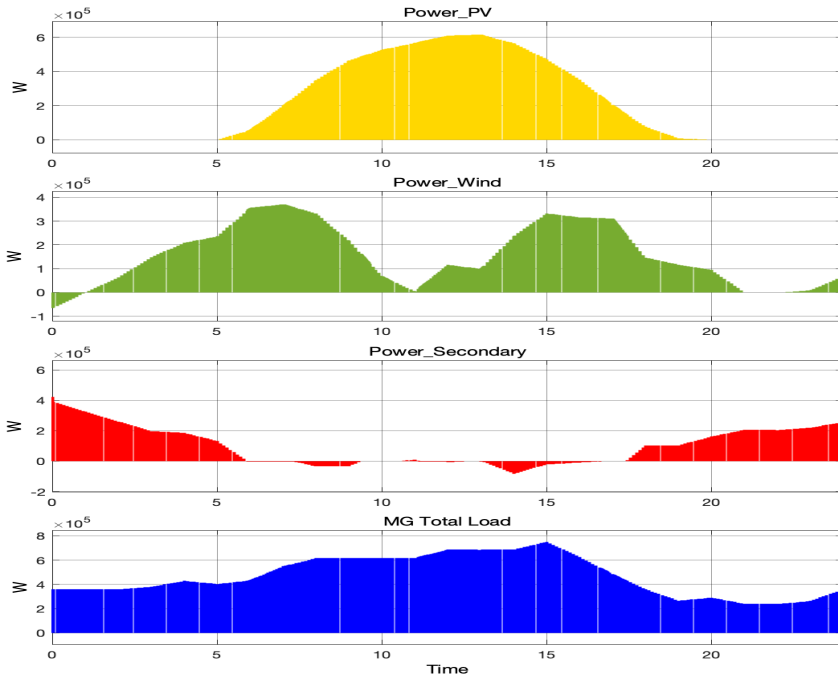


Figure 6.24: Case 2: MG test-bed response to the DSM.

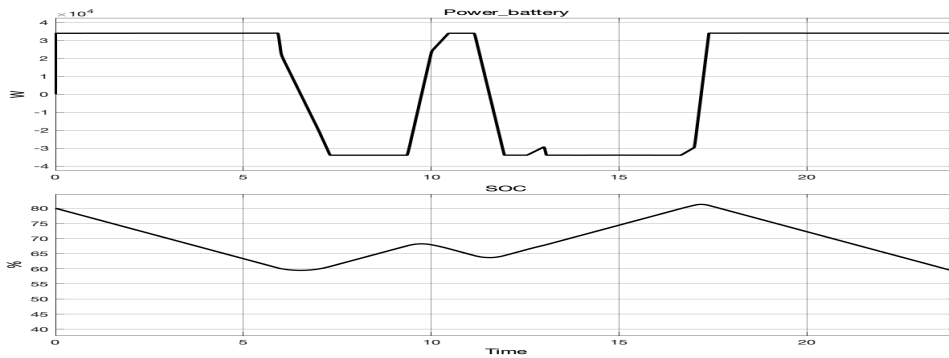


Figure 6.25: Case 2: MG test-bed battery response to the DSM.

category occurs while the load is at the bottom of the priority list then its peak will be clipped with a high percentage rate, whereas if the peak of that load type occurred while it was listed top in priority then no curtailment will be done to that load. Note that here, we deal with the peak of each load type not the peak of the aggregated microgrid load. The aggregated load before and after the peak shaving is shown in Figure 6.26 and the peak shaving of each load type is shown in Figures.6.27-6.30. Note

Table 6.3: Inputs and outputs of energy balance based DSM with LPL

Hour	Inputs to the FL system			Outputs of the FL system (Curtailed(%))			
	$P_{difference}(\%)$	Period	Priority	Residential	Commercial	Industrial	Hospital
1	95.02550117	P1	1	0	63.30	48.31	0
2	85.47	P1	1	0	63.17	48.17	0
3	73.07	P1	1	0	56.31	45.11	0
4	64.21	P1	1	0	49.60	37.48	0
5	55.87	P1	1	0	48.29	35	0
6	7.23	P1	1	0	23.17	10	0
7	-3.73	P1	1	0	0	0	0
8	-10.68	P1,P2	2	0	0	0	0
9	-10.71	P1,P2	2	0	0	0	0
10	8.36	P1,P2	2	23.13	10	10	0
11	11.59	P2	2	22.98	10	10	0
12	-5.74	P2	2	0	0	0	0
13	-4.25	P2	2	0	0	0	0
14	-16.67	P2	2	0	0	0	0
15	-7.06	P2	2	0	0	0	0
16	-2.19	P2,P3	2	20.90	8.97	8.97	0
17	11.83	P2,P3	3	9.41	10	22.97	0
18	62.42	P2,P3	3	0	36.45	49.06	0
19	74.08	P3	3	0	46.54	59.04	0
20	82.83	P3	3	0	48.12	63.11	0
21	94.52	P3	3	0	48.30	63.30	0
22	94.51	P3	3	0	48.30	63.30	0
23	93.69	P3	3	0	48.29	63.29	0
24	84.89	P3	1	0	63.16	48.16	0

that the hospital peak was not clipped and this is due to the effect of LPL. The daily load factor of each load type, which was defined in Eq.2.4, have increased except for the hospital load (Table 6.4). The microgrid response is shown in Figures.6.31-6.32 and the energy sum bought from the utility decreased from 6.28 MWh to 5.99 MWh

Table 6.4: Daily load factor before and after peak clipping

Load type	Before DR	After DR	Energy curtailed (KWh)
Residential	91.48	94.52	1.372
Commercial	88.17	89.07	0.609
Industrial	87.12	94	291.64
Hospital	84.17	84.17	0

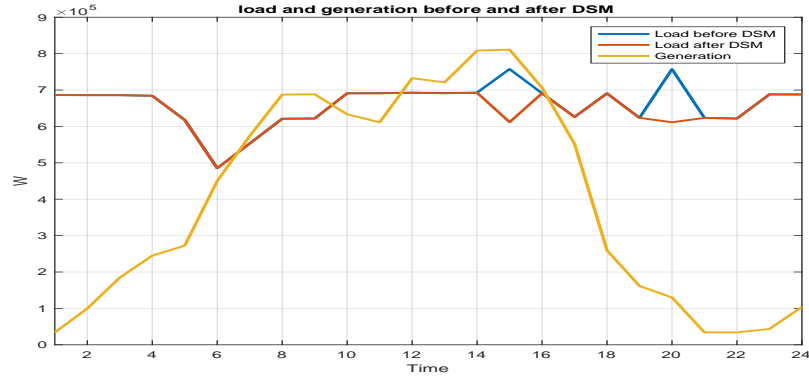


Figure 6.26: MG Loads before and after peak shaving.

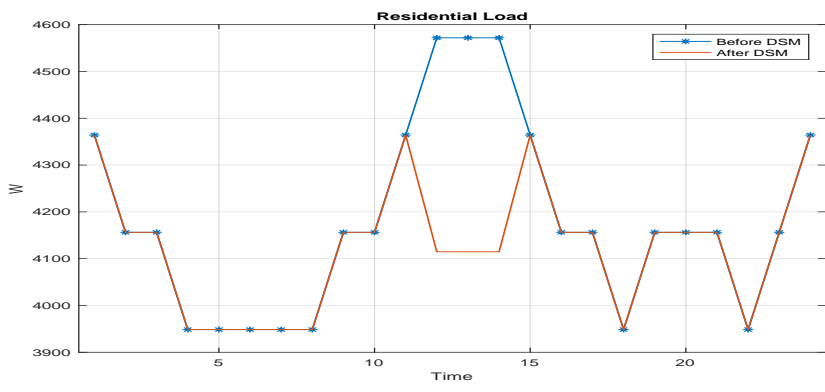


Figure 6.27: Residential load peak shaving.

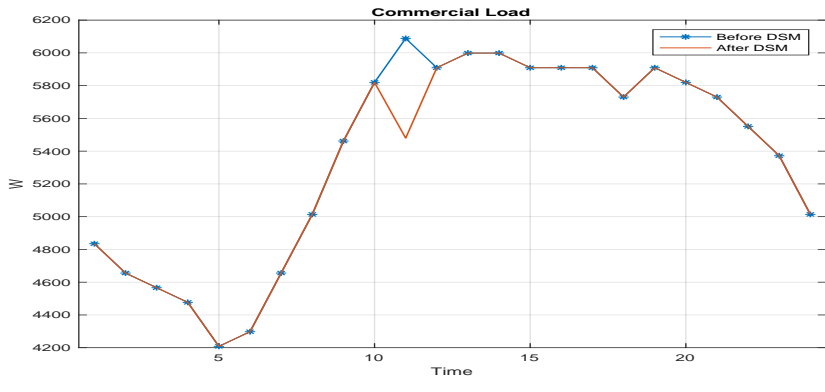


Figure 6.28: Commercial load peak shaving.

6.2.4 Peak Shifting LPL based DSM on Each Load Category

Unlike peak clipping, which reduces the total energy, the peak shifting DSM doesn't change the load sum, but instead it fills the signal's trough from the peak load, thus

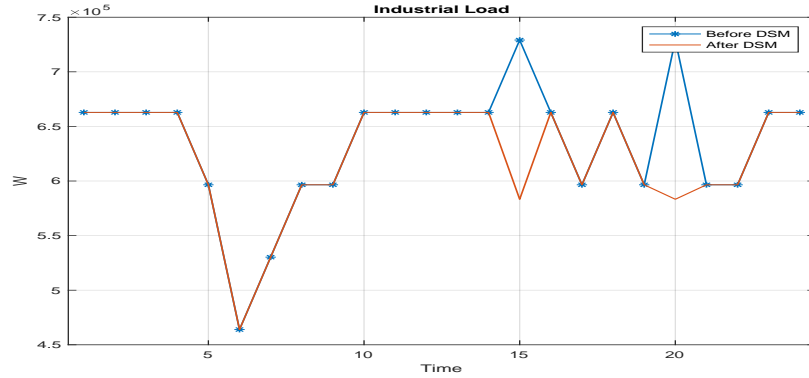


Figure 6.29: Industrial load peak shaving.

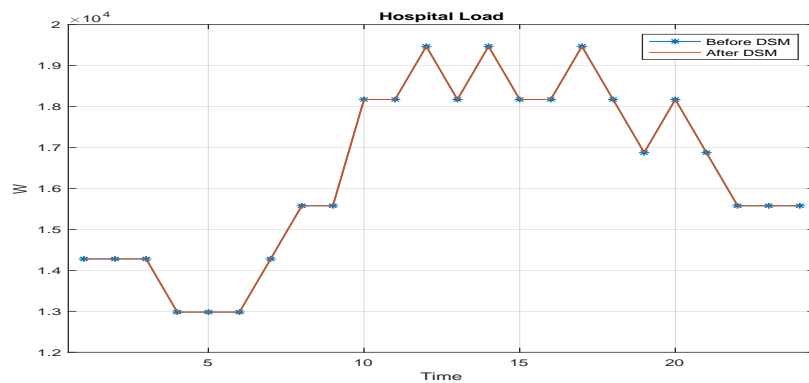


Figure 6.30: Hospital load peak shaving.

it involves clipping the peak and placing it in the troughs of the curve, simultaneously (Figure 6.3). Just as in the previous case, the peak shifting will also depend on the priority list. Figure 6.33, shows the microgrid total load and generation before and after the peak shifting effect, while Figures.6.34-6.37 show the peak shaving of each load type. The daily load factor of each load type have increased to values that are higher than in peak clipping because here we are reducing the signal sparks from both sides up and down (Table 6.5). Observe that the energy curtailed during the day is zero, however we succeeded in shaving the peaks and increasing the load factors. The microgrid response is shown in Figures.6.38-6.39.

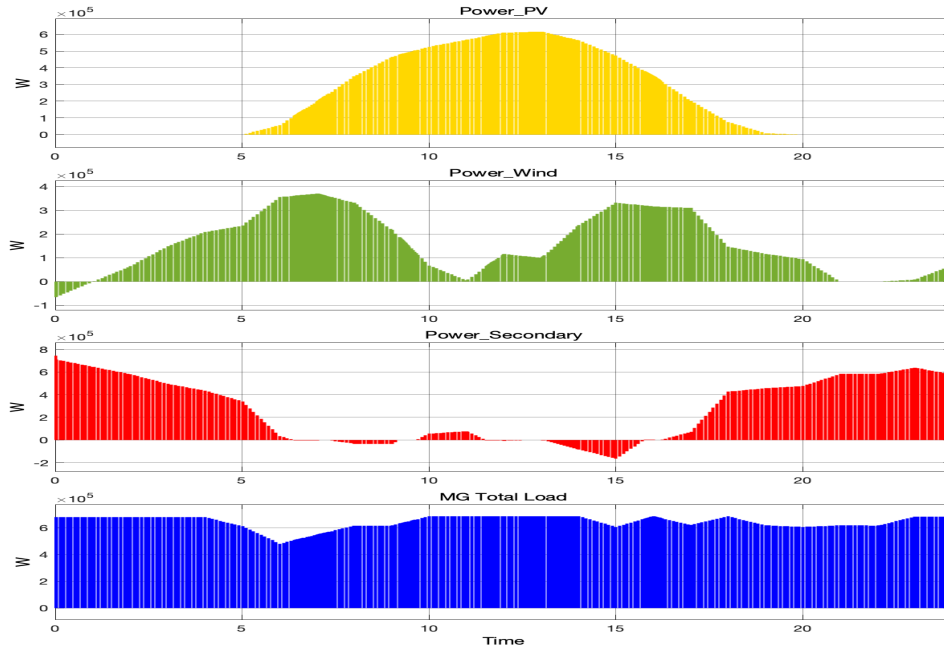


Figure 6.31: Case 3: MG test-bed response to the DSM.

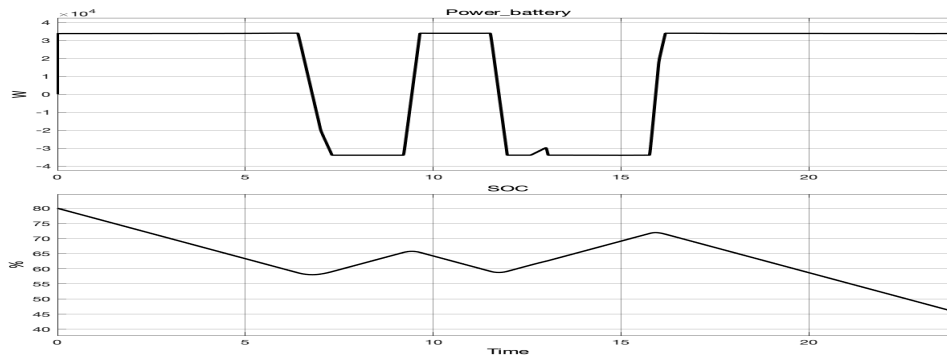


Figure 6.32: Case 3: MG test-bed battery response to the DSM.

Table 6.5: Daily load factor before and after peak shifting

Load type	Before DR	After DR	Energy curtailed (KWh)
Residential	91.48	95.83	0
Commercial	88.17	89.49	0
Industrial	87.12	94	0
Hospital	84.17	84.17	0

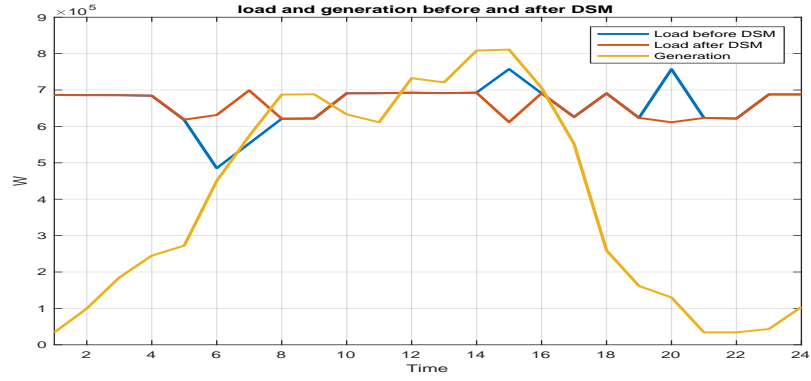


Figure 6.33: MG Loads before and after peak shifting.

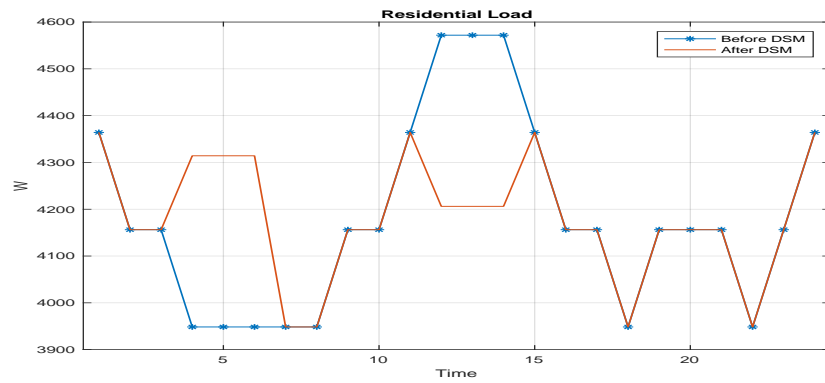


Figure 6.34: Residential load peak shifting.

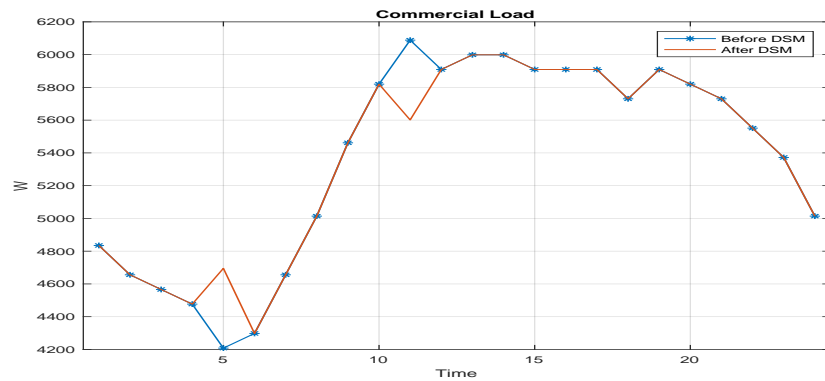


Figure 6.35: Commercial load peak shifting.

6.2.5 Peak Shaving LPL based DSM of The Total Aggregated Load

As we are operating our microgrid, we are concerned more about the aggregated load rather than each load type, thus the peak shaving exercise will be repeated

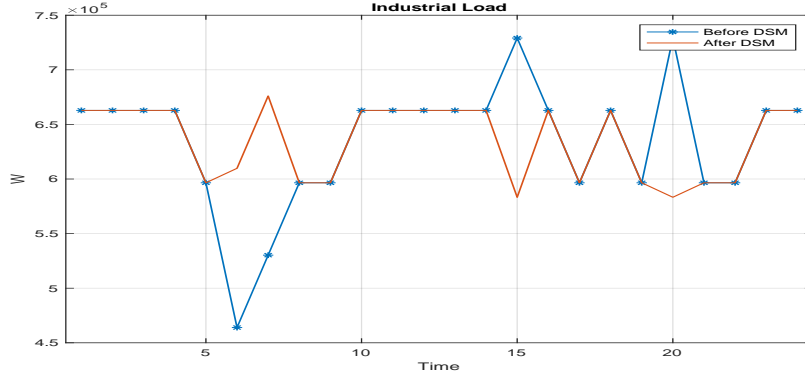


Figure 6.36: Industrial load peak shifting.

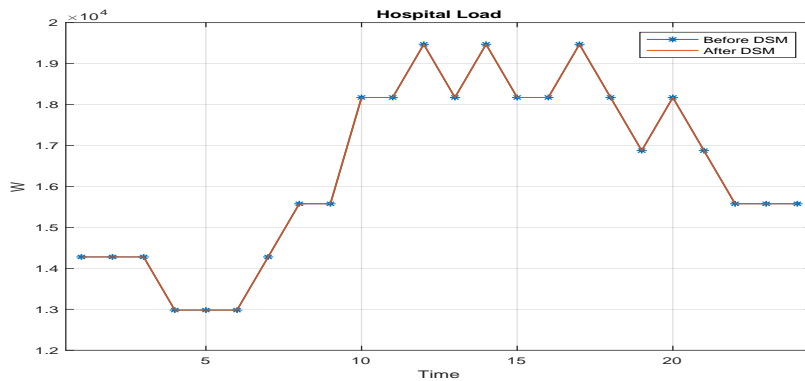


Figure 6.37: Hospital load peak shaving.

here but with a small alteration. Now, the peak of the aggregated MG load will be curtailed instead of shaving each load's peak, which might not yield the clipping of the aggregated load's peak. The idea is as follows; the peak of the aggregated load will be spotted. Accordingly, the algorithm will read the priority list at that hour, then the load of the least and before least important types at that hour will be clipped with a higher clipping percentage for the least important load. The MG load and generation before and after DSM is shown in Figure 6.40 and the corresponding curtailment of each load type is shown in figures.6.41-6.44. Again no curtailment occurred to the hospital load as it is a critical load (Table 6.6). The energy sum bought from the utility decreased from 6.28 MWh to 5.99 MWh. Notice that this case is very similar to

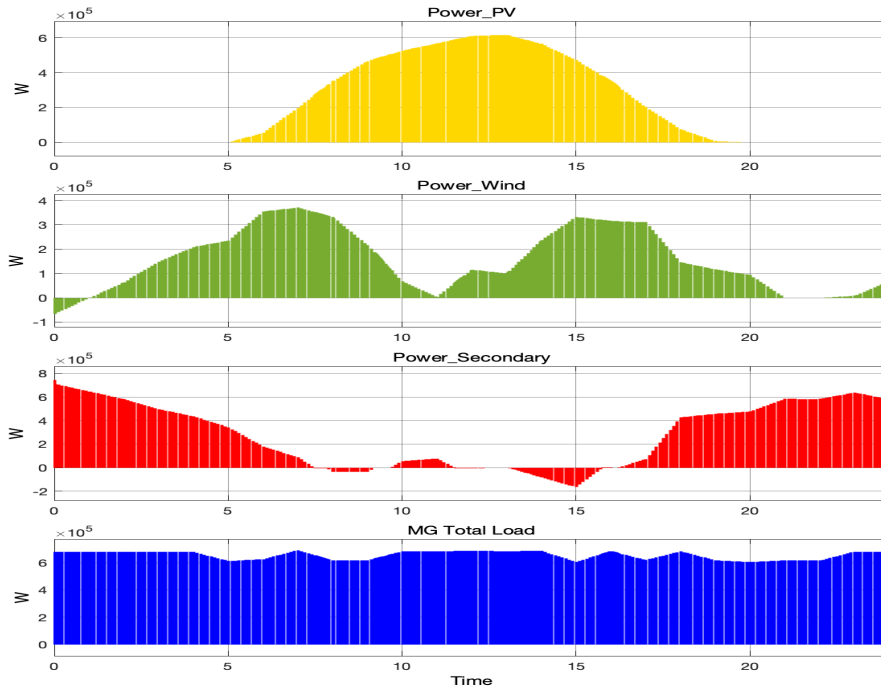


Figure 6.38: Case 4: MG test-bed response to the DSM.

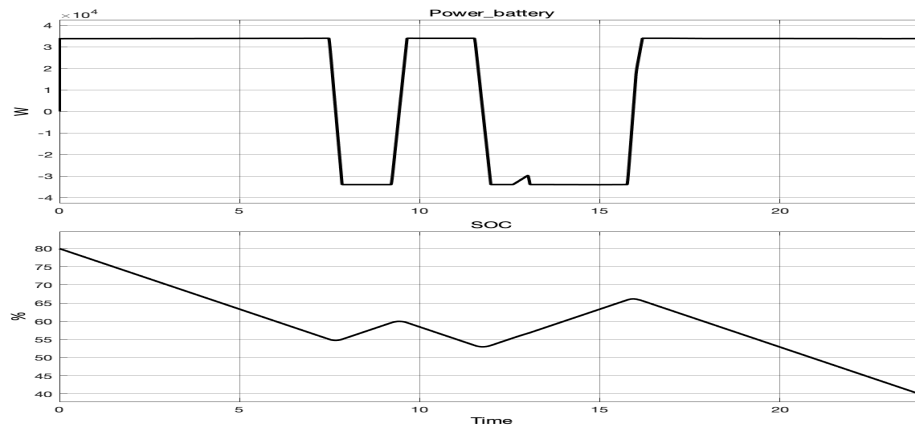


Figure 6.39: Case 4: MG test-bed battery response to the DSM.

case 3 because the industrial load contributed most of the profile of our microgrid and thus the difference between the individual peak clipping scheme and the aggregated one is very negligible.

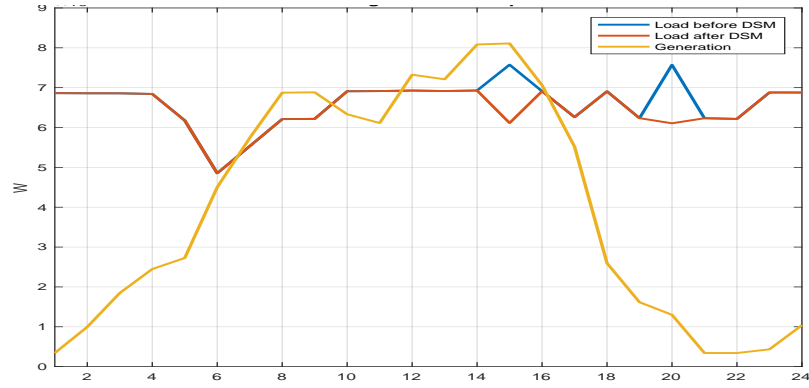


Figure 6.40: MG Loads before and after peak shaving.

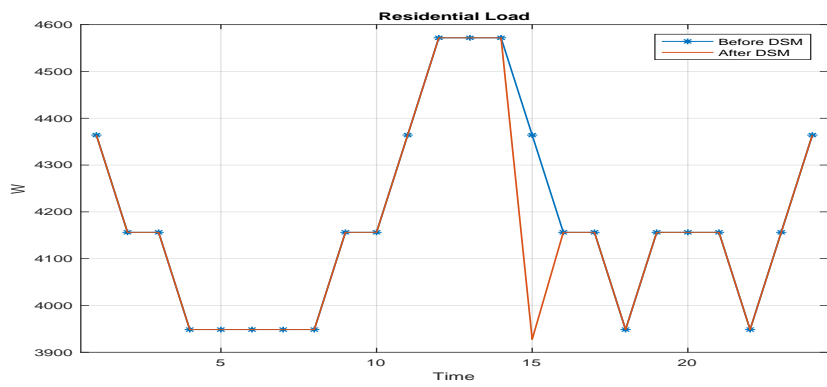


Figure 6.41: Residential load peak shaving.

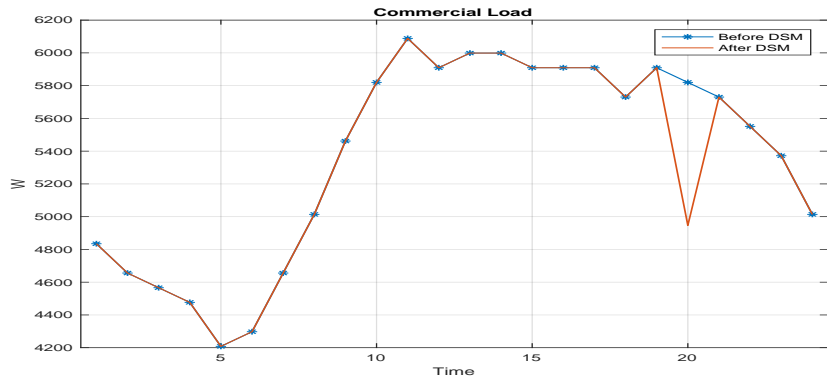


Figure 6.42: Commercial load peak shaving.

6.2.6 Residential Load DSM Using Load Composition

This is a special case where DSM will be done only to the residential costumers using the load composition acquired in Chapter.2. The biggest percentage of consumption

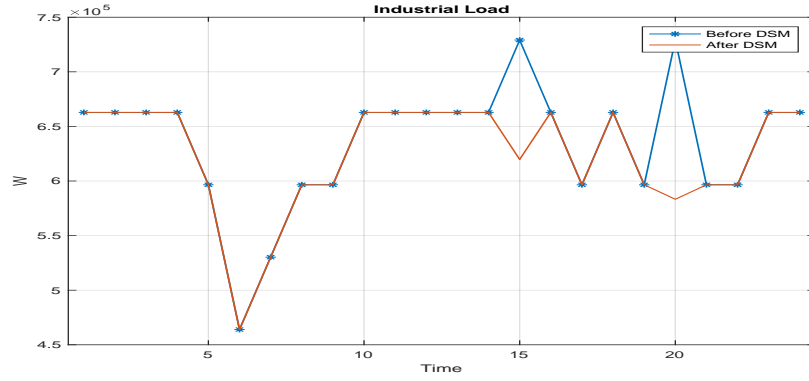


Figure 6.43: Industrial load peak shaving.

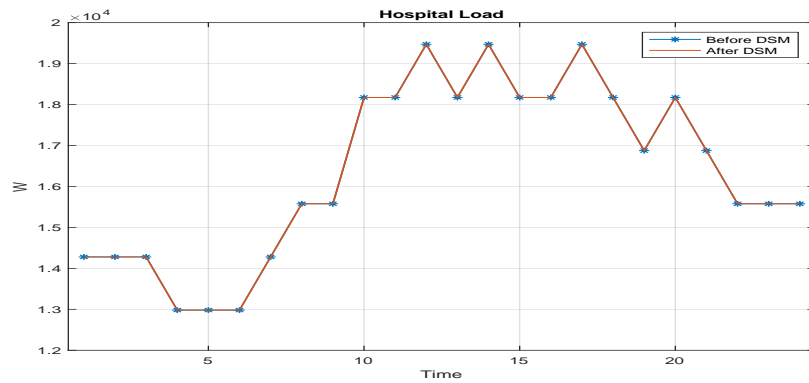


Figure 6.44: Hospital load peak shaving.

Table 6.6: Daily load factor before and after peak shaving the aggregated load

Load type	Before DR	After DR	Energy curtailed (KWh)
Residential	91.48	91.08	0.436
Commercial	88.17	87.58	0.873
Industrial	87.12	94.23	255
Hospital	84.17	84.17	0

in residential loads in Saudi Arabia is attributed to air conditioning loads. Thus, the direct load control will be done to the AC loads only, which were found to occupy 62% of the total residential load profile. The study includes three residential homes with the load composition and percentages found in Chapter.2. As a result, four inputs were given to the fuzzy controller, three of them are the hourly load profile input of each home, and the fourth input is the time of the day. Three outputs are considered,

which are the amount of shedding for each home. To determine if the current input load is at peak or not, the scaled power of the three houses is calculated as follows:

$$P_{S,z}(t) = \frac{P_{H,z}(t)}{\max(P_{H,z})} \quad (6.6)$$

where, z is the house number and t is time. $P_{S,z}(t)$ is the scaled power and $P_{H,z}(t)$ is the house power. Having three outputs from the FL controller. The new curtailed load of each household $P_{Cu,z}(t)$ will be as follows:

$$P_{Cu,z}(t) = \left(1 - \left(\frac{FL_z(t)}{2}\right)\right) \times 0.62 \times P_{S,z}(t) + 0.38 \times P_{S,z}(t) \times \max(P_{H,z}) \quad (6.7)$$

Where $FL_z(t)$ represents each output of the FL controller, and the 62% is the percentage of AC load to the total house consumption. The input and output FL mapping is shown in Figure 6.45 and the corresponding membership functions are shown in Figure 6.46-6.47. It can be seen from Figure 6.48, how demand response was different in each period. At P_2 the shedding was very severe and it decrease in severity in P_3 then P_1 . The aggregated load shows a successful curtailment of on AC loads which caused a substantial decrease and smoothing of the load profile for the sake of avoiding the swelling peak at P_2 (Figure 6.49). The verbal mapping of the AC response resulted from the FL, and the action that should be taken is summarized in Table 6.7. The microgrid response is shown in Figures.6.50-6.51 and the energy sum bought from the utility decreased from 6.28 MWh to 5.99 MWh. The detailed fuzzy rules are listed in Appendix.B.

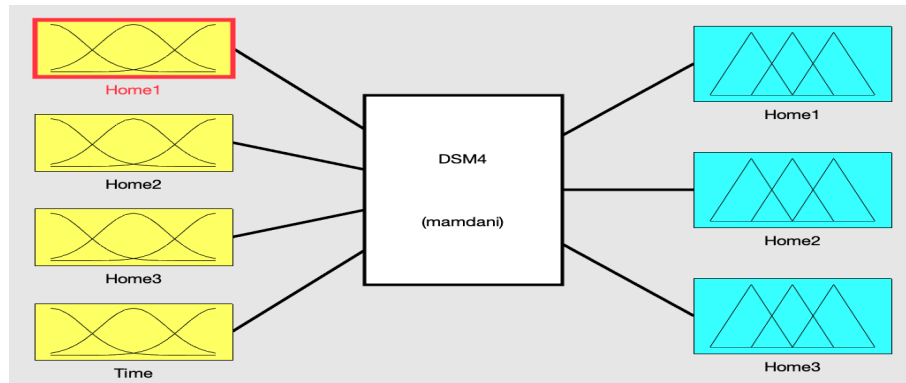


Figure 6.45: Residential AC demand response FL map.

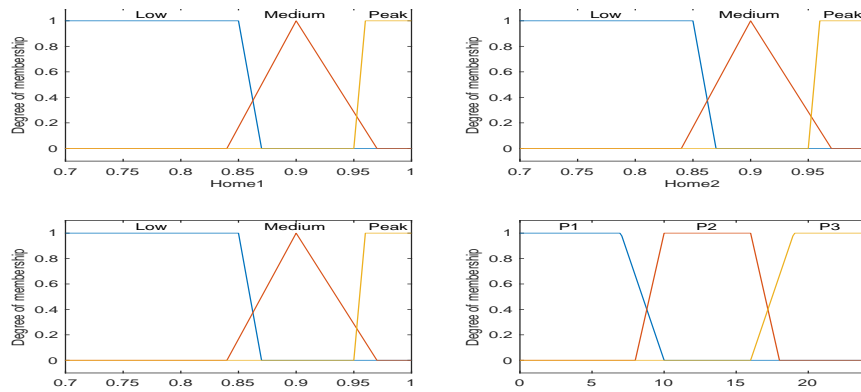


Figure 6.46: Inputs membership functions.

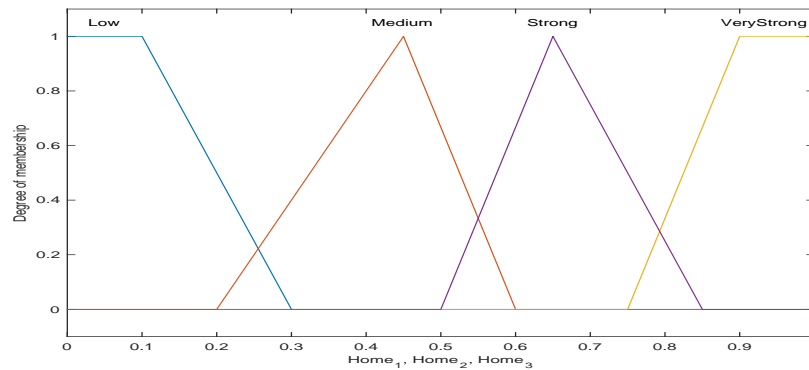


Figure 6.47: Outputs membership functions.

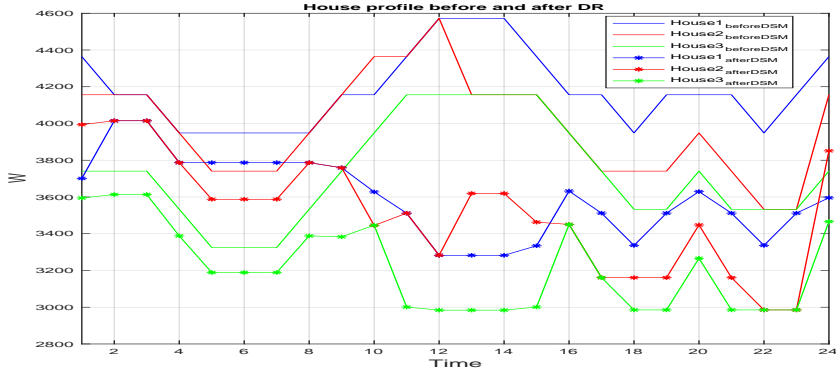


Figure 6.48: Profile of three houses before and after AC DSM.

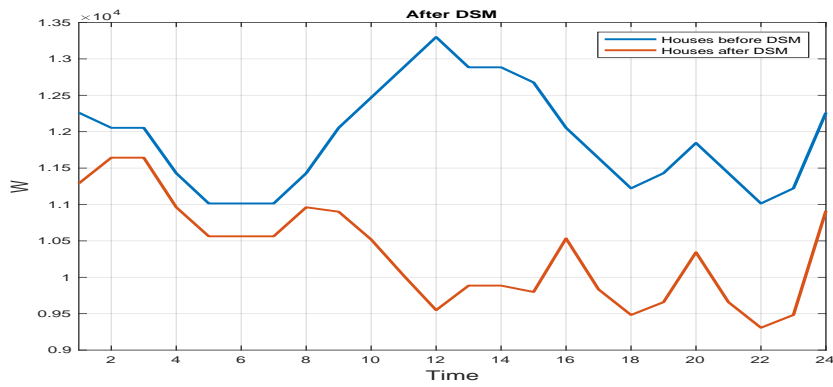


Figure 6.49: Aggregated profile of the three houses before and after AC DSM.

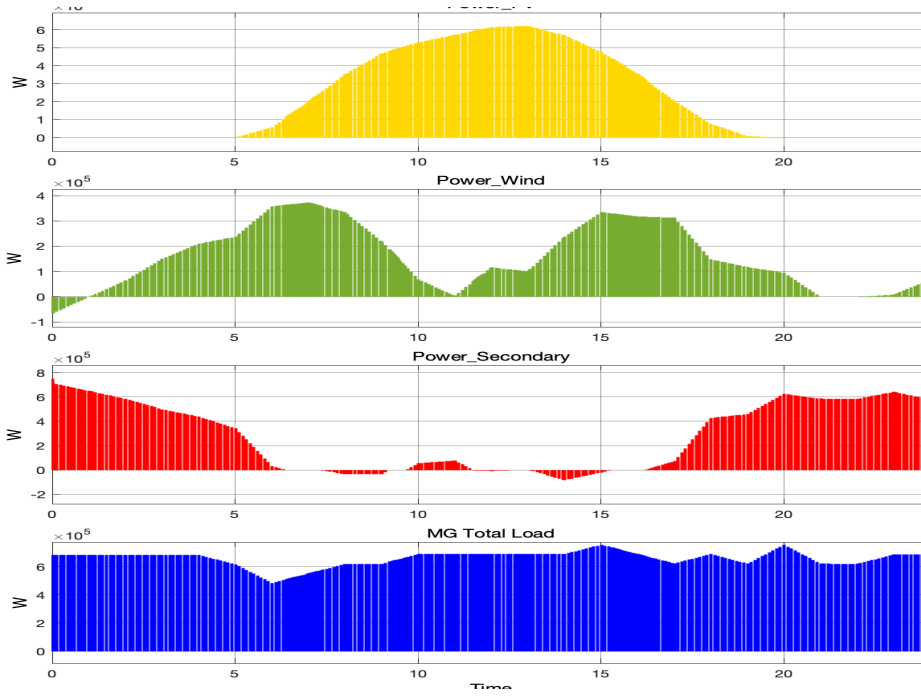


Figure 6.50: Case 6: MG test-bed response to the DSM.

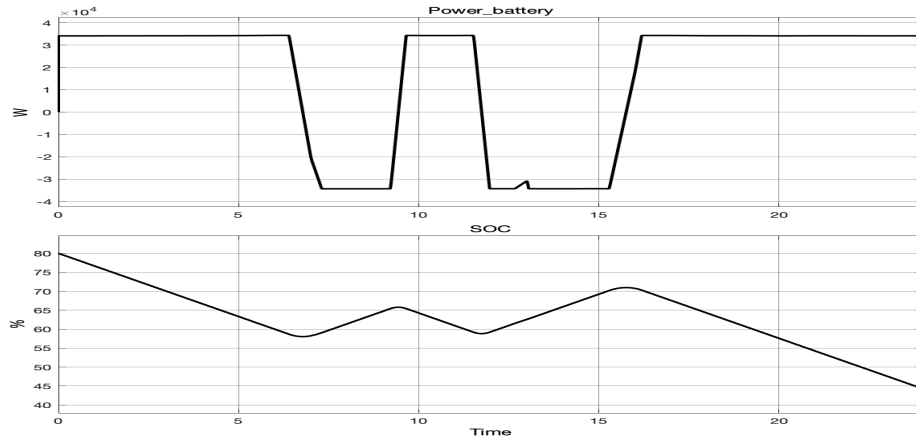


Figure 6.51: Case 6: MG test-bed battery response to the DSM.

Table 6.7: Mapping of FL output and AC action

FL output	Suggested AC action
Low or none	AC ON
Medium	Increase the temperature
Strong	Fan only
Very strong	AC OFF

CHAPTER 7

INCENTIVE-BASED FEASIBILITY STUDY OF AN EFFICIENT HYBRID AC/DC MICROGRID IN SAUDI ARABIA

Most of our household appliances and devices are operating on DC. In fact some of the appliances such as refrigerators, they tend to have more efficiency than AC based ones. Even at the industrial level, DC drives and motors have gained immense popularity. Thus, DC microgrid can be an excellent option to increase the total efficiency of the system. In this chapter, the economic feasibility of a hybrid DC/AC microgrid will be scrutinized. The proposed hybrid DC/AC microgrid shown in Figure 7.1 ensures that the DC-based energy resources such as PV and batteries are directly connected to the DC bus, while the AC based generation such as wind will be directly connected

to the AC bus. This guarantees fewer converters in between which should be reflected in the increased efficiency and cost.

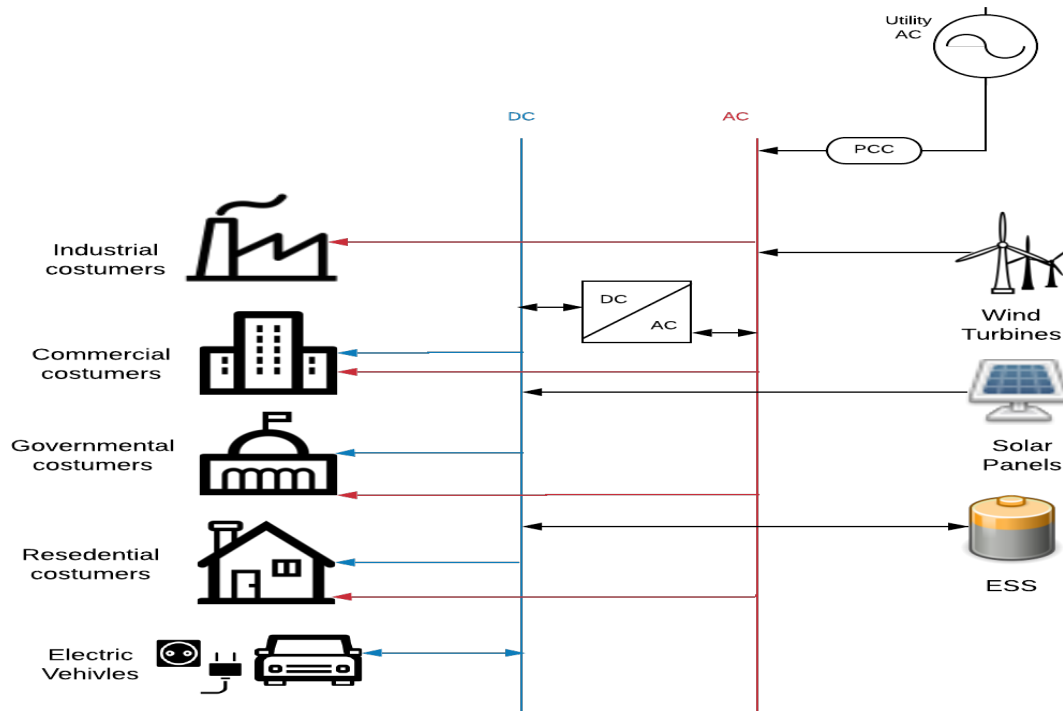


Figure 7.1: Hybrid AC/DC microgrid configuration.

The rest of the chapter is organized as follows: firstly a brief literature review about AC/DC microgrids will be provided, then the financial cost programs that are used for the feasibility study will be illustrated. Lastly, the analysis and results will be shown and a conclusion will be drawn about their viability.

7.1 Literature Review

Various studies in the literature have been done on the hybrid AC/DC microgrid. In [109], a microgrid test-bed was proposed containing different Distributed Energy Resources (DER). Control and protection schemes were investigated and the overall

performance of the microgrid was evaluated, however, the economic feasibility of the MG was not introduced. In [110], an economic feasibility study was implemented on an AC based microgrid using a real-valued cultural algorithm (RVCA). The authors found that under certain circumstances, there will be a reduction of 8.1% of the annual cost. The study though does not tackle the incorporation of DC microgrid at all. On the other hand, [111] evaluates the feasibility of a DC microgrid serving DC homes. The paper proposes alterations in users consumption habits and aims to optimize PV and batteries to yield an economically feasible microgrid based on different locations. The study, however, does not tackle hybrid microgrids and is limited to one load type, i.e., residential. In [112], Zhang et al. tested a DC microgrid for a commercial building to feed its DC loads such as LED lamps. An economical study has been implemented where PV is considered as a DG source, shows that the installation cost is around 2.2\$/W. They concluded that a hybrid DC/AC microgrid would be a better option, but without further verifying and implementing this statement.

7.2 Hybrid MG Distributed Energy Resources Sizing

In the hybrid DC/AC microgrid, it will be assumed that the PV and the battery will directly supply the DC load, while the wind energy output will feed the AC load.

7.2.1 PV Sizing

One of the main objectives of the presented microgrid is to eliminate the use of inverters which are the main cause of decreasing efficiency in microgrids. Thus, the annual energy consumption of DC load in the presented microgrid must be equal to its annual energy production of PV panels. A storage unit is required to level the energy consumption of the DC load with energy production during a year.

To estimate the capacity of the required solar panel suitable for the DC load of the presented microgrid, the annual energy consumption must be known (Table 7.1). From the last row in Table 7.1, the annual consumption of energy in each sector can be extracted. These values are used for calculating the annual energy production of PV modules to meet the net DC energy demand of the microgrid. From table 3.1, the average annual sun peak hours can be calculated, which is found to be 8.8 [hr/day] and then the required capacity to cover the annual power consumption can be found using equation 7.1.

$$P_{PV} = \frac{E_y \ 35\%}{8.8_{hr} \ 30_{day} \ 12_{Month}} \quad (7.1)$$

Where E_y is the sum of all DC load of different demand sectors. The DC load is estimated to be 35% of the hospital, residential and commercial and 0% of the industrial load [109].

Table 7.1: Consumption of the four load types

Month	Residential (KWh)	Commercial (KWh)	Hospital (KWh)	Industrial (KWh)
JAN	2600	1426.4	8750	11703
FEB	2637.5	1626.5	6058	7842
MAR	3315.625	2009.8	6332	6654
APR	4810	2847.9	7347	5948
MAY	7326.25	3950.2	8387	6203
JUN	9120	4416.3	8776	6531
JUL	7693.75	4417.5	9644	6494
AUG	7191.875	4338.1	9706	6275
SEP	7008.75	3900.7	8805	5709
OCT	5481.875	3426.4	8407	5797
NOV	3548.75	2340.4	7095	5011
DEC	3033.75	2015.3	6695	5303
SUM	63768.13	36715.5	96002	79470

7.2.2 Wind Sizing

Since the usage of the PV modules is to increase the efficiency of the proposed micro-grid by eliminating the usage of the AC/DC converters, the AC loads in the microgrid must be supplied by an AC source, wind generator. To estimate the capacity of the Wind generator, the same wind model as in Chapter 3 will be used. The total wind generation is shown Table 7.2.

7.2.3 Battery Sizing

To estimate the battery sizing, we estimate the PV capacity required, where we can calculate the annual energy production from PV and compare it to the annual energy consumption by the DC load. The DC load is estimated to be 35% of the hospital, residential and commercial and 0% of the industrial load. Since the demand increases during the summer and decreases during the winter, then by calculating the total extra

Table 7.2: Wind monthly energy generation

Month	Wind Energy generation (KWh)	AC Energy consumption (KWh)
JAN	17695.11	20007.66
FEB	21272.94	14551.3
MAR	17695.11	14231.32
APR	22792.44	15701.18
MAY	23552.19	18984.24
JUN	37622.08	21034
JUL	30577.15	20634.91
AUG	17695.11	20078.38
SEP	12483.61	18523.39
OCT	12899.73	17051.93
NOV	12483.61	13450.70
DEC	17695.11	12936.63
Total	244464.2	207185.6

energy production during the winter and subtracting the extra energy production of the PV during the year, then the battery size can be estimated Table 7.3. The sizing were based on adding on adding the negative numbers in the last column, to ensure that repetitive deficit between the PV generation and the DC load is compensated by the battery.

7.3 Financial Costs Programs

To design financial incentive programs that meet the investor criteria, a complete and detailed financial calculations must be given. In this chapter, the discount rate, inflation rate, interest rate, tax and loan duration will be all considered in the model. Besides, the the calculation of the energy consumption of each month of the year, taking into account the number of days in each month and the peak sun hours in that month, from historical data will be the basis of the financial study. To provide accurate

Table 7.3: Battery size calculation

Month	PV Gen (KWh)	DC Cons (KWh)	ESS (KWh)
JAN	4774	4471.74	302.26
FEB	4928	3612.7	1315.3
MAR	4774	4080.10	693.90
APR	5280	5251.72	28.285
MAY	6138	6882.21	-744.21
JUN	7260	7809.305	-549.31
JUL	7502	7614.34	-112.34
AUG	6820	7432.59	-612.59
SEP	5940	6900.06	-960.06
OCT	6820	6060.35	759.65
NOV	5940	4544.452	1395.55
DEC	4774	4110.42	663.58
Total	70950	68769.97	2180.03
ESS size (KWh)=		2978.50	

financial incentive programs for investment, the same real data modeled in Chapter 2 is used. The understanding of load categorization will ensure advising more certain incentive program for each of them. The incentive programs are designed to motivate the consumer to invest in renewable energy. The diversity of incentives are designed to meet the range of consumers. The proposed incentive programs are zero interest rate funding and business energy investment tax credit. To find out the optimal incentive program, the total cost of the installed system must be considered. The inflation rate, discount rate, interest rate, and the price of the electricity generated by the renewable energy sources compared to the price of the grid are also considered. These incentive programs must be viable economic options to motivate the investors in the renewable energy sector.

One of the main objectives of the presented hybrid microgrid is to eliminate the use of inverters which are leading cause of decreasing efficiency in such networks. Thus,

the annual energy consumption of DC load in the presented microgrid must be equal to its annual energy production of PV panels. A storage unit is required to level the energy consumption of the DC load with energy production during a year. The financial outcomes of the investment after a certain period of time must meet with the expectations and have a low cost of energy production compared to the grid cost, otherwise investors will not be motivated and willing to take the risk of the investment [89]. Also, The energy companies, the distributors, must facilitate and utilize the use of smart energy metering to sell and buy the energy from the customers without any limitations on quantities. The Saudi Electricity Company (SEC) just issued new tariff for all sectors (residential, commercial, hospital, industrial) (Table 2.2).

To investigate if the proposed design is economically feasible, a detailed and complete financial calculations must be implemented. The proposed financial model in this paper tests if the presented model is an economical choice and hence should be adopted. The model is shown in equation 7.2.

$$\begin{aligned}
& -(Tax\%) \left[\frac{[(1+r_{inf})^n - 1](1+r_{inf})(O\&M\ Cost)}{r_{inf}} + C_1 \right. \\
& \quad \left. + C_2 + C_3 \right] - \frac{r_{int}(1+r_{int})^{n_1}}{(1+r_{int})^{n_1} - 1} n_1 C_1 \\
& \quad - \frac{r_{int}(1+r_{int})^{n_2}}{(1+r_{int})^{n_2} - 1} n_2 C_2 - \frac{r_{int}(1+r_{int})^{n_3}}{(1+r_{int})^{n_3} - 1} n_3 C_3 \\
& \quad - \frac{((1+r_{inf})^{inf} - 1)(1+r_{inf})(C_1 OM)}{r_{inf}} - Bill_1 \\
& \quad + (\text{annual Energy production of PV}) n \\
& \quad + C_1 \left(\frac{r_{int}(1+r_{int})^{n_1}}{(1+r_{int})^{n_1} - 1} n_1 - 1 \right) \\
& \quad + C_2 \left(\frac{r_{int}(1+r_{int})^{n_2}}{(1+r_{int})^{n_2} - 1} n_2 - 1 \right) \\
& \quad + C_3 \left(\frac{r_{int}(1+r_{int})^{n_3}}{(1+r_{int})^{n_3} - 1} n_3 - 1 \right) = 0
\end{aligned} \tag{7.2}$$

Breaking Equation 7.2 to small parts can help in simplifying the presented model.

All the costs involved in this investment must be known to be implemented in the model. To start an investment, a loan is needed, thus, the cost due to loan and its interest is:

$$\begin{aligned}
Loan\ Cost = & \frac{r_{int}(1+r_{int})^{n_1}}{(1+r_{int})^{n_1} - 1} n_1 C_1 + \frac{r_{int}(1+r_{int})^{n_2}}{(1+r_{int})^{n_2} - 1} n_2 C_2 \\
& + \frac{r_{int}(1+r_{int})^{n_3}}{(1+r_{int})^{n_3} - 1} n_3 C_3
\end{aligned} \tag{7.3}$$

The second cost is considered in this model is operation and maintenance. The operation and maintenance cost is calculated by considering the inflation rate.

$$Total\ O\&M\ Cost = \frac{((1+r_{inf})^{inf} - 1)(1+r_{inf})(C_1 OM)}{r_{inf}} \tag{7.4}$$

In addition, taxes cost must be included for the capital cost and operation and maintenance cost. Since the new 2030 vision in the Kingdom of Saudi Arabia, taxes must be included in every transaction.

$$Tax\ Cost = (Tax\%) \left[\frac{[(1 + r_{inf})^n - 1](1 + r_{inf})(O\&M\ Cost)}{r_{inf}} + C_1 + C_2 + C_3 \right] \quad (7.5)$$

The last cost that should be considered is the last electric bill the investor should pay while the PV system is installed.

$$Energy\ bill\ of\ the\ first\ Year = Bill_1 \quad (7.6)$$

The proposed incentives that should be given to balance equation 7.2 and make the hybrid DC/AC microgrid a feasible option are the following term in the preceding equation 7.2:

$$Incentives = C_1 \frac{r_{int}(1 + r_{int})^{n_1}}{(1 + r_{int})^{n_1} - 1} n_1 - 1 + C_2 \frac{r_{int}(1 + r_{int})^{n_2}}{(1 + r_{int})^{n_2} - 1} n_2 - 1 + C_3 \frac{r_{int}(1 + r_{int})^{n_3}}{(1 + r_{int})^{n_3} - 1} n_3 - 1 \quad (7.7)$$

On the other hand, the saving the investor have is the cost of the annual energy bill, which the installed PV system covered it after installing it, in addition to the energy sold by the system to the grid.

$$Saving = (annual\ Energy\ production\ of\ PV) n \quad (7.8)$$

After calculating the costs and the savings, if the investment is successful then the saving will amount for more than the cost of the system, otherwise, it is not worth investing it net zero energy building. since the main objective is to motivate an investor into investing while the price of energy bought from the utility is lower than the energy production from the distributed generations, then it is not enough to make the costs equal to the saving, because the net of the investment is zero after the end of the investment lifetime. Thus, to encourage the investor, a couple of incentives are proposed.

Equation.7.9 is used to calculate the cost of energy production of the installed PV and wind generator

$$Cost\ of\ Energy[\$/KWh] = \frac{Total\ Cost}{Total\ Energy\ Production} \quad (7.9)$$

There are many financial terms that must be known before starting designing a financial model. After calculating the savings in the investment for the period of the project, its present worth value must be found:

$$PWF(r_d, n) = \frac{1}{(1 + r_d)^n} \quad (7.10)$$

In addition, the effect of inflation rate on the discount and interest rate has to be incorporated:

$$r_{int0} = \frac{(r_{int} - r_{inf})}{(1 + r_{inf})} \quad (7.11)$$

$$r_{d0} = \frac{(r_d - r_{inf})}{(1 + r_{inf})} \quad (7.12)$$

Equations.7.11, and 7.12 show that we can eliminate the inflation rate effects on the interest rate and discount rate from the start by adjusting them. In addition, the inflation rate has an impact on the services provided during the lifetime of the project, such as operation and maintenance.

For the loan, we have to level the payment during the investment time.

$$CRF(r_d, n) = \frac{r_d}{1 - (1 + r_d)^{-n}} \quad (7.13)$$

Since the energy prices set by Saudi Electricity Company are constant, the energy price escalation was ignored in this study.

7.4 Analysis and Results

The case study presented in this chapter are for high residential income homes, low residential income homes, industrial, hospital and commercial. To give accurate results, a detailed average price of the recent PV system (fixed and variable prices) is shown in Table 7.4 and the interest rate, inflation rate, discount rate, taxes and lifetime of the investment are shown in Table 7.10. Batteries was not included in the study due to the increase in the capital cost, and operation and maintenance cost. Since the selling price of energy equals to the buying price of electricity, there is no need to invest in an energy storage system.

Using Eq.7.1 to calculate the capacity required for installation to meet the net zero energy building and using Table 2.2 to calculate the monthly energy bill, we can estimate the annual saving that the renewable energy system PV can obtain, see Tables 7.5,7.6,7.7,7.8 and 7.9. The first column is the month of the year and the second and third months are the energy produced and consumed by PV, respectively. The fourth and last column are the electricity bill before and after installing the PV. The 5th column is the difference between the PV consumption and the PV production.

Table 7.4: PV technology specifications

	Fixed Cost (SAR/W)	Variable Cost (SAR/W year)	Area ($m^2/100W$)	Lifetime (Year)
PV	4.125	3% -5% of capital cost	0.5	30
Inverter	1.5	Capital cost	-	10
Installation	4.125	-	-	-
Implementation Area	1 m^2 for each 200 W			
Inverter Efficiency	95%			

Table 7.5: High income residential customers

Month	PV Prod (KWh)	PV Cons (KWh)	Bills Without PV	Net Cons (KWh)	Bills With PV
JAN	4535.3	2600	468	-1935	-348
FEB	4681.6	2637.5	475	-2044	-368
MAR	4535.3	3315.625	597	-1220	-220
APR	5016	4810	866	-206	-37
MAY	5831.1	7326.25	1478	1495	269
JUN	6897	9120	2016	2223	400
JUL	7126.9	7693.75	1588	567	102
AUG	6479	7191.875	1438	713	128
SEP	5643	7008.75	1383	1366	246
OCT	6479	5481.875	987	-997	-179
NOV	5643	3548.75	639	-2094	-377
DEC	4535.3	3033.75	546	-1502	-270
SUM	67402.5	63768.13	12659		-654
Annual Saving			13313		

Table 7.6: Low income residential customers

Month	PV Prod (KWh)	PV Cons (KWh)	Bills Without PV	Net Cons (KWh)	Bills With PV
JAN	1443.05	800	144	-643	-116
FEB	1489.6	844	151.92	-645	-116
MAR	1443.05	1061	190.98	-382	-69
APR	1596	1539.2	277.056	-57	-10
MAY	1855.35	2344.4	421.992	489	88
JUN	2194.5	2918.4	525.312	724	130
JUL	2267.65	2462	443.16	194	35
AUG	2061.5	2301.4	414.252	240	43
SEP	1795.5	2242.8	403.704	447	81
OCT	2061.5	1754.2	315.756	-307	-55
NOV	1795.5	1135.6	204.408	-660	-118
DEC	1443.05	970.8	174.744	-472	-85
SUM	21446.25	20373.8	3847.28		-193
Annual Saving			4040.32		

After calculating the annual energy consumption of industrial, commercial, hospital, and residential, equation 7.1 can be used to determine which incentive can be used. This is due to the range of prices difference between the residential, commercial, hospital and industrial and their annual consumption, the incentive program differs from one to the other. The economical feasibility and risk taking in the investment may not be worth it to invest in net zero energy building for the industrial sector, since the energy cost is minimal. For the residential sector, the capital cost and the small size of PV system may not cover its costs. To have the optimal PV system which will produce energy at lower cost than the price of energy bought from the grid, size of energy production and corresponding costs must be considered, the amount of energy the utility company is willing to buy and at what price is also crucial. In addition to the high interest rate and its long duration, which will add more to the investment cost. Many factors are in play, see equation 7.2, to determine the optimum option for

Table 7.7: Commercial customers

Month	PV Prod (KWh)	PV Cons (KWh)	Bills Without PV	Net Cons (KWh)	Bills With PV
JAN	2577	1426.4	285.28	-1150	-230
FEB	2660	1626.5	325.3	-1034	-207
MAR	2577	2009.8	401.96	-567	-113
APR	2850	2847.9	569.58	-2	-0.42
MAY	3313	3950.2	790.04	637	127
JUN	3919	4416.3	883.26	498	100
JUL	4049	4417.5	883.5	368	74
AUG	3681	4338.1	867.62	657	131
SEP	3206	3900.7	780.14	694	139
OCT	3681	3426.4	685.28	-255	-51
NOV	3206	2340.4	468.08	-866	-173
DEC	2577	2015.3	403.06	-562	-112
SUM	38297	36715.5	7523.1		-316
Annual Saving			7839.4		

either the incentive or the energy production cost.

Tables 7.11, 7.12, 7.13, 7.14 and 7.15 shows the results of the study of net-zero energy building in KSA. As these tables show that investing in net-zero energy building with financial parameters presented in table 7.10 may not be the best economical options. Unless these parameters changed or the prices of PV system reduced even further.

All in all, a detailed case study of residential, commercial, hospital and industrial is presented to study the economic feasibility of the presented microgrid in the Kingdom of Saudi Arabia in addition to the governmental incentive programs to promote for renewable energy and reduce the eco-impact of the traditional power generation plant, such as oil and gas. The results show that the presented microgrid will not be a viable economic option unless the government supports it. This does not mean that the distributed generation sources could not help in reducing the billing cost, but it says

Table 7.8: Hospital load

Month	PV Prod (KWh)	PV Cons (KWh)	Bills Without PV	Net Cons (KWh)	Bills With PV
JAN	6596.8	8750	2800	2153	689
FEB	6809.6	6058	1938.56	-752	-241
MAR	6596.8	6332	2026.24	-265	-85
APR	7296	7347	2351.04	51	16
MAY	8481.6	8387	2683.84	-95	-30
JUN	10032	8776	2808.32	-1256	-402
JUL	10366	9644	3086	-722	-231
AUG	9424	9706	3106	282	90
SEP	8208	8805	2817.6	597	191
OCT	9424	8407	2690.24	-1017	-325
NOV	8208	7095	2270.4	-1113	-356
DEC	6596.8	6695	2142.4	98.2	31
SUM	98040	96002	30901		-652
Annual Saving			31552.8		

that the microgrid working in island operations may not be an economical option without the support of the government. For high-income residential, a minimum incentive must be 0 % interest rate on loan and 40 % capital reduction to meet the price of the grid. While for the low-income residential a minimum incentive must be 0 % interest rate on loan and 35 % capital reduction to meet the price of the grid. For the hospital (governmental) section a 4% interest rate on loan will be enough to match the cost of the grid. While for the low industrial sector a minimum incentive must be 0 % interest rate on loan and 45 % capital reduction to meet the price of the grid. These are due to the low cost of electrical energy from the traditional power generation plants compared to renewable energy. Keep in mind that the renewable energy price can be reduced dramatically when the size of power production increases. In conclusion, at this point of time, it would be better to opt for the AC microgrid

Table 7.9: Industrial customers

Month	PV Prod (KWh)	PV Cons (KWh)	Bills Without PV	Net Cons (KWh)	Bills With PV
JAN	5566.05	11703	2106.54	6137	1104
FEB	5745.6	7842	1411.56	2096	377
MAR	5566.05	6654	1197.72	1088	196
APR	6156	5948	1070.64	-208	-37
MAY	7156.35	6203	1116.54	-953	-172
JUN	8464.5	6531	1175.58	-1934	-348
JUL	8746.65	6494	1168.92	-2253	-405
AUG	7951.5	6275	1129.5	-1677	-302
SEP	6925.5	5709	1027.62	-1217	-219
OCT	7951.5	5797	1043.46	-2155	-388
NOV	6925.5	5011	901.98	-1915	-345
DEC	5566.05	5303	954.54	-263	-47
SUM	82721.25	79470	14484.6		-585
Annual Saving			15069.8		

Table 7.10: Financial parameters

r_{inf} [%]	r_{int} [%]	r_d [%]	Tax [%]	Life [year]
1%	5%	5%	5%	30

Table 7.11: Case study: High income residential customers

High Income Residential	
Without Incentive	
Size[kW]	Cost of Energy [SAR/W]
21	0.342573694
Profit [SAR]	Area m^2
-308393.647	105
With Incentive (Tax =40%+0% interest)	
Profit [SAR]	Cost of Energy [SAR/W]
627.899	0.182472383
With Incentive (Tax =50%+0% interest)	
Profit [SAR]	Cost of Energy [SAR/W]
22143.027	0.171325587

option since installing a hybrid DC-AC network is not worth it from an economical point of view. An AC-based MG testbed will be build in the next section.

Table 7.12: Case Study: Low income residential customers

Low Income Residential	
Without Incentive	
Size[kW]	Cost of Energy [SAR/W]
7	0.342513383
Profit [SAR]	Area m^2
-99159.079	35
With Incentive (Tax =35%+0% interest)	
Profit [SAR]	Cost of Energy [SAR/W]
314.538	0.187904197
With Incentive (Tax =50%+0% interest)	
Profit [SAR]	Cost of Energy [SAR/W]
11063.913	0.171196732

Table 7.13: Case study: Commercial customers

Commercial	
Without Incentive	
Size[kW]	Cost of Energy [SAR/W]
12.5	0.343081706
Profit [SAR]	Area m^2
-159936.291	62.5
With Incentive (Tax =25%+0% interest)	
Profit [SAR]	Cost of Energy [SAR/W]
4909.743	0.199600866
With Incentive (Tax =50%+0% interest)	
Profit [SAR]	Cost of Energy [SAR/W]
36899.222	0.171757446

Table 7.14: Case study: Hospital load

Hospital	
Without Incentive	
Size[kW]	Cost of Energy [SAR/W]
32	0.347039785
Profit [SAR]	Area m^2
-74129.417	160
With Incentive (Tax =0%+4% interest)	
Profit [SAR]	Cost of Energy [SAR/W]
2839.234	0.320870654
With Incentive (Tax =0%+0% interest)	
Profit [SAR]	Cost of Energy [SAR/W]
265620.729	0.23152566

Table 7.15: Case study: Industrial customers

Industrial	
Without Incentive	
Size[kW]	Cost of Energy [SAR/W]
27	0.342370363
Profit [SAR]	Area m^2
-397544.380	135
With Incentive (Tax =45%+0% interest)	
Profit [SAR]	Cost of Energy [SAR/W]
13600.190	0.176695653
With Incentive (Tax =50%+0% interest)	
Profit [SAR]	Cost of Energy [SAR/W]
27431.344	0.171122255

CHAPTER 8

CONCLUSION AND FUTURE WORK

In this chapter, a conclusion about the work done is drawn. The method, simulation, and findings of the thesis will be summarized, and the contributions of the study will be discussed. Lastly, the test system designed sets the cornerstone for future studies. Some of the future work that can be done to the test-bed will be discussed.

8.1 Conclusion

In this study, an integrated energy management systems with hybrid renewable generation, battery energy storage and controllable loads was designed. The proposed testbed is capable of the following:

- Incorporating the hourly renewable generation from photovoltaics and wind energy.
- Acquiring hourly residential, commercial, industrial and governmental load pro-

file.

- Installing a battery energy storage system that is capable of smoothing the changing nature of renewable resources and minimizing the total energy bought from the utility.
- Prioritizing the loads smartly and flexibly using Artificial Neural Networks (ANN).
- Implementing different Demand Side Management (DSM) schemes to curtail loads based on supply and demand balance, peak shaving or peak shifting.

The microgrid test bed is AC based, and thus an incentive-based economical feasibility study on a hybrid DC/AC microgrid was proposed to show that according to the current energy situation in Saudi Arabia, the adoption of such configurations may not be feasible unless big incentives are enforced.

The simulation results of the test-bed showed that the microgrid would firstly feed its load from the distributed generation. If the load demand is higher than generation, the battery will take action to match the deficit. The battery, of course, has a maximum power limit that it can not exceed. If the battery power and distributed generation are not able to adequately feed the microgrid demand, then a signal will be sent to the utility to feed discrepancy. The discrepancy can be high sometimes especially if it happens during peak hours where the power bought from the grid will be costly, thus microgrid should attempt to minimize the power received from the main network at this period. Demand Side Management (DSM) was implemented to prevent the microgrid from buying expensive energy. Since our microgrid has different

load types, a flexible demand priority list that updates itself each hour to inform the DSM on which loads should be curtailed and which loads are uninterruptible. The DSM will operate accordingly and shed loads that are not-critical and eventually managing microgrid demand and generation. Different DSM schemes were tested and evaluated based on the amount of power curtailed and their successfulness to mitigate power purchasing during peak periods. Another contribution of this thesis is the incentive-based feasibility study of the hybrid DC/AC microgrid that studied how economically viable is replacing the AC test-bed system with a hybrid DC/AC one and what are the needed incentives to make this configuration compete.

8.2 Future Work

The test-bed is a foundation for many studies that can be implemented. Studies can be done on the control part, cable sizing, generation, and battery optimal sizing techniques. A list of applicable interesting future work is suggested below:

- Optimizing the sizing of the battery using Evolutionary Algorithms (EA). The optimization objective function is to reduce the amount of power bought from the utility.
- Using the load percentages and composition found in Chapter.2, a detailed DSM model can be formulated and applied to residential costumers.
- Addition of another generation sources in the microgrid test-bed such as diesel generators, CHP and Fuel Cells (FC).

- Developing and evaluating different algorithms to implement load and generation forecasting using the given historical data.
- Mapping the ANN priority list parameters to the fuzzy logic input parameters by developing a fuzzy basis function network (FBFN), which will provide a solid framework for combining numerical and linguistic information in a uniform fashion.

APPENDIX A

MICROGRID TEST SYSTEM

A.1 SIMULINK Simulation

The simulation of the energy management microgrid with the hybrid renewable energy resources and controllable loads was done in SIMULINK MATLAB. The designed microgrid configuration is shown in Figure A.1. The load and renewable generation data is calculated in an m.file and received by SIMULINK (Figure A.2). It can be seen from the microgrid that four load types: residential, commercial, industrial and hospital are acquired and two renewable resources: PV and wind energy. The battery controller in Figure A.3 will take the secondary voltage and current to acquire the secondary real and imaginary power. The power will be passed through a switch. If signal 3, which is the battery trigger ON and OFF signal, is 0 then the battery is deactivated, and 0 will be assigned to the RMS current, which is the current going in or out of the battery. If signal 3 (shown in Figure A.4) is not 0 then the extra or deficit power will be passed through the switch and the RMS current will be positive or negative depending on the energy balance case of the microgrid. This RMS now

is inputted to the battery dynamics blocks (Figure A.5). The RMS current and its phase angle are converted to real and imaginary form and multiplied by the SoC block to make sure that no current will be triggered from the battery if the SoC is less than 20%. Furthermore, if the battery SoC is equal to 90%, the battery will not accept any further current. The last block "*Battery_I*" is fed to the microgrid. Lastly, the most important dynamics of the battery is in its Ampere-hour which is acquired from the m.file and its SoC which was modeled to be in the range of 90% to 20%. The battery dynamics block (Figure A.6) simulates the setting of the battery SoC limits and the AH hourly variations. Lastly, all figures and simulation results can be investigated from the scopes block (Figure A.7).

A.2 Microgrid Testbed Web-page

A webpage was designed for the microgrid to make it accessible for researcher to do studies. All of the load, generation and battery data are included in the page. A link to download the test system in SIMULINK is available too. A special window in the web-page is dedicated for the recent studies on the grid. The showcasing of the studies implemented on the test system will enable researchers to be aware of the literature state and so that replicated studies are minimized. The webpage can be found at: <https://www.ahmedsa.me/kfup2mg>

KFUP2MG

Microgrid System with RES, ESS and Diverse loads (Residential, Commercial, Hospital and Industrial) Based on Local & Real Data from Saudi Arabia

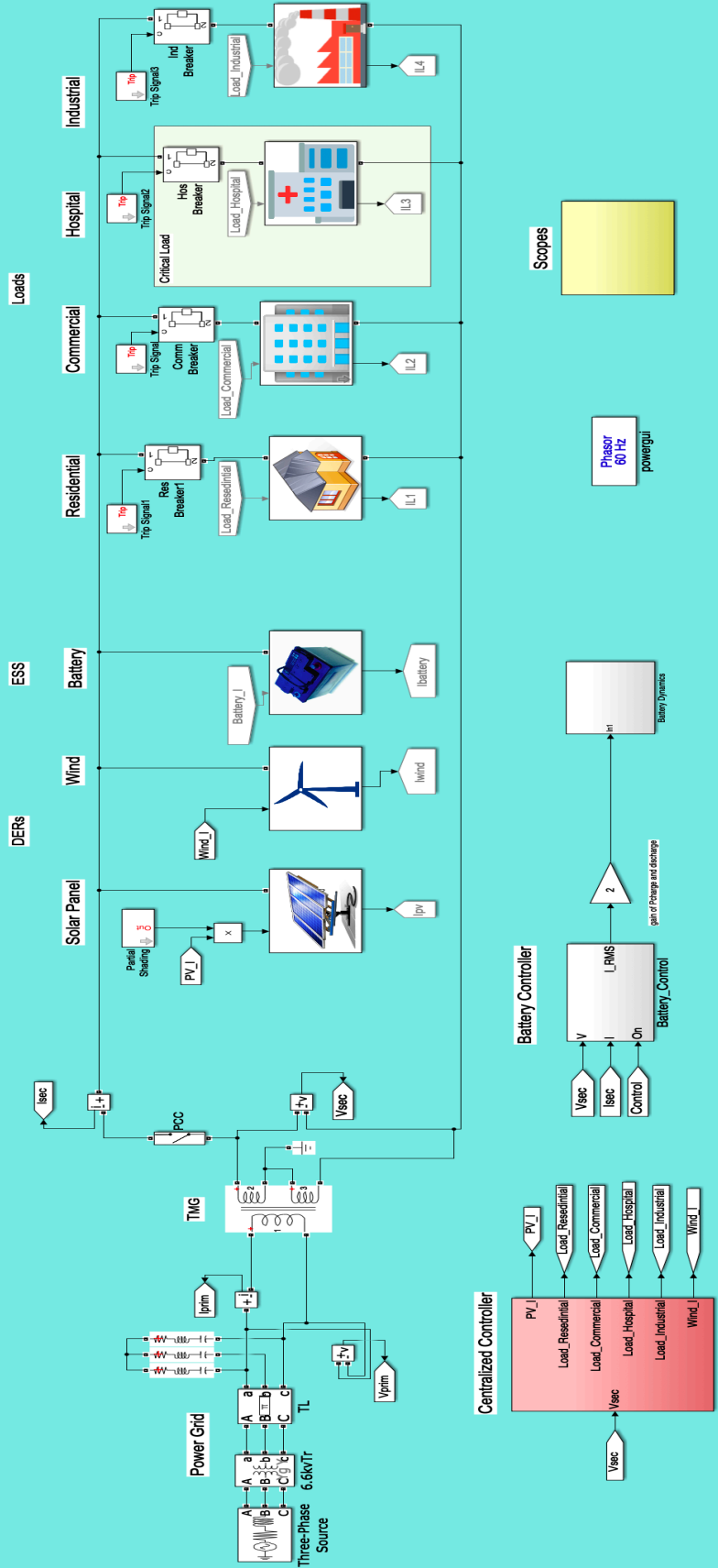


Figure A.1: KFUP2MG microgrid.

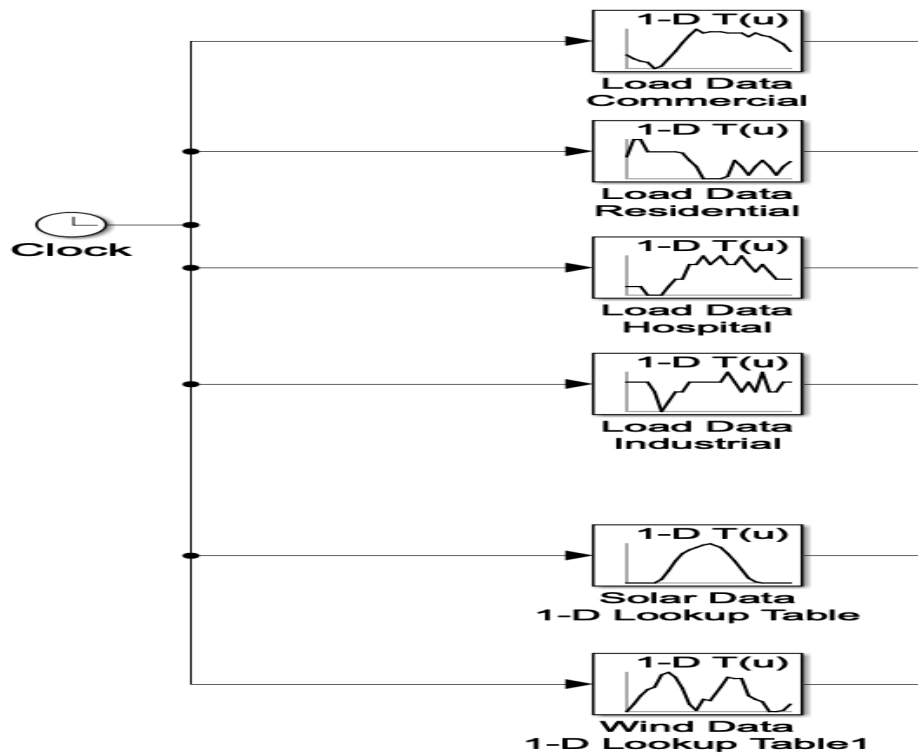


Figure A.2: Load and renewable generation from m.file

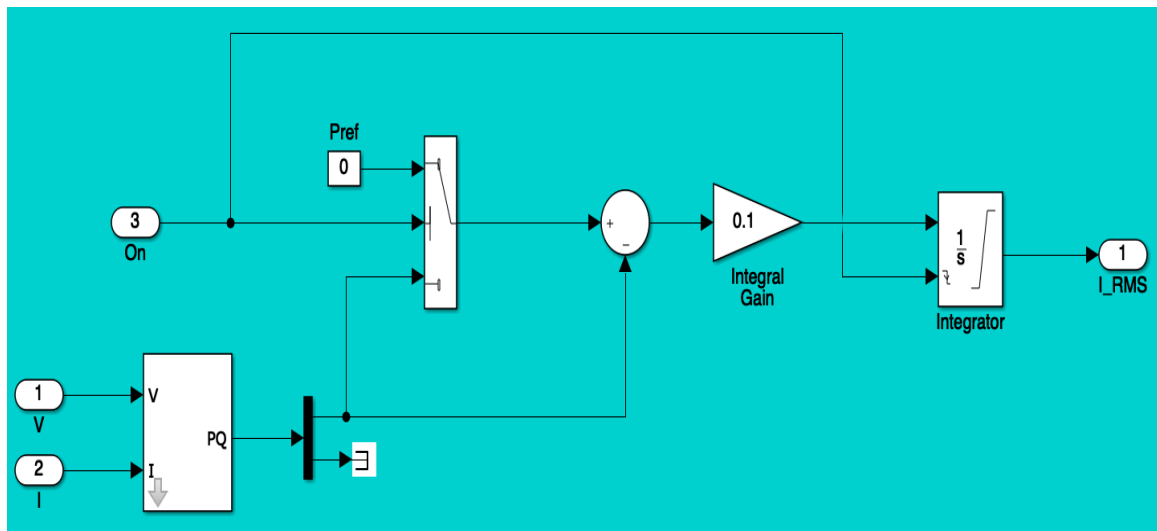


Figure A.3: Battery controller

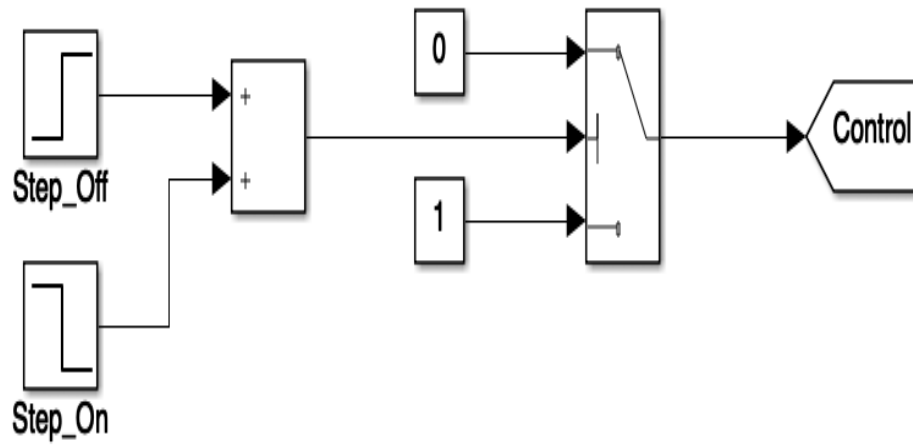


Figure A.4: Battery ON or OFF trigger

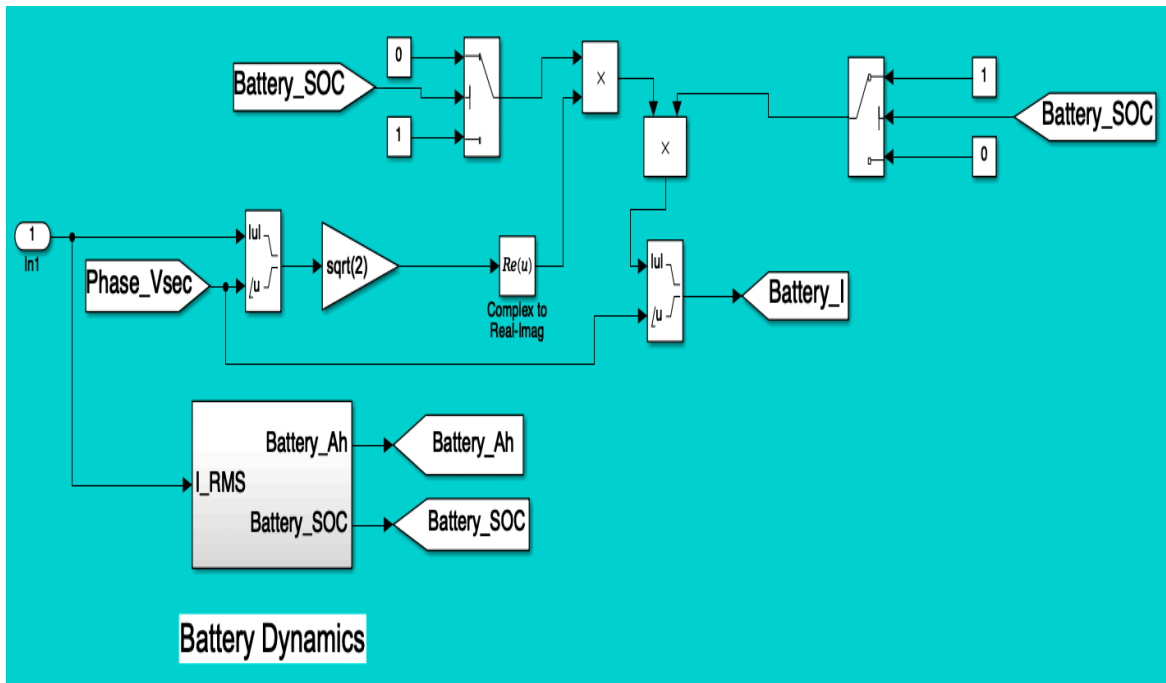


Figure A.5: Battery dynamics 1

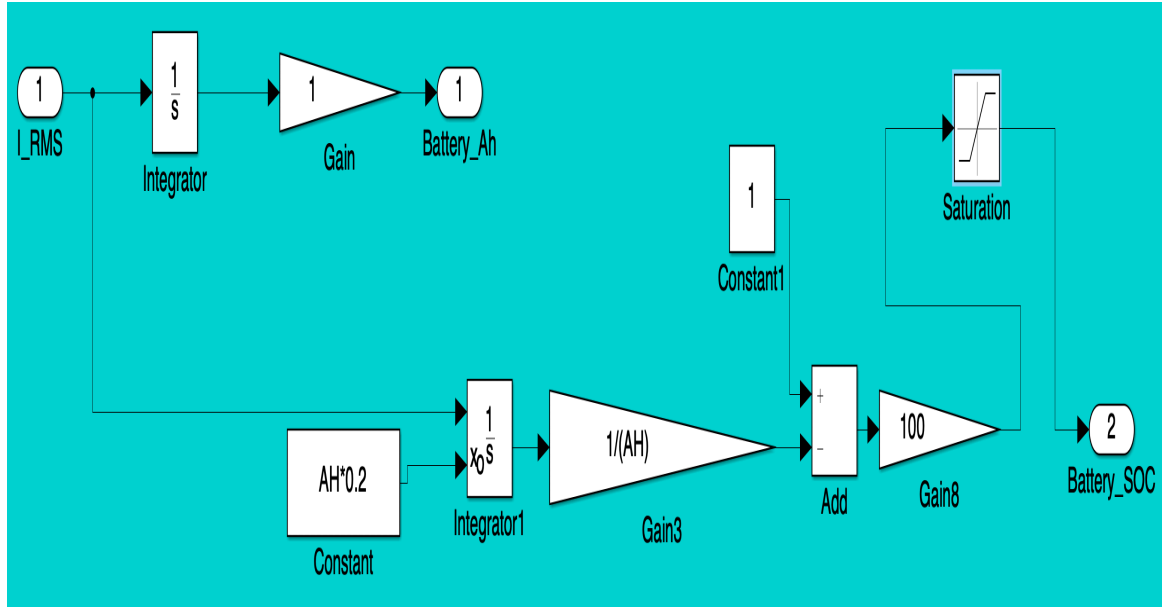


Figure A.6: Battery dynamics 2

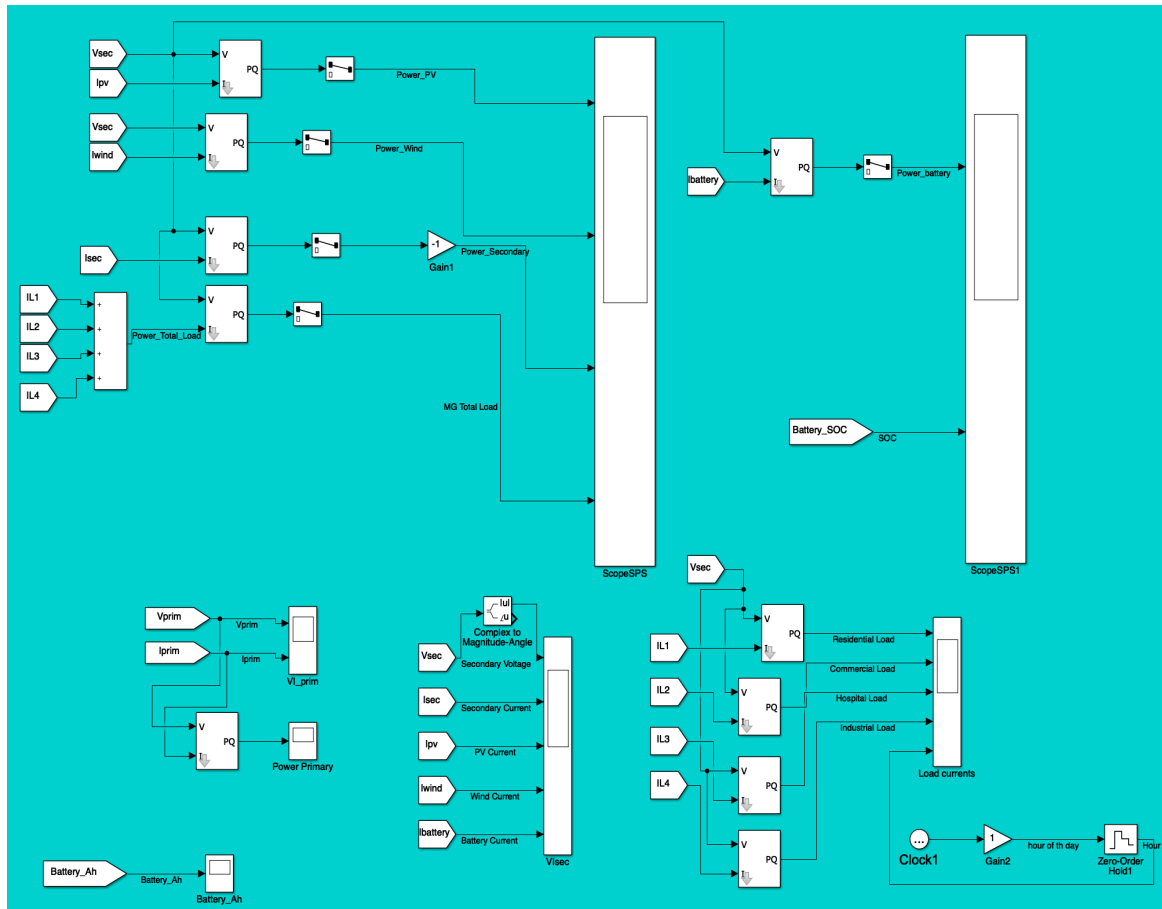


Figure A.7: Scopes to simulate the microgrid system

APPENDIX B

FUZZY RULES

Fuzzy Inference System (FIS) was used to implement Demand Side Management (DSM) in three of the six presented cases. In this appendix the set of if-then rules used to map the input and output will be listed in different sections.

B.1 Case 1

For the energy balance case, 2 inputs and 1 output are considered. 13 rules were implemented the subscripts listed below stand for: EB is energy balance in the microgrid, G & L are the aggregated load and local generation of the microgrid at a certain hour and P_1, P_2 and P_3 are three periods during the 24 hour span. DLC is the direct load control decision and curtailment percentage.

Table B.1: Fuzzy rules of the 1st case

Fuzzy Rules
1. If (EB is G>L) then (DLC is DoNothing) (1)
2. If (EB is L>G) and (Time is P1) then (DLC is Low) (1)
3. If (EB is L>G) and (Time is P2) then (DLC is Medium) (1)
4. If (EB is L>G) and (Time is P3) then (DLC is Low) (1)
5. If (EB is L>>G) and (Time is P1) then (DLC is Low) (1)
6. If (EB is L>>G) and (Time is P2) then (DLC is Medium) (1)
7. If (EB is L>>G) and (Time is P3) then (DLC is Medium) (1)
8. If (EB is L>>G) and (Time is P1) then (DLC is Medium) (1)
9. If (EB is L>>G) and (Time is P2) then (DLC is VeryHigh) (1)
10. If (EB is L>>G) and (Time is P3) then (DLC is High) (1)
11. If (EB is L>>>G) and (Time is P1) then (DLC is High) (1)
12. If (EB is L>>>G) and (Time is P3) then (DLC is VeryHigh) (1)
13. If (EB is L>>>G) and (Time is P2) then (DLC is Extreme) (1)

B.2 Case 2

This case applies same concept as Case.1 but with the incorporation of priority list.

The variable xx is the priority list at each hour. There are 3 inputs and 4 outputs in this case and the rules to map the inputs and outputs are listed below.

Table B.2: Fuzzy rules of the 2nd case

Fuzzy Rules
1. If (EB is G>L) then (RES DLC is DoNothing)(COMMDLC is DoNothing) (INDDLC is DoNothing)(HOS DLC is DoNothing) (1)
2. If (EB is L>G) and (Time is not P2) and (xx is 3120) then (RES DLC is DoNothing) (COMMDLC is Medium)(INDDLC is Low)(HOS DLC is DoNothing) (1)
3. If (EB is L>G) and (Time is not P2) and (xx is 3021) then (RES DLC is Medium) (COMMDLC is DoNothing)(INDDLC is Low)(HOS DLC is DoNothing) (1)
4. If (EB is L>G) and (Time is not P2) and (xx is 3102) then (RES DLC is DoNothing) (COMMDLC is Low)(INDDLC is Medium)(HOS DLC is DoNothing) (1)
5. If (EB is L>>G) and (Time is not P2) and (xx is 3120) then (RES DLC is DoNothing) (COMMDLC is High)(INDDLC is Medium)(HOS DLC is DoNothing) (1)
6. If (EB is L>>G) and (Time is not P2) and (xx is 3021) then (RES DLC is High) (COMMDLC is DoNothing)(INDDLC is Medium)(HOS DLC is DoNothing) (1)
7. If (EB is L>>G) and (Time is not P2) and (xx is 3102) then (RES DLC is DoNothing) (COMMDLC is Medium)(INDDLC is High)(HOS DLC is DoNothing) (1)
8. If (EB is L>>>G) and (Time is not P2) and (xx is 3120) then (RES DLC is DoNothing) (COMMDLC is VeryHigh)(INDDLC is High)(HOS DLC is DoNothing) (1)
9. If (EB is L>>>G) and (Time is not P2) and (xx is 3021) then (RES DLC is VeryHigh) (COMMDLC is DoNothing)(INDDLC is High)(HOS DLC is DoNothing) (1)
10. If (EB is L>>>G) and (Time is not P2) and (xx is 3102) then (RES DLC is DoNothing) (COMMDLC is High)(INDDLC is VeryHigh)(HOS DLC is DoNothing) (1)

Table B.2 continued from previous page

Fuzzy Rules
11. If (EB is L>>>>G) and (Time is not P2) and (xx is 3120) then (RES DLC is DoNothing) (COMMDLC is Extreme)(INDDL C is VeryHigh)(HOSDLC is DoNothing) (1)
12. If (EB is L>>>>G) and (Time is not P2) and (xx is 3021) then (RES DLC is Extreme) (COMMDLC is DoNothing)(INDDL C is VeryHigh)(HOSDLC is DoNothing) (1)
13. If (EB is L>>>>G) and (Time is not P2) and (xx is 3102) then (RES DLC is DoNothing) (COMMDLC is VeryHigh)(INDDL C is Extreme)(HOSDLC is DoNothing) (1)
14. If (EB is L>G) and (Time is P2) and (xx is 3120) then (RES DLC is Low) (COMMDLC is Medium)(INDDL C is Low)(HOSDLC is DoNothing) (1)
15. If (EB is L>G) and (Time is P2) and (xx is 3102) then (RES DLC is Low) (COMMDLC is Low)(INDDL C is Medium)(HOSDLC is DoNothing) (1)
16. If (EB is L>>G) and (Time is P2) and (xx is 3120) then (RES DLC is Low) (COMMDLC is High)(INDDL C is Medium)(HOSDLC is DoNothing) (1)
17. If (EB is L>>G) and (Time is P2) and (xx is 3021) then (RES DLC is High) (COMMDLC is Low)(INDDL C is Medium)(HOSDLC is DoNothing) (1)
18. If (EB is L>>G) and (Time is P2) and (xx is 3102) then (RES DLC is Low) (COMMDLC is Medium)(INDDL C is High)(HOSDLC is DoNothing) (1)
19. If (EB is L>>>G) and (Time is P2) and (xx is 3120) then (RES DLC is Low) (COMMDLC is VeryHigh)(INDDL C is High)(HOSDLC is DoNothing) (1)
20. If (EB is L>>>>G) and (Time is P2) and (xx is 3021) then (RES DLC is VeryHigh) (COMMDLC is Low)(INDDL C is High)(HOSDLC is DoNothing) (1)

Table B.2 continued from previous page

Fuzzy Rules
21. If (EB is L>>>G) and (Time is P2) and (xx is 3102) then (RES DLC is Low) (COMMDLC is High)(INDDL C is VeryHigh)(HOSDLC is DoNothing) (1)
22. If (EB is L>>>>G) and (Time is P2) and (xx is 3120) then (RES DLC is Low) (COMMDLC is Extreme)(INDDL C is VeryHigh)(HOSDLC is DoNothing) (1)
23. If (EB is L>>>>G) and (Time is P2) and (xx is 3021) then (RES DLC is Extreme) (COMMDLC is Low)(INDDL C is VeryHigh)(HOSDLC is DoNothing) (1)
24. If (EB is L>>>>G) and (Time is P2) and (xx is 3102) then (RES DLC is Low) (COMMDLC is VeryHigh)(INDDL C is Extreme)(HOSDLC is DoNothing) (1)
25. If (EB is L>G) and (Time is not P2) and (xx is 3012) then (RES DLC is Low) (COMMDLC is DoNothing)(INDDL C is Medium)(HOSDLC is DoNothing) (1)
26. If (EB is L>>G) and (Time is not P2) and (xx is 3012) then (RES DLC is Medium) (COMMDLC is DoNothing)(INDDL C is High)(HOSDLC is DoNothing) (1)
27. If (EB is L>>>G) and (Time is not P2) and (xx is 3012) then (RES DLC is High) (COMMDLC is DoNothing)(INDDL C is VeryHigh)(HOSDLC is DoNothing) (1)
28. If (EB is L>>>>G) and (Time is not P2) and (xx is 3012) then (RES DLC is VeryHigh) (COMMDLC is DoNothing)(INDDL C is Extreme)(HOSDLC is DoNothing) (1)
29. If (EB is L>G) and (Time is P2) and (xx is 3012) then (RES DLC is Low) (COMMDLC is Low)(INDDL C is Medium)(HOSDLC is DoNothing) (1)
30. If (EB is L>>G) and (Time is P2) and (xx is 3012) then (RES DLC is Medium) (COMMDLC is Low)(INDDL C is High)(HOSDLC is DoNothing) (1)

Table B.2 continued from previous page

Fuzzy Rules
31. If (EB is L>>>G) and (Time is P2) and (xx is 3012) then (RES DLC is High) (COMMDLC is Low)(INDDLDC is VeryHigh)(HOSDLC is DoNothing) (1)
32. If (EB is L>>>>G) and (Time is P2) and (xx is 3012) then (RES DLC is VeryHigh) (COMMDLC is Low)(INDDLDC is Extreme)(HOSDLC is DoNothing) (1)
33. If (EB is L>G) and (Time is P2) and (xx is 3021) then (RES DLC is Medium) (COMMDLC is Low)(INDDLDC is Low)(HOSDLC is DoNothing) (1)

B.3 Case 6

In this case, a special DSM scheme was tested, which is only applied to Residential costumers, particularly AC loads. The load profile of three houses is inputted alongside with time. The output is the action that should be taken on the air condntioning loads at each house.

Table B.3: Fuzzy rules of the 6th case

Fuzzy Rules
1. If (Home1 is Low) and (Home2 is Low) and (Home3 is Low) and (Time is P1) then (Home1 is Low)(Home2 is AC_ON)(Home3 is AC_{ON}) (1)
2. If (Home1 is Medium) and (Home2 is Medium) and (Home3 is Medium) and (Time is P1) then (Home1 is Low)(Home2 is AC_ON)(Home3 is AC_{ON}) (1)

Table B.3 continued from previous page

Fuzzy Rules
3. If (Home1 is Medium) and (Home2 is Medium) and (Home3 is Medium) and (Time is P2) then (Home1 is Medium)(Home2 is T_{23})(Home3 is T_{23}) (1)
4. If (Home1 is Medium) and (Home2 is Medium) and (Home3 is Medium) and (Time is P3) then (Home1 is Medium)(Home2 is T_{23})(Home3 is T_{23}) (1)
5. If (Home1 is Peak) and (Home2 is Peak) and (Home3 is Peak) and (Time is P1) then (Home1 is Medium)(Home2 is T_{23})(Home3 is T_{23}) (1)
6. If (Home1 is Peak) and (Home2 is Peak) and (Home3 is Peak) and (Time is P2) then (Home1 is VeryStrong)(Home2 is AC_{OFF})(Home3 is AC_{OFF}) (1)
7. If (Home1 is Peak) and (Home2 is Peak) and (Home3 is Peak) and (Time is P3) then (Home1 is Strong)(Home2 is T_{26})(Home3 is T_{26}) (1)
8. If (Home1 is Peak) and (Home2 is not Peak) and (Home3 is not Peak) and (Time is P1) then (Home1 is Strong)(Home2 is AC_ON)(Home3 is AC_{ON}) (1)
9. If (Home1 is Peak) and (Home2 is not Peak) and (Home3 is not Peak) and (Time is P3) then (Home1 is Strong)(Home2 is AC_ON)(Home3 is AC_{ON}) (1)
10. If (Home1 is Peak) and (Home2 is not Peak) and (Home3 is not Peak) and (Time is P2) then (Home1 is VeryStrong)(Home2 is T_{23})(Home3 is T_{23}) (1)
11. If (Home1 is not Peak) and (Home2 is Peak) and (Home3 is not Peak) and (Time is P2) then (Home1 is Medium)(Home2 is AC_{OFF})(Home3 is T_{23}) (1)
12. If (Home1 is not Peak) and (Home2 is Peak) and (Home3 is not Peak) and (Time is P1) then (Home1 is Low)(Home2 is T_{26})(Home3 is AC_{ON}) (1)

Table B.3 continued from previous page

Fuzzy Rules
13. If (Home1 is not Peak) and (Home2 is Peak) and (Home3 is not Peak) and (Time is P3) then (Home1 is Low)(Home2 is T_{26})(Home3 is AC_{ON}) (1)
14. If (Home1 is not Peak) and (Home2 is not Peak) and (Home3 is Peak) and (Time is P1) then (Home1 is Low)(Home2 is AC_ON)(Home3 is T_{26}) (1)
15. If (Home1 is not Peak) and (Home2 is not Peak) and (Home3 is Peak) and (Time is P2) then (Home1 is Strong)(Home2 is T_{26})(Home3 is AC_{OFF}) (1)
16. If (Home1 is not Peak) and (Home2 is not Peak) and (Home3 is Peak) and (Time is P3) then (Home1 is Medium)(Home2 is T_{23})(Home3 is T_{26}) (1)
17. If (Home1 is Peak) and (Home2 is not Peak) and (Home3 is Peak) and (Time is P1) then (Home1 is Strong)(Home2 is AC_ON)(Home3 is T_{23}) (1)
18. If (Home1 is Peak) and (Home2 is Peak) and (Home3 is not Peak) and (Time is P1) then (Home1 is Strong)(Home2 is T_{23})(Home3 is AC_{ON}) (1)
19. If (Home1 is Peak) and (Home2 is not Peak) and (Home3 is Peak) and (Time is P3) then (Home1 is Strong)(Home2 is AC_ON)(Home3 is T_{26}) (1)
20. If (Home1 is Peak) and (Home2 is Peak) and (Home3 is not Peak) and (Time is P3) then (Home1 is Strong)(Home2 is T_{26})(Home3 is AC_{ON}) (1)
21. If (Home1 is Peak) and (Home2 is not Peak) and (Home3 is Peak) and (Time is P2) then (Home1 is VeryStrong)(Home2 is T_{23})(Home3 is AC_{OFF}) (1)
22. If (Home1 is Peak) and (Home2 is Peak) and (Home3 is not Peak) and (Time is P2) then (Home1 is VeryStrong)(Home2 is AC_{OFF})(Home3 is T_{23}) (1)

Table B.3 continued from previous page

Fuzzy Rules
23. If (Home1 is Peak) and (Home2 is Peak) and (Home3 is not Peak) and (Time is P2) then (Home1 is VeryStrong)(Home2 is AC_{OFF})(Home3 is T_{23}) (1)
24. If (Home1 is not Peak) and (Home2 is Peak) and (Home3 is Peak) and (Time is P2) then (Home1 is Medium)(Home2 is AC_{OFF})(Home3 is AC_{OFF}) (1)
25. If (Home1 is Peak) and (Home2 is Peak) and (Home3 is not Peak) and (Time is P1) then (Home1 is Medium)(Home2 is T_{26})(Home3 is AC_{ON}) (1)
26. If (Home1 is not Peak) and (Home2 is Peak) and (Home3 is Peak) and (Time is P1) then (Home1 is Low)(Home2 is T_{26})(Home3 is T_{23}) (1)
27. If (Home1 is Peak) and (Home2 is Peak) and (Home3 is not Peak) and (Time is P3) then (Home1 is Strong)(Home2 is T_{26})(Home3 is AC_{ON}) (1)
28. If (Home1 is not Peak) and (Home2 is Peak) and (Home3 is Peak) and (Time is P3) then (Home1 is Low)(Home2 is T_{26})(Home3 is T_{26}) (1)
29. If (Home1 is Peak) and (Home2 is not Peak) and (Home3 is Peak) and (Time is P1) then (Home1 is Medium)(Home2 is AC_ON)(Home3 is T_{26}) (1)
30. If (Home1 is not Peak) and (Home2 is Peak) and (Home3 is Peak) and (Time is P1) then (Home1 is Low)(Home2 is T_{23})(Home3 is T_{26}) (1)
31. If (Home1 is Peak) and (Home2 is not Peak) and (Home3 is Peak) and (Time is P2) then (Home1 is VeryStrong)(Home2 is T_{23})(Home3 is AC_{OFF}) (1)
32. If (Home1 is not Peak) and (Home2 is Peak) and (Home3 is Peak) and (Time is P2) then (Home1 is Medium)(Home2 is AC_{OFF})(Home3 is AC_{OFF}) (1)

Table B.3 continued from previous page

Fuzzy Rules
33. If (Home1 is Peak) and (Home2 is not Peak) and (Home3 is Peak) and (Time is P3) then (Home1 is Strong)(Home2 is AC_ON)(Home3 is T_{26}) (1)
34. If (Home1 is not Peak) and (Home2 is Peak) and (Home3 is Peak) and (Time is P3) then (Home1 is Low)(Home2 is T_{26})(Home3 is T_{26}) (1)

REFERENCES

- [1] [Online]. Available: <https://www.se.com.sa/en-us/Pages/home.aspx>
- [2] “Engineering toolbox (2008), wind shear.” [Online]. Available: https://www.engineeringtoolbox.com/wind-shear-d_1215.html
- [3] “World energy outlook 2009,” *World Energy Outlook - International Energy Agency*, 2009.
- [4] E. Dupont, R. Koppelaar, and H. Jeanmart, “Global available wind energy with physical and energy return on investment constraints,” *Applied Energy*, 10 2017.
- [5] “vestas v47-700 - 700,00 kw - windkraftanlage.” [Online]. Available: <https://www.wind-turbine-models.com/turbines/1724-vestas-v47-700>
- [6] D. E. Olivares, A. Mehrizi-Sani, A. H. Etemadi, C. A. Cañizares, R. Iravani, M. Kazerani, A. H. Hajimiragha, O. Gomis-Bellmunt, M. Saeedifard, R. Palma-Behnke, G. A. Jiménez-Estévez, and N. D. Hatziargyriou, “Trends in microgrid control,” *IEEE Transactions on Smart Grid*, vol. 5, no. 4, pp. 1905–1919, July 2014.

- [7] “WG C6.22 microgrids.” [Online]. Available: <http://c6.cigre.org/WG-Area/WG-C6.22-Microgrids>
- [8] S. Chowdhury, S. P. Chowdhury, and P. Crossley, *Microgrids and active distribution networks*. Institution of Engineering and Technology, 2009.
- [9] A. Parida, S. Choudhury, and D. Chatterjee, “Microgrid based hybrid energy co-operative for grid-isolated remote rural village power supply for east coast zone of india,” *IEEE Transactions on Sustainable Energy*, vol. 9, no. 3, pp. 1375–1383, July 2018.
- [10] S. Mashayekh, M. Stadler, G. Cardoso, M. Heleno, S. C. Madathil, H. Nagarajan, R. Bent, M. Mueller-Stoffels, X. Lu, and J. Wang, “Security-constrained design of isolated multi-energy microgrids,” *IEEE Transactions on Power Systems*, vol. 33, no. 3, pp. 2452–2462, May 2018.
- [11] R. Morsali and R. Kowalczyk, “Demand response based day-ahead scheduling and battery sizing in microgrid management in rural areas,” *IET Renewable Power Generation*, vol. 12, no. 14, pp. 1651–1658, 2018.
- [12] S. Uski, K. Forssén, and J. Shemeikka, “Sensitivity assessment of microgrid investment options to guarantee reliability of power supply in rural networks as an alternative to underground cabling,” *Energies*, vol. 11, no. 10, p. 2831, 2018.
- [13] J. Xiao, P. Wang, and L. Setyawan, “Implementation of multiple-slack-terminal dc microgrids for smooth transitions between grid-tied and islanded states,” *IEEE Transactions on Smart Grid*, vol. 7, no. 1, pp. 273–281, Jan 2016.

- [14] M. Tariq and H. V. Poor, "Electricity theft detection and localization in grid-tied microgrids," *IEEE Transactions on Smart Grid*, vol. 9, no. 3, pp. 1920–1929, May 2018.
- [15] Y. Yang, Z. Fang, F. Zeng, and P. Liu, "Research and prospect of virtual microgrids based on energy internet," in *2017 IEEE Conference on Energy Internet and Energy System Integration (EI2)*, Nov 2017, pp. 1–5.
- [16] "Utility microgrids - where is the value?" Mar 2018. [Online]. Available: <https://www.engerati.com/transmission-and-distribution/article/microgrids/utility-microgrids-where-value>
- [17] "Household energy survey 2017." [Online]. Available: <https://www.stats.gov.sa/en>
- [18] X. Yu, "Interplay of smart grids and intelligent systems and control," May 2011.
- [19] G. Rietveld, P. Clarkson *et al.*, "Measurement infrastructure for observing and controlling smart electrical grids, 3rd IEEE PES innovative smart grid technologies Europe (ISGT Europe), berlin," 2012.
- [20] M. Hashmi, S. Hanninen, and K. Maki, "Survey of smart grid concepts, architectures and technological demonstrations worldwide, 2011 IEEE PES conference on innovative smart grid technologies (ISGT latin america)," 2011.
- [21] V. Koutsoumpas and P. K. Gupta, "Towards a constraint based approach for self-healing smart grids, 2013 2nd international workshop on software engineering challenges for the smart grid (SE4sg), san francisco, CA," 2013.

- [22] L. M. Zhu Min-jie, “The study of distribution grid distributed self-healing under dynamic operating modes, china international conference on electricity distribution (CICED 2012), shanghai,” 2012.
- [23] Y. Oualmakran, J. Melendez *et al.*, “Self-healing for smart grids: Problem formulation and considerations,” *3rd IEEE PES Innovative Smart Grid Technologies Europe (ISGT Europe), Berlin*, 2012.
- [24] K. Ishaque and Z. Salam, “A review of maximum power point tracking techniques of PV system for uniform insolation and partial shading condition,” *Renew. Sustain*, vol. 19, pp. 475–488, 2013.
- [25] A. R. Reisi, M. H. Moradi, and S. Jamasb, “Classification and comparison of maximum power point tracking techniques for photovoltaic system: A review,” *Renew. Sustain*, vol. 19, pp. 433–443, 2013.
- [26] A. Safari and S. Mekhilef, “Simulation and hardware implementation of incremental conductance MPPT with direct control method using cuk converter,” *IEEE Trans. Ind. Electron.*, vol. 58, no. 4, pp. 1154–1161, 2011.
- [27] B. Alajmi, K. Ahmed, S. Finney, and B. Williams, “Fuzzy logic controlled approach of a modified hill climbing method for maximum power point in micro-grid stand-alone photovoltaic system,” *IEEE Trans. Power Electron.*, vol. 26, no. 4, pp. 1022–1030, 2011.

- [28] Y. Zheng, C. Wei, and S. Lin, "A maximum power point tracking method based on tabu search for PV systems under partially shaded conditions," *IET Conference Renewable Power Generation (RPG)*, pp. 52–52, 2011.
- [29] R. Ramaprabha, V. Gothandaraman, K. Kanimozhi, R. Divya, and B. L. Mathur, "Maximum power point tracking using GA-optimized artificial neural network for Solar PV system," *2011 1st Int. Conf. Electr. Energy Syst.*, no. vol. 1, pp. 264–268, 2011.
- [30] J. S. R. Jang, "Anfis: adaptive-network-based fuzzy inference system," *IEEE Trans. Syst. Man Cybern.*, vol. 23, no. 3, pp. 665–685, 1993.
- [31] A. M. S. Aldobhani, "Maximum power point tracking of PV system using ANFIS prediction and fuzzy logic tracking." vol. II, pp. 19–21, 2008.
- [32] Syafaruddin, E. Karatepe, and T. Hiyama, "Artificial neural network-polar coordinated fuzzy controller based maximum power point tracking control under partially shaded conditions," *IET Renewable Power Generation*, vol. 3, no. 2, p. 239, 2009.
- [33] N. Femia, G. Petrone, G. Spagnuolo, and M. Vitelli, "Optimization of perturb and observe maximum power point tracking method," *IEEE Trans. Power Electron.*, vol. 20, no. 4, pp. 963–973, 2005.
- [34] M. B. Smida and A. Sakly, "Genetic based algorithm for maximum power point tracking (mppt) for grid connected pv systems operating under partial shaded

- conditions,” *2015 7th International Conference on Modelling, Identification and Control (ICMIC)*, 2015.
- [35] P. Lei, Y. Li, and J. E. Seem, “Sequential esc-based global mppt control for photovoltaic array with variable shading,” *IEEE Transactions on Sustainable Energy*, vol. 2, no. 3, pp. 348–358, 2011.
- [36] Y. H. Liu, S. C. Huang, J. W. Huang, and W. C. Liang, “A particle swarm optimization-based maximum power point tracking algorithm for pv systems operating under partially shaded conditions,” *IEEE Transactions on Energy Conversion*, vol. 27, no. 4, pp. 1027–1035, Dec 2012.
- [37] G. J. Falco and W. R. Webb, “Water microgrids: The future of water infrastructure resilience,” *Procedia Engineering*, vol. 118, pp. 50–57, 2015.
- [38] X. Tan, Q. Li, and H. Wang, “Advances and trends of energy storage technology in Microgrid,” *Int. J. Electr. Power Energy Syst.*, vol. 44, no. 1, pp. 179–191, 2013.
- [39] A. Rufer, D. Hotellier, and P. Barrade, “A supercapacitor-based energy storage substation for voltage compensation in weak transportation networks,” *IEEE Trans. Power Deliv.*, vol. 19, no. 2, pp. 629–636, 2004.
- [40] Y. Cheng, “Assessments of energy capacity and energy losses of supercapacitors in fast charging-discharging cycles,” *IEEE Trans. Energy Convers.*, vol. 25, no. 1, pp. 253–261, 2010.

- [41] Z. Yang, C. Shen, L. Zhang, M. L. Crow, and S. Atcitty, “Integration of a StatCom and battery energy storage,” *IEEE Trans. Power Syst.*, vol. 16, no. 2, pp. 254–260, 2001.
- [42] T. Zhao, Z. Zuo, and Z. Ding, “Cooperative control of distributed battery energy storage systems in microgrids,” in *2016 35th Chinese Control Conference (CCC)*, July 2016, pp. 10 019–10 024.
- [43] A. Khatamianfar, M. Khalid, A. V. Savkin, and V. G. Agelidis, “Improving wind farm dispatch in the Australian electricity market with battery energy storage using model predictive control,” *IEEE Transactions on Sustainable Energy*, vol. 4, no. 3, pp. 745–755, 2013.
- [44] J. P. Fossati, A. Galarza, A. Martin-Villate, and L. Fontan, “A method for optimal sizing energy storage systems for microgrids,” *Renewable Energy*, vol. 77, pp. 539–549, 2015.
- [45] A. Zahedi, “Maximizing solar PV energy penetration using energy storage technology,” *Renewable and Sustainable Energy Reviews*, vol. 15, no. 1, pp. 866–870, 2011.
- [46] P. Denholm and R. M. Margolis, “Evaluating the limits of solar photovoltaics (PV) in electric power systems utilizing energy storage and other enabling technologies,” *Energy Policy*, vol. 35, no. 9, pp. 4424–4433, 2007.

- [47] P. Denholm and M. Hand, “Grid flexibility and storage required to achieve very high penetration of variable renewable electricity, *Energy Policy*,” vol. 39, no. 3, pp. 1817–1830, 2011.
- [48] A. Khodaei, “Microgrid optimal scheduling with multi-period islanding constraints,” *IEEE Transactions on Power Systems*, vol. 29, no. 3, pp. 1383–1392, 2014.
- [49] M. Izadbakhsh, M. Gandomkar, A. Rezvani, and A. Ahmadi, “Short-term resource scheduling of a renewable energy based micro grid, *Renewable Energy*,” vol. 75, pp. 598–606, 2015.
- [50] G. Graditi, M. L. D. Silvestre, R. Gallea, and E. R. Sanseverino, “Heuristic-based shiftable loads optimal management in smart micro-grids, *IEEE Transactions on Industrial Informatics*,” vol. 11, no. 1, pp. 271–280, 2015.
- [51] H. Farzin, M. Fotuhi-Firuzabad, and M. Moeini-Aghaie, “A stochastic multi-objective framework for optimal scheduling of energy storage systems in microgrids,” *IEEE Transactions on Smart Grid*, vol. 8, no. 1, pp. 117–127, Jan 2017.
- [52] M. D. Somma, B. Yan, N. Bianco, G. Graditi, P. B. Luh, L. Mongibello, and V. Naso, “Operation optimization of a distributed energy system considering energy costs and energy efficiency, *Energy Conversion and Management*,” vol. 103, pp. 739–751, 2015.

- [53] I. Aldaouab, M. Daniels, and K. Hallinan, “Microgrid cost optimization for a mixed-use building,” in *2017 IEEE Texas Power and Energy Conference (TPEC)*, Feb 2017, pp. 1–5.
- [54] L. Yu, T. Jiang, and Y. Cao, “Energy cost minimization for distributed internet data centers in smart microgrids considering power outages, *IEEE Transactions on Parallel and Distributed Systems*,” vol. 26, no. 1, pp. 120–130, 2015.
- [55] Y. Liu, C. Yuen, N. U. Hassan, S. Huang, R. Yu, and S. Xie, “Electricity cost minimization for a microgrid with distributed energy resource under different information availability, *IEEE Transactions on Industrial Electronics*,” vol. 62, no. 4, pp. 2571–2583, 2015.
- [56] R. Mallol-Poyato, S. Salcedo-Sanz, S. Jimenez-Fernaandez, and P. Diaz-Villar, “Optimal discharge scheduling of energy storage systems in microgrids based on hyper-heuristics, *Renewable Energy*,” vol. 83, pp. 13–24, 2015.
- [57] B. Zhao, X. Zhang, J. Chen, C. Wang, and L. Guo, “Operation optimization of standalone microgrids considering lifetime characteristics of battery energy storage system, *IEEE Transactions on Sustainable Energy*,” vol. 4, no. 4, pp. 934–943, 2013.
- [58] Y. Atwa, E. El-Saadany, M. Salama, and R. Seethapathy, “Optimal renewable resources mix for distribution system energy loss minimization, *IEEE Transactions on Power Systems*,” vol. 25, no. 1, pp. 360–370, 2010.

- [59] “Bibliography on load models for power flow and dynamic performance simulation,” *IEEE Transactions on Power Systems*, vol. 10, no. 1, pp. 523–538, 1995.
- [60] A. Maitra, A. Gaikwad, P. Zhang, M. Ingram, D. Mercado, and W. Woitt, “Using system disturbance measurement data to develop improved load models,” *2006 IEEE PES Power Systems Conference and Exposition*, 2006.
- [61] L. M. Korunovic, S. Sterpu, S. Djokic, K. Yamashita, S. M. Villanueva, and J. V. Milanovic, “Processing of load parameters based on existing load models,” *2012 3rd IEEE PES Innovative Smart Grid Technologies Europe (ISGT Europe)*, 2012.
- [62] P. Kundur, *Power System Stability and Control*, vol. New York: I, 1994.4.
- [63] “Load representation for dynamic performance analysis (of power systems),” *IEEE Transactions on Power Systems*, vol. 8, no. 2, pp. 472–482, 1993.
- [64] M. Bostanci, J. Koplowitz, and C. Taylor, “Identification of power system load dynamics using artificial neural networks,” *IEEE Transactions on Power Systems*, vol. 12, no. 4, pp. 1468–1473, 1997.
- [65] A. Arif, Z. Wang, J. Wang, B. Mather, H. Bashualdo, and D. Zhao, “Load modeling - a review,” *IEEE Transactions on Smart Grid*, pp. 1–1, 2017.
- [66] J. Lim, P. Ji, A. Ozdemir, and C. Singh, “Component-based load modeling including capacitor banks,” *2001 Power Engineering Society Summer Meeting. Conference Proceedings (Cat. No.01CH37262)*, 2001.

- [67] K. E. Wong, M. E. Haque, and M. Davies, "Component-based dynamic load modeling of a paper mill," pp. 1–6, 2012.
- [68] L. Zhu, X. Li, H. Ouyang, Y. Wang, W. Liu, and K. Shao, "Research on component-based approach load modeling based on energy management system and load control system," pp. 1–6, 2012.
- [69] T. Porsinger, P. Janik, Z. Leonowicz, and R. Gono, "Component modelling for microgrids," *2016 IEEE 16th International Conference on Environment and Electrical Engineering (EEEIC)*, 2016.
- [70] T. Papadopoulos, E. Tzanidakis, P. Papadopoulos, P. Crolla, G. Papagiannis, and G. Burt, "Aggregate load modeling in microgrids using online measurements," *MedPower 2014*, 2014.
- [71] B.-K. Choi, H.-D. Chiang, Y. Li, H. Li, Y.-T. Chen, D.-H. Huang, and M. Lauby, "Measurement-based dynamic load models: Derivation, comparison, and validation," *IEEE Transactions on Power Systems*, vol. 21, no. 3, pp. 1276–1283, 2006.
- [72] J. Hou, Z. Xu, and Z. Y. Dong, "Measurement-based load modeling at distribution level with complete model structure," *2012 IEEE Power and Energy Society General Meeting*, 2012.
- [73] D. P. Stojanovic, L. M. Korunovic, and J. Milanovic, "Dynamic load modelling based on measurements in medium voltage distribution network," *Electric Power Systems Research*, vol. 78, no. 2, pp. 228–238, 2008.

- [74] E. O. Kontis, T. A. Papadopoulos, A. I. Chrysochos, and G. K. Papagiannis, “Measurement-based dynamic load modeling using the vector fitting technique,” *IEEE Transactions on Power Systems*, vol. 33, no. 1, pp. 338–351, 2018.
- [75] M. Tasdighi, H. Ghasemi, and A. Rahimi-Kian, “Residential microgrid scheduling based on smart meters data and temperature dependent thermal load modeling,” *IEEE Transactions on Smart Grid*, vol. 5, no. 1, pp. 349–357, 2014.
- [76] H. Li, C. Yao, J. Wang, L. Zhu, and S. Yang, “Events identification based load modeling for residential microgrid,” *2015 IEEE Energy Conversion Congress and Exposition (ECCE)*, 2015.
- [77] J. V. Milanovic and S. M. Zali, “Validation of equivalent dynamic model of active distribution network cell,” *IEEE Transactions on Power Systems*, vol. 28, no. 3, pp. 2101–2110, 2013.
- [78] Z. Baharlouei and M. Hashemi, “Demand side management challenges in smart grid: A review,” in *2013 Smart Grid Conference (SGC)*, Dec 2013, pp. 96–101.
- [79] “Matlab - mathworks.” [Online]. Available: <https://www.mathworks.com/products/matlab.html>
- [80] L. He and N. Liu, “Load profile analysis for commercial buildings microgrids under demand response,” in *2017 12th IEEE Conference on Industrial Electronics and Applications (ICIEA)*, June 2017, pp. 461–465.
- [81] H. R. Atia, A. Shakya, P. Tandukar, U. Tamrakar, T. M. Hansen, and R. Tonkoski, “Efficiency analysis of ac coupled and dc coupled microgrids consid-

- ering load profile variations,” in *2016 IEEE International Conference on Electro Information Technology (EIT)*, May 2016, pp. 0695–0699.
- [82] *Renewable 2018: Global Status Report*, REN21 Secretariat, Paris.
- [83] P. Janik, J. Rezmer, Z. Waclawek, P. Kostyła, T. Porsinger, and H. Schwarz, “Potentials of microgrids - res infeed, stationary storage and controllable loads modelling,” in *2014 16th International Conference on Harmonics and Quality of Power (ICHQP)*, May 2014, pp. 655–658.
- [84] J. Li, W. Wei, and J. Xiang, “A simple sizing algorithm for stand-alone pv/wind/battery hybrid microgrids,” *Energies*, vol. 5, no. 12, p. 5307–5323, 2012.
- [85] R. Tito, T. T. Lie, and T. Anderson, “A simple sizing optimization method for wind-photovoltaic-battery hybrid renewable energy systems,” 2013.
- [86] M. Sheraz and M. A. Abido, “An efficient mppt controller using differential evolution and neural network,” in *2012 IEEE International Conference on Power and Energy (PECon)*, Dec 2012, pp. 378–383.
- [87] D. Y. Goswami, “Principle of solar engineering,” *Taylor and Francis Group, LLC*, 2015.
- [88] E. Skoplaki and J. Palyvos, “On the temperature dependence of photovoltaic module electrical performance: A review of efficiency/power correlations,” *Solar Energy*, vol. 83, no. 5, pp. 614–624, 2009.

- [89] A. Ghalebani and T. K. Das, "Design of financial incentive programs to promote net zero energy buildings," *IEEE Transactions on Power Systems*, vol. 32, no. 1, p. 75 to 84, 2017.
- [90] "Department of Energy (DoE)." [Online]. Available: <http://www.energy.gov/>
- [91] Z. Chen, D. Pattabiraman, R. H. Lasseter, and T. M. Jahns, "Certs microgrids with photovoltaic microsources and feeder flow control," in *2016 IEEE Energy Conversion Congress and Exposition (ECCE)*, Sept 2016, pp. 1–8.
- [92] E. Hossain, E. Kabalci, R. Bayindir, and R. Perez, "Microgrid testbeds around the world: State of art," May 2014. [Online]. Available: <https://www.sciencedirect.com/science/article/pii/S0196890414004233>
- [93] V. A. Kleftakis, D. T. Lagos, C. N. Papadimitriou, and N. D. Hatziargyriou, "Seamless transition between interconnected and islanded operation of dc microgrids," *IEEE Transactions on Smart Grid*, vol. PP, no. 99, pp. 1–1, 2017.
- [94] J. H. Eto, R. Lasseter, B. Schenkman, D. Klapp, E. Linton, H. Hurtado, J. Roy, N. J. Lewis, J. Stevens, and et al., "Certs microgrid laboratory test bed - pier final project report," 2008.
- [95] K. J. Mun, J. H. Park, H.-S. Kim, and J.-I. Seo, "Development of real-time-service restoration system for distribution automation system," in *ISIE 2001. 2001 IEEE International Symposium on Industrial Electronics Proceedings (Cat. No.01TH8570)*, vol. 3, June 2001, pp. 1514–1519 vol.3.

- [96] H. Yu, H. Liu, and J. Liu, "Service restoration reconfiguration in distribution networks based on a multi-objective optimization algorithm," in *2011 International Conference on Electrical and Control Engineering*, Sept 2011, pp. 3624–3627.
- [97] Q. Zhou, D. Shirmohammadi, and W. . E. Liu, "Distribution feeder reconfiguration for operation cost reduction," *IEEE Transactions on Power Systems*, vol. 12, no. 2, pp. 730–735, May 1997.
- [98] X. Chen, B. Kong, F. Liu, X. Gong, and X. Shen, "System service restoration of distribution network based on multi-agent technology," in *2013 Fourth International Conference on Digital Manufacturing Automation*, June 2013, pp. 1371–1374.
- [99] K. S. Kumar, K. Rajalakshmi, and S. P. Karthikeyan, "A modified artificial neural network based distribution system reconfiguration for loss minimization," in *2014 International Conference on Advances in Electrical Engineering (ICAEE)*, Jan 2014, pp. 1–5.
- [100] Y. Kumar, B. Das, and J. Sharma, "Multiobjective, multiconstraint service restoration of electric power distribution system with priority customers," *IEEE Transactions on Power Delivery*, vol. 23, no. 1, pp. 261–270, Jan 2008.
- [101] L. T. Marques, A. C. B. Delbem, J. B. A. London, and M. H. M. Camillo, "Service restoration in large-scale distribution systems considering three levels of priority customers," in *2015 IEEE Eindhoven PowerTech*, June 2015, pp. 1–6.

- [102] L. T. Marques, A. C. B. Delbem, and J. B. A. London, "Service restoration with prioritization of customers and switches and determination of switching sequence," *IEEE Transactions on Smart Grid*, vol. 9, no. 3, pp. 2359–2370, May 2018.
- [103] R. Hardwar, "Prioritizing the restoration of network distribution transformers using distribution system loading and network reliability indices," Ph.D. dissertation, 2014. [Online]. Available: <https://search.proquest.com/docview/1562269564?accountid=27795>
- [104] M. H. M. Camillo, M. E. V. Romero, R. Z. Fanucchi, T. W. D. Lima, A. B. C. Delbem, and J. B. A. London, "Exhaustive search and multi-objective evolutionary algorithm for single fault service restoration in a real large-scale distribution system," *2015 IEEE Power & Energy Society General Meeting*, 2015.
- [105] J. Hou, Z. Xu, Z. Y. Dong, and K. P. Wong, "Permutation-based power system restoration in smart grid considering load prioritization," *Electric Power Components and Systems*, vol. 42, no. 3-4, p. 361–371, May 2014.
- [106] A. Abraham and B. Nath, "Artificial neural networks for intelligent real time."
- [107] S. Biansoongnern and B. Plangklang, "Nonintrusive load monitoring (nilm) using an artificial neural network in embedded system with low sampling rate," *2016 13th International Conference on Electrical Engineering/Electronics, Computer, Telecommunications and Information Technology (ECTI-CON)*, 2016.

- [108] [Online]. Available: <http://www.iyfipun.com/#1050%231680%231%230%23784%23294>
- [109] C. Wang, X. Yang, Z. Wu, Y. Che, L. Guo, S. Zhang, and Y. Liu, "A highly integrated and reconfigurable microgrid testbed with hybrid distributed energy sources," *IEEE Transactions on Smart Grid*, vol. 7, no. 1, pp. 451–459, Jan 2016.
- [110] T. Som and N. Chakraborty, "Studies on economic feasibility of an autonomous power delivery system utilizing alternative hybrid distributed energy resources," *IEEE Transactions on Power Systems*, vol. 29, no. 1, pp. 172–181, Jan 2014.
- [111] K. Palaniappan, S. Veerapeneni, R. Cuzner, and Y. Zhao, "Assessment of the feasibility of interconnected smart dc homes in a dc microgrid to reduce utility costs of low income households," in *2017 IEEE Second International Conference on DC Microgrids (ICDCM)*, June 2017, pp. 467–473.
- [112] F. Zhang, C. Meng, Y. Yang, C. Sun, C. Ji, Y. Chen, W. Wei, H. Qiu, and G. Yang, "Advantages and challenges of dc microgrid for commercial building a case study from xiamen university dc microgrid," in *2015 IEEE First International Conference on DC Microgrids (ICDCM)*, June 2015, pp. 355–358.

VITAE

- Name: Ahmed Saleh Alahmed
- Nationality: Saudi
- Date of Birth: 09/14/1993
- Email: *alahmed6593@gmail.com*
- Permanent Address: KFUPM Academic Belt Road, Dhahran, Saudi Arabia
- Website: <https://www.ahmedsa.me>

Academic Background:

- 2017 - 2019, ” **King Fahd University of Petroleum and Minerals**”, Master of Science degree in power and energy engineering with honors recognition.
- 2016 - 2017, ”**KTH Royal Institute of Technology**”, ABB scholarship with electric power engineering department at KTH.
- 2011 - 2016, ” **King Fahd University of Petroleum and Minerals**”, Bachelor of Science degree in electrical engineering with honors recognition.

Experience:

- 2017 - current, " **King Fahd University of Petroleum and Minerals**", Graduate assistant.
- 2018, " **University of Tokyo**", Leadership Program on Sustainable Energy Systems, Tokyo, Japan.
- 2018, " **Saudi Aramco EXPEC Advanced Research Center (ARC)**", Summer researcher at the Production Technology Division (PTD), Dhahran.
- 2015, " **Buro Happold Engineering**", Abroad summer training with MEP team, London, UK.
- 2014, " **Georgia Institute of Technology**", Exchange program student, Atlanta, Georgia, USA.

Publications:

A. Posters

- **A. S. Alahmed** and M. M. Almuahini, " **Modelling of microgrid demands and load composition for highly reliable systems**", *Best poster award* at IEEE Saudi Arabia Smart Grid (SASG) Conference, Jeddah, Saudi Arabia, 2018.

B. Conferences

- **A. S. Alahmed**, S. O. Taiwo and M. A. Abido and M. M. Almuahini " **Intelligent Flexible Priority List for Reconfiguration of Microgrid**

Demands Using Deep Neural Network", Accepted at IEEE PES ISGT ASIA, China, 2019.

- **A. S. Alahmed**, S. O. Taiwo and M. A. Abido, "**Implementation and evaluation of grey wolf optimization algorithm on power system stability enhancement**", 10th IEEE GCC Conference, Kuwait, 2019.
- H. Adel, **A. S. Alahmed** and I. Elamin, "**Possible privatization schemes for power generation sector in saudi arabia**", IEEE International Conference on Smart Energy Grid Engineering (SEGE), Oshawa, Canada, 2018.
- **A. S. Alahmed**, O. T. Alafif, A. H. Muqaibel and A. T. Abdalla, "**Path-loss compensation in through-the-wall radar imaging**", IEEE International Conference on Radar, Antenna, Microwave, Electronics and Telecommunications (ICRAMET), Jakarta, 2016.

C. Journals

- **A. S. Alahmed** and M. Ghandhari "**Performance of controlled FACTS and VSC-HVDC in a power system subject to inter-area oscillation**", Journal of Automation & Systems Engineering (JASE), 2018.
- **A. S. Alahmed**, H. S. Alharbi, I. Elamin and M. M. Almuahini, "**Incentive-Based Feasibility Study of a Hybrid AC/DC Microgrid in Saudi Arabia With Hybrid Distributed Energy Resources**", Submitted to Energies smartgrids and microgrids, 2019.